

**EVALUATING RESERVOIR PRODUCTION STRATEGIES IN  
MISCIBLE AND IMMISCIBLE GAS-INJECTION PROJECTS**

A Thesis

by

IMAN FARZAD

Submitted to the Office of Graduate Studies of  
Texas A&M University  
in partial fulfillment of the requirements for the degree of  
MASTER OF SCIENCE

August 2004

Major Subject: Petroleum Engineering

**EVALUATING RESERVOIR PRODUCTION STRATEGIES IN  
MISCIBLE AND IMMISCIBLE GAS-INJECTION PROJECTS**

A Thesis

by

IMAN FARZAD

Submitted to the Office of Graduate Studies of  
Texas A&M University  
in partial fulfillment of the requirements for the degree of

MASTER OF SCIENCE

Approved as to style and content by:

---

Maria A. Barrufet  
(Chair of Committee)

---

Richard A. Startzman  
(Member)

---

Philip T. Eubank  
(Member)

---

Stephen A. Holditch  
(Head of Department)

August 2004

Major Subject: Petroleum Engineering

## ABSTRACT

Evaluating Reservoir Production Strategies in Miscible and Immiscible Gas-Injection

Projects. (August 2004)

Iman Farzad, B.S., Sharif University of Technology

Chair of Advisory Committee: Dr. Maria A. Barrufet

Miscible gas injection processes could be among the most widely used enhanced oil recovery processes. Successful design and implementation of a miscible gas injection project depends upon the accurate determination of the minimum miscibility pressure (MMP) and other factors such as reservoir and fluid characterization. The MMP indicates the lowest pressure at which the displacement process becomes multicontact miscible. The experimental methods available for determining MMP are both costly and time consuming. Therefore, the use of correlations that prove to be reliable for a wide range of fluid types would likely be considered acceptable for preliminary screening studies. This work includes a comparative and critical evaluation of MMP correlations and thermodynamic models using an equation of state by PVTsim software.

Application of gas injection usually entails substantial risk because of the technological sophistication and financial requirements to initiate the project. More detailed, comprehensive reservoir engineering and project monitoring are necessary for typical miscible flood projects than for other recovery methods. This project evaluated effects of important factors such as injection pressure, vertical-to-horizontal permeability ratio, well completion, relative permeability, and permeability stratification on the recovery efficiency from the reservoir for both miscible and immiscible displacements. A three-dimensional, three-phase, Peng-Robinson equation of state (PR-EOS) compositional simulator based on the implicit-pressure explicit-saturation (IMPES) technique was used to determine the sensitivity

of miscible or immiscible oil recovery to suitable ranges of these reservoir parameters.

Most of the MMP correlations evaluated in this study have proven not to consider the effect of fluid composition properly. In most cases, EOS-based models are more conservative in predicting MMP values. If screening methods identify a reservoir as a candidate for a miscible injection project, experimental MMP measurements should be conducted for specific gas-injection purposes.

Simulation results indicated that injection pressure was a key parameter that influences oil recovery to a high degree. MMP appears to be the optimum injection pressure since the incremental oil recovery at pressures above the MMP is negligible and at pressures below the MMP recovery is substantially lower.

Stratification, injection-well completion pattern, and vertical-to-horizontal permeability ratios could also affect the recovery efficiency of the reservoir in a variety of ways discussed in this work.

## **DEDICATION**

This effort is dedicated to my parents and my sisters for their patience, understanding, and encouragement in preparing this thesis.

## **ACKNOWLEDGEMENTS**

I would like to express my sincere thanks to Dr. Maria Barrufet, chair of my advisory committee, for her guidance and support in completing and conducting this research.

I would also like to thank Dr. Richard A. Startzman and Dr. Philip T. Eubank for their help as members of my committee.

## TABLE OF CONTENTS

	Page
ABSTRACT .....	iii
DEDICATION.....	v
ACKNOWLEDGEMENTS.....	vi
TABLE OF CONTENTS .....	vii
LIST OF FIGURES .....	ix
LIST OF TABLES.....	xiv
1. INTRODUCTION .....	1
2. LITERATURE REVIEW .....	3
2.1 Phase Behavior .....	3
2.1.1 Ternary Systems .....	3
2.1.2 Pressure/Composition Diagrams .....	4
2.2 Classification of Miscible Displacement .....	5
2.2.1 First Contact Miscibility Process (FCMP) .....	5
2.2.2 Vaporizing-Gas Drive Mechanism .....	9
2.2.3 Condensing-Gas Drive Mechanism .....	11
2.2.4 Combined Condensing-Vaporizing Drive Mechanism .....	12
2.2.5 The CO <sub>2</sub> Miscible Process .....	14
2.3 Experimental Methods for Determining MMP .....	14
2.3.1 Slim-tube Experiments .....	14
2.3.2 Rising-Bubble Apparatus .....	16
2.4 Minimum Miscibility Pressure Calculations .....	17
2.4.1 Glasø Correlation.....	21
2.4.2 Firoozabadi <i>et al.</i> Correlation.....	23
2.4.3 Eakin <i>et al.</i> Correlation.....	24
2.5 Thermodynamic Method .....	26
2.6 Simulator Eclipse.....	27
3. RESULTS.....	30
3.1 Comparative Investigation of MMP Correlations .....	30

	Page
3.1.1 Reservoir Fluid Composition.....	31
3.1.2 Injection Gas Composition.....	32
3.1.3 Correlation Results .....	33
3.1.4 Comparison of Simulation and Correlation Results .....	35
3.2 Evaluation of Parameters on Miscible and Immiscible Gas Injection Projects .....	36
3.2.1 Field Description .....	37
3.2.2 Relative Permeability .....	40
3.2.3 Injection Pressure Effect.....	48
3.2.4 Vertical Permeability Effect.....	56
3.2.5 Effect of Well Completion on Recovery Efficiency .....	59
3.2.6 Stratification Effect.....	91
3.2.7 In What Condition Miscible Flooding Is a Competitive EOR Method?.....	102
4. CONCLUSIONS .....	109
NOMENCLATURE .....	111
REFERENCES .....	114
APPENDIX A.....	118
VITA.....	128



## LIST OF FIGURES

FIGURE	Page
2.1 A typical pseudocomponent ternary diagram at specified pressure and temperature .....	4
2.2 First-contact miscibility in pseudoternary diagrams (from Stalkup <sup>1</sup> ) .....	6
2.3 Phase behavior considerations for first-contact miscibility; Pressure-temperature diagram (from Stalkup <sup>1</sup> ).....	7
2.4 A typical pressure/composition diagram for a reservoir fluid .....	8
2.5 Vaporizing gas-drive miscibility .....	9
2.6 Condensing-gas drive miscibility (from Stalkup <sup>1</sup> ).....	11
2.7 Schematic diagram of the slim-tube apparatus.....	15
2.8 A typical diagram of rising bubble apparatus.....	16
3.1 Phase envelope of reservoir fluids (using PVTsim). Higher API gravities cause extension of the phase envelope toward higher temperatures.....	31
3.2 Three-dimensional grid configuration. Injection and production wells are located on the (1,1) and (9,9) coordinates of the X-Y plane .....	39
3.3 Variation in oil saturation during immiscible gas injection of the first layer (for miscible relative permeability curves).....	41
3.4 Variation in oil saturation during immiscible gas injection of the second layer (using immiscible relative permeability curve).....	42
3.5 Variation in oil saturation of the first layer (miscible $k_r$ ) .....	43
3.6 Variation in oil saturation of the second layer (miscible $k_r$ ) .....	43
3.7 Higher oil saturation for bottom layer using immiscible $k_r$ .....	44
3.8 Comparison of average gas saturation using miscible and immiscible $k_r$ ...	45
3.9 Comparison of production well gas/oil ratio using different relative permeability curves.....	45

FIGURE	Page
3.10 Pressure disturbance in the reservoir at the early days of production causes unsteady gas injection rate .....	46
3.11 Higher injection rates (using miscible $k_r$ ) cause greater average reservoir pressure in this displacement.....	46
3.12 Comparison of cumulative oil production for two relative permeabilities.....	47
3.13 Significant incremental oil recovery using miscible $k_r$ .....	48
3.14 Variation in oil saturation of grids (5,5,1) and (5,5,2).....	50
3.15 Higher pressure gradient along the diagonal streamlines located on the shortest distance between wells makes sweep efficiency of this region higher.....	51
3.16 Saturation profiles at 4,400 psi ( $p < \text{MMP}$ ).....	51
3.17 Saturation profiles at $\text{MMP}=5,000$ .....	52
3.18 Saturation profiles at 5,600 psi ( $p > \text{MMP}$ ).....	53
3.19 Variation in oil saturation during gas injection at different injection pressures .....	54
3.20 Incremental oil recovery after around 4 pore volume of injected gas is marginal at pressures above MMP .....	55
3.21 Cumulative oil production at above MMP and below the MMP injection pressure .....	55
3.22 Oil saturation profile of grids (5,5,1) and (5,5,2) for vertical permeability of 0.009 and different injection pressures .....	56
3.23 Lower vertical permeability ( $k_v=0.009$ md) decreases the average reservoir pressure 200 psi greater than that of reservoir with $k_v=9$ md .....	58
3.24 Different completion patterns.....	59
3.25 Significant increase in miscible oil recovery in case a completion pattern compared to immiscible displacement .....	63
3.26 Oil and gas saturation profiles of grids (5,5,1) & (5,5,2) .....	64

FIGURE	Page
3.27 Oil saturation profiles at 4,400 psi (case a: injection to the first and production from the second layers) .....	65
3.28 Oil saturation profiles at 4,400 psi (case b: injection and production from the second layers).....	66
3.29 Oil saturation profiles at 5,600 psi (case a: injection to the first and production from the second layers) .....	67
3.30 Oil saturation profiles at 5,600 psi (case b: injection and production from the second layers). Invaded gas into the second layer (rows three and four) sweeps this layer at earlier times .....	68
3.31 Effect of well completion on average reservoir pressure .....	70
3.32 pressure distribution at 4,400 psi (case a: injection to the first and production from the second layers) .....	71
3.33 pressure distribution at 4,400 psi (case b: injection and production from the second layers).....	72
3.34 pressure distribution at 5,600 psi (case a: injection to the first and production from the second layers).....	73
3.35 pressure distribution at 5,600 psi (case b: injection and production from the second layers).....	74
3.36 Variation in reservoir pressure during gas injection.....	75
3.37 Fluid accumulation (Reservoir volume difference in total injected and produced fluids) during injection of gas at 4,400 psi at completion case b .....	77
3.38 Typical relative permeability curve .....	78
3.39 Variation in gas viscosity of the first and second layers at 4,400 .....	79
3.40 Variation in gas viscosity during gas injection at 5,600 psi .....	81
3.41 Higher degree of miscibility in the first layer where the injection well is completed .....	82

FIGURE	Page
3.42 Variation in gas viscosity at 4,400 psi (case a: injection to the first and production from the second layers).....	82
3.43 Variation in gas viscosity at 4,400 psi (case b: injection and production from the second layers) .....	83
3.44 Variation in gas viscosity at 5,600 psi (case a: injection to the first and production from the second layers).....	84
3.45 Variation in gas viscosity at 5,600 psi (case b: injection and production from the second layers) .....	85
3.46 Oil viscosity profile at 4,400 psi ( case a) .....	87
3.47 Variation in oil viscosity during miscible gas injection (case a, 5,600 psi) .....	88
3.48 Oil viscosity profile during immiscible gas injection (case a, 4,400 psi) .....	89
3.49 Oil viscosity profile during miscible gas injection (case a, 5,600 psi).....	90
3.50 Estimated oil recovery at injection pressure of 4,400 psi.....	93
3.51 Estimated oil recovery at Minimum miscibility pressure of 5000 psi.....	93
3.52 Estimated oil recovery at injection pressure of 5600 psi.....	94
3.53 Comparison of GOR at immiscible and miscible gas flooding .....	95
3.54 Gas production rate of the individual layers at 5,000 psi .....	96
3.55 Oil production rate of the individual layers at 5,000 psi .....	96
3.56 Dependence of miscibility to pressure.....	97
3.57 Oil saturation profile at injection pressure of 4,400 psi (x-z cross-section view, $k_1 > k_2$ ) .....	98
3.58 Oil saturation profile at injection pressure of 4,400 psi (x-z cross-section view, $k_2 > k_1$ ) .....	99
3.59 Oil saturation profile at injection pressure of 5,000 psi (x-z cross-section view, $k_1 > k_2$ ).....	100

FIGURE	Page
3.60 Oil saturation profile at injection pressure of 5,000 psi ( x-z cross-section view, $k_2 > k_1$ ).....	101
3.61 High mobility ratio in gas injection project decreases the oil recovery from the reservoir .....	106
3.62 Absence of unfavorable mobility ratio in miscible flooding improves the oil recovery to a high degree.....	107
3.63 Comparison of GOR for two displacement mechanisms .....	107
3.64 Comparison of tracer concentration in gas and water injection projects.....	108

## LIST OF TABLES

TABLE	Page
2.1	Constant Parameters of Reduced temperature equation .....26
3.1	Reservoir oil compositions (reported by Core Laboratories, INC.) .....30
3.2	Bubble point pressures of the reservoir fluids .....31
3.3	Injection gas composition (mole %) for oil A .....32
3.4	Injection gas composition (mole %) for oil B .....33
3.5	Predicted MMP using Eakin <i>et al.</i> correlation. This correlation accounts for effect of CO <sub>2</sub> in decreasing miscibility pressure .....34
3.6	Predicted MMPs by Firoozabadi <i>et al.</i> correlation. This correlation like majority of lean gas MMP correlations ignores the effect of injection gas composition.....34
3.7	Predicted MMP using Glasø correlation. This correlation predicts unreliable MMPs for oil A (order of plots from top to bottom: A2, A1 order instead of A1, A2) and very low values for injection gas B2 .....35
3.8	Comparison of simulation and correlation results for fluid B/injection gas B1 system.....36
3.9	Reservoir grid data and water properties .....38
3.10	Gas relative permeability data.....39
3.11	Three phase saturation data .....39
3.12	Reservoir fluid and injection gas composition.....40
3.13	Comparison of oil saturation profiles for different $k_v / k_h$ ratio .....57
3.14	Effect of $k_v / k_h$ ratio on calculated oil recovery.....58
3.15	Performance of the homogeneous reservoir at 1.2 pore volume of injection .....61
3.16	Heterogeneous-reservoir performance at 1.2 pore volume (22,700 MMscf) of miscible or immiscible injection gas.....62

TABLE	Page
3.17 Comparison of oil recovery and GOR at 1.2 pore volume of injected gas.....	92
3.18 Reservoir properties .....	104
3.19 Reservoir fluid and injection gas compositions .....	105

## 1. INTRODUCTION

Through the past decades, miscible displacement processes have been developed as a successful oil recovery method in many reservoirs. The successful design and employment of a gas injection project is dependent on the favorable fluid and rock properties. The case studies using Eclipse compositional simulator considered the effect of key parameters, such as relative permeability, injection pressure, well completion, stratification, and mobility ratio, on the performance recovery in miscible and immiscible flooding of the reservoir. However, accurate estimation of the minimum miscibility pressure is important in conducting numerous simulation runs. MMP is the minimum miscibility pressure which defines whether the displacement mechanism in the reservoir is miscible or immiscible. Thermodynamic models using an equation of state and appropriate MMP correlations were used in determining the reliable MMP.

Numerous compositional simulation runs determined the sensitivity of the oil recovery to the variations in above mentioned parameters.

Significant increase in oil recovery was observed when miscible relative permeability curve was used. Miscible relative permeability curve which is an additional accounting for miscibility in Eclipse compositional simulator is the weighted average between fully miscible and immiscible relative permeability curves. Miscible relative permeability is dependent on the surface tension value between the displacing and displaced fluid. Surface tension determines the interpolation factor which is used in obtaining a weighted average of immiscible (entered saturation data curves) and miscible (straight line) relative permeabilities.

Simulation runs performed at pressures below, equal to, and greater than estimated MMP for particular reservoir fluid/ injection gas system. Oil recovery was greatest when miscibility achieved.



Well completion pattern was found as one of the important parameters which influence the recovery from the homogeneous or heterogeneous reservoir miscible and immiscible displacement mechanisms. Higher oil recovery was predicted when the injection well is perforated on the first layer.

To investigate the effect of stratification on the performance recovery of the reservoir, the base relative permeability of two layers changed. Location of the permeable layer (up or bottom layer) in the stratified reservoir greatly influenced the efficiency of the reservoir.

Understanding the effect of interfacial tension and adverse mobility ratio on the efficiency of the gas injection project was the last case study. Injection gas compositions differed in such a way to have interfacial tension and mobility dominated mechanism. The base quarter five-spot model increased twice in x and y dimensions to represent the gravity effect in displacement. To investigate the effect of interfacial tension water was considered as a fluid with much higher surface tension values with the oil. Lower surface tension values between rich gas and reservoir fluid (interfacial tension dominated) made gas injection project the competitive recovery method compare with waterflooding. In mobility dominated displacement mechanism (lean gas/reservoir fluid system) the viscous instabilities were more important than the interfacial tension effect. For this case waterflooding with favorable mobility ratio resulted in higher oil recoveries.

## 2. LITERATURE REVIEW

This chapter is a review and study of basic principles that are general to miscible displacement processes.

### 2.1 Phase Behavior

#### 2.1.1 Ternary Systems

A useful method for representing the phase behavior of multicomponent hydrocarbon mixtures is using a pseudoternary diagram. Such a diagram is shown in **Fig. 2.1**. The components of the reservoir fluid are grouped into three pseudocomponents located on the corners of the ternary plot. The reservoir fluid components are usually classified into the following three groups: a volatile pseudocomponent composed of methane and nitrogen located on the uppermost of the triangle, an intermediate pseudocomponent composed of intermediate hydrocarbon components such as ethane through hexane located on the lower right corner of the plot, and a relatively heavy fraction of the petroleum fluid such as  $C_{7+}$ . Each corner of the triangular plot represents 100% of a given component. Binary mixtures are located on the sides of the ternary diagram, and three component mixtures are located inside the triangle.

Ternary diagrams indicate all possible equilibrium compositions for three pseudocomponent systems at a fixed temperature and pressure. Fig. 2.1 shows the mixture with overall composition  $z$  located on the two phase region. An equilibrium liquid phase with composition  $x$  and an equilibrium gas phase with composition  $y$ , form the fluid with composition  $z$ . The dashed lines connecting the equilibrium liquid and gas phases are called tie lines. The bubble point curve joins the dew point curve at the critical or plait point.

This is the point where composition and properties of the liquid and gas phases become identical. At the particular pressure and temperature, any system whose composition is inside the phase boundary curve form two phases. Any system with composition outside that boundary will form a single phase. Single phase liquid

region is below the bubble point curve, while the single phase gas region exists above the dew point curve.

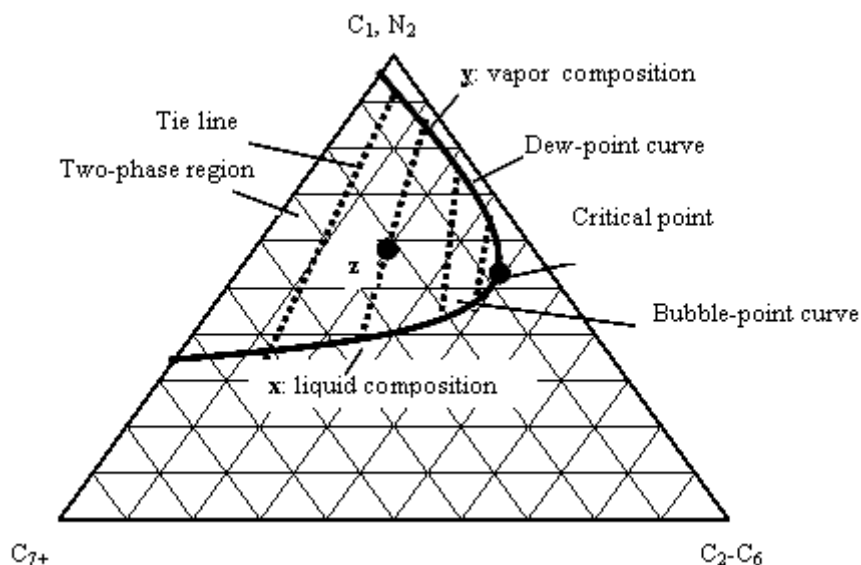


Fig. 2.1— A typical pseudocomponent ternary diagram at specified pressure and temperature

The extent of the two phase region depends upon the pressure and temperature. For a constant temperature, the size of the two phase region increases as pressure decreases. An increase in temperature increases the size of the two phase region for a fixed pressure.

### 2.1.2 Pressure/composition Diagrams

Pressure/composition (P-X) diagram is a useful method for displacing phase behavior for mixture of fluids. Pressure/composition diagrams for reservoir fluids are obtained by adding injection fluid into the reservoir oil and measuring the saturation pressure of the resultant mixture. Initially, as injection gas is added, mixtures will have bubble points at the saturation pressure but as concentration of the injection gas in the mixture increases, the mixtures formed will exhibit dewpoints. Single-phase mixture exists at pressures above the bubblepoint or dewpoint curves. The highest pressure at which two phases coexist in equilibrium is called the cricondenbar. As will state later, this pressure is equal to first contact miscibility pressure (FCMP).

Since the pressure/composition diagram is obtained by batch contacting of injection gas and reservoir fluid, it does not contain information about all the mixtures that might be of interest in a miscible displacement.

## **2.2 Classification of Miscible Displacements**

Miscible displacement processes in the oil reservoirs are usually divided into two classes:

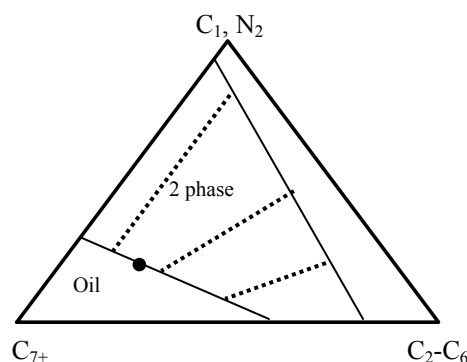
1. First contact miscible processes: Displacements in which the injection fluid and the in-situ reservoir fluid form a single phase mixture for all mixing proportions.
2. Multi-contact miscible processes: Processes in which the injected fluid and the reservoir oil are not miscible in the first contact but miscibility could develop after multiple contacts (dynamic miscibility). These processes are categorized into vaporizing, condensing, and combined vaporizing-condensing drive mechanisms.

### **2.2.1 First Contact Miscible Process**

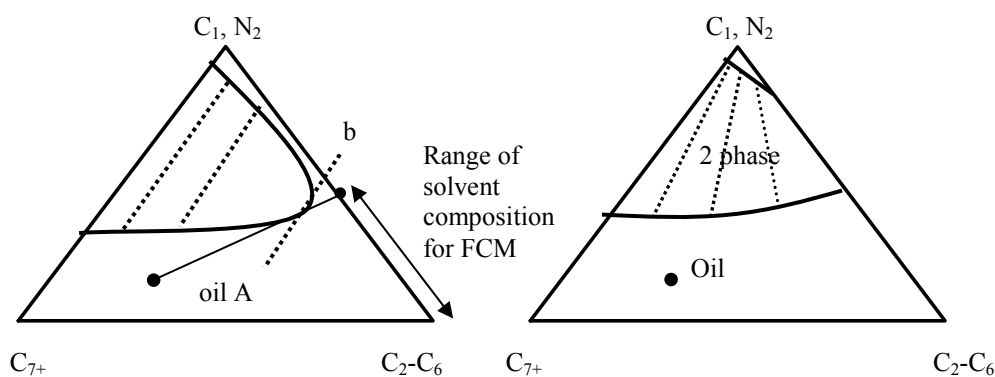
For petroleum reservoirs, miscibility is defined as the ability of two or more fluids (liquid or gas) to form a single homogeneous phase without the existence of an interface when mixed in all proportions. If two phases form after some proportion of one fluid is added, the fluids are considered immiscible. Liquefiable petroleum gas (LPG) or low molecular weight hydrocarbons such as ethane, propane, and butane are the frequent solvents that have been used for first-contact miscible flooding. These solvents will form a single phase upon the first contact with the reservoir oil in all proportion.

In practice, LPG solvents that are first-contact miscible with reservoir fluids are too expensive to be injected continuously into the reservoir. Instead the solvent, or slug, is injected in a limited volume, and the slug, is miscibly displaced with a less expensive fluid such as natural gas, or flue gas. The basic requirement for slug injection is that the solvent slug must be miscible with both the reservoir oil and the drive gas, which is mostly methane. **Fig. 2.2** illustrates the phase behavior requirements for first contact miscibility at both the leading and trailing edges of an LPG slug. Drive gas and LPG solvent on this pseudoternary diagram are represented

by the  $C_1$ ,  $N_2$ , and  $C_2$ - $C_6$  pseudocomponents. For achieving first-contact miscibility between LPG and reservoir oil, the straight line connecting reservoir oil composition



a) Solvent-drive gas miscibility; solvent oil immiscibility ( $P_1$ ,  $T_1$ )



b) Solvent-drive gas and solvent-oil miscibility ( $P_2 > P_1$ ,  $T_1$ )

c) Solvent-oil miscibility; solvent-drive gas immiscibility ( $P_2$ ,  $T_2 > T_1$ )

Fig. 2.2—First-contact miscibility in pseudoternary diagrams (from Stalkup<sup>1</sup>)

and LPG must not pass through the multiphase region. This is not the case in Fig. 2.2a. Fig. 2.2.b represents the situation that LPG can be diluted with methane up to the limiting composition a. This maximum permissible methane concentration in the slug at a given pressure decreases with increasing temperature because the size of two-phase region increases. Conversely, the pressure required to achieve first-contact

miscibility with a given mixture of LPG and light components increases with increasing reservoir temperature.

Pressure/temperature diagram is also a useful tool for studying the miscibility relationships between injection gas and solvent. Such a diagram is shown in **Fig. 2.3**. This figure shows how the cricondenbars for oil/solvent and drive gas/solvent might vary with temperature. At temperature  $T_1$ , pressure  $P_1$  is below the solvent vapor pressure and falls within the two-phase region for solvent/oil mixture. This condition also is depicted by Fig. 2.2a. Pressure  $P_2$  is above the vapor pressure of the solvent but lies within the two-phase region for solvent/drive gas. This situation is depicted by Fig. 2.2.c. Pressure  $P_3$  is the pressure at which all drive gas/solvent mixture and also oil/solvent mixtures are single phases (Fig. 2.2.b).

In terms of ternary diagrams, the gas composition located on the critical tie line passing through the oil composition is the leanest composition that can provide FCM with the oil at the specified pressure and temperature of the ternary system. The pressure of the ternary system is the FCMP corresponding to that composition.

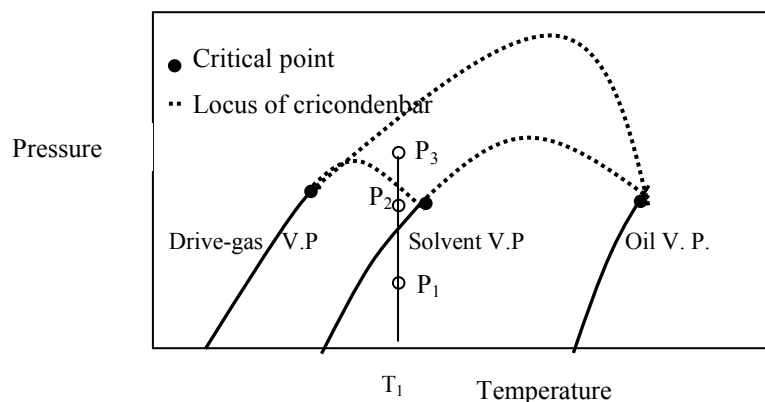


**Fig. 2.3—Phase behavior considerations for first-contact miscibility; Pressure-temperature diagram (from Stalkup<sup>1</sup>)**

FCMP is an important property which indicates the upper limit for multi contact miscibility pressure (MCMP).

FCMP can also be obtained by locating the maximum saturation pressure (cricondenbar pressure) on the p-x diagram which corresponds to the results of the swelling test. The displacement pressure must be above the cricondenbar pressure of

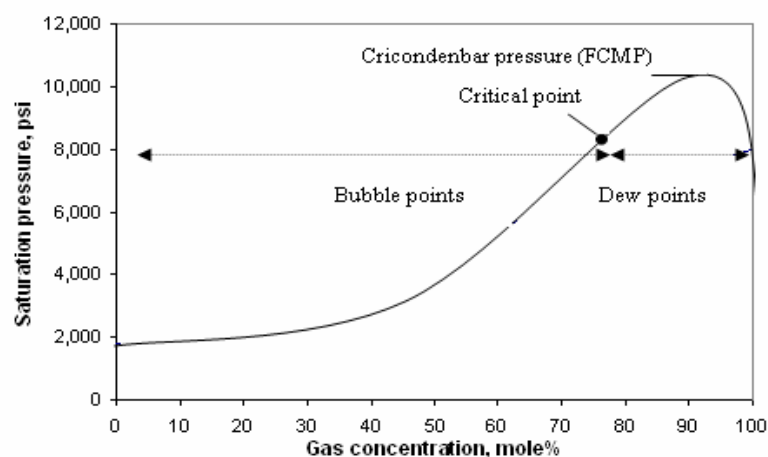


**Fig. 2.4— A typical pressure/composition diagram for a reservoir fluid**

all the possible mixtures of reservoir fluid and the injected solvent at the reservoir temperature, to ascertain the formation of single phase in the reservoir.

**Fig. 2.4** indicates the variation in saturation pressure of the mixture with the injection gas for a fixed temperature. The saturation point of the reservoir oil is the point on the p-x diagram where the gas concentration is zero. The incremental increase of the injection gas results in the critical point where mixture behaves gas like with further injection. The dew point of this reservoir fluid initially increases then decreases with addition of the gas. For this oil/solvent combination, first contact miscibility (maximum saturation pressure) occurs after 92% of the injected gas and is equal to 10,700 psi. It is clearly seen that for this fluid the cricondenbar pressure is impractically high for first contact miscibility. When this happens, dynamic miscibility can be achieved by vaporizing, condensing or combined drive displacement mechanisms. The composition at FCMP, which is the result of the mixing of reservoir oil with the injection gas at the cricondenbar pressure, can be calculated as follows:





which the vaporizing-gas drive miscibility is achieved by injecting lean hydrocarbon gas  $G$ , into the reservoir fluid  $B$ . Reservoir oil  $B$  is located on the right side of the extension of the critical tie line passing through the plait point. Since the injection gas and reservoir fluid are not miscible in the first contact, the injection gas initially displaces oil immiscibly but leaves some oil behind the gas front and creates a mixture with overall composition  $M_1$ . The tie line passing through point  $M_1$  shows the equilibrium liquid  $L_1$ , and vapor phase  $G_1$  at this point in the reservoir. Subsequent injection of lean gas into the reservoir pushes the gas  $G_1$ , left after the first contact, further into the reservoir, where it contacts fresh reservoir oil and a new overall composition,  $M_2$ , is reached with corresponding equilibrium gas and liquid,  $G_2$  and  $L_2$ . Further contacts of injection gas with fresh reservoir oil, cause the composition of the injection gas at the displacing front to alter progressively along the dew point curve until it reaches the plait-point composition. The plait-point fluid is directly miscible with the reservoir fluid  $B$ <sup>1</sup>.

The reservoir oil composition must lie on or to the right of limiting tie line for miscibility to be attained by the vaporizing-gas drive mechanism with natural gas that has a composition lying to the left of the limiting tie line. This implies that only oils that are undersaturated in methane can be miscibly displaced by methane or natural gas. Miscibility pressure with lean hydrocarbon gas decreases with decreasing concentration of methane and nitrogen in the oil. If the oil composition lies to the left of the limiting tie line, gas enriches only to the point on the dew point curve lying on the tie line that can be extended to pass through the oil composition. For example, the injected gas into the reservoir oil  $A$  would be enriched to the composition of equilibrium gas  $G_2$  (Fig. 2.5).

Continuous injection of the miscible solvent without ever switching to a drive gas is an important characteristic of vaporizing-drive mechanism. This may be the main reason for the relative success of vaporizing-drive floods<sup>1</sup>. The high pressure gas itself serves as both solvent and drive gas, and miscibility can not be lost unless pressure at the gas front falls below miscibility pressure. Lower overall mobility ratio

compared with first-contact miscible and condensing-drive floods could also contribute to the relative success of these displacement mechanisms. Because higher API gravity and lower-viscosity oil are generally displaced in vaporizing-gas drive projects rather than the other hydrocarbon projects. On average more favorable viscosity ratio is observed in these miscible projects.

### 2.2.3 Condensing-Gas Drive Mechanism

In this process, injection gas containing low molecular weight hydrocarbon components ( $C_2$ - $C_6$ ), condenses in the oil to generate a critical mixture at the displacing front.

Several laboratory experiments by Kehn<sup>2</sup> *et al.* were conducted with a wide composition range of injection gases and reservoir fluids, at displacement pressures equal to, greater than, or less than saturation pressure of the displaced fluid. In most of these experiments, high oil recoveries were obtained regardless of whether the oil was initially saturated or unsaturated with injected gas at displacement pressure.

**Fig. 2.6** illustrates the phase relation in condensing-gas drive process. Gas composition B is defined by extending the limiting tie line through the through the plait point, P, until it intersects the right side of the triangle. Injection gases with composition ranges between points A and B have the capability to displace the reservoir oil miscibly. The multiple-contacting or enriched-gas mechanism creates a

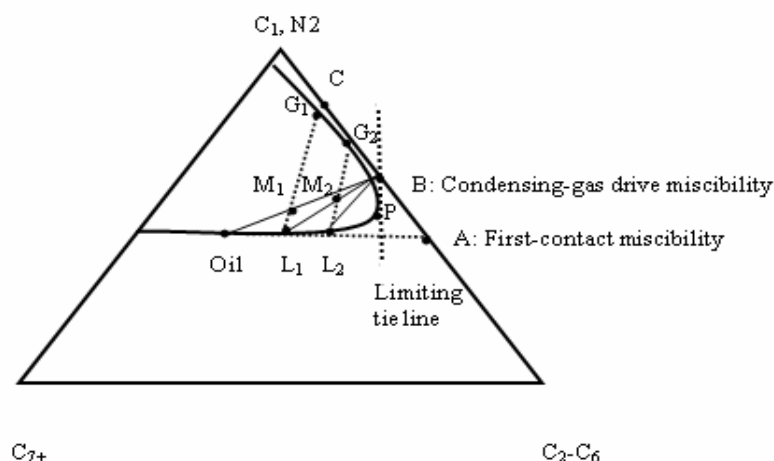


**Fig. 2.6—Condensing-gas drive miscibility(from Stalkup<sup>1</sup>)**

transition zone of continuously miscible liquid compositions varying from original reservoir oil through compositions  $L_1$ ,  $L_2$ ,  $L_3$ ,  $P$  on the bubble-point composition to injected gas composition. At the same time, multiple contacts of the reservoir fluid and injected gas develop a transition zone of gas compositions from  $G_1$  to  $P$  along the dew-point curve.

If an extended tie line passes through the injected gas composition, an immiscible displacement will result. For example, gas composition  $C$  lies on the extension of the tie line  $G_1 L_1$ . Enrichment of the oil to composition  $L_1$  would occur if gas  $C$  were the injected gas. Further contacts would always result in  $L_1$  and  $V_1$  as the equilibrium gas and liquid.

It should be noted that the simplification of a flowing gas phase contacting a nonflowing oil phase in a batch contact manner, is not accurate but it fairly describes<sup>3</sup> the compositional part of the mechanism.

#### **2.2.4 Combined Condensing-vaporizing Drive Mechanism**

There is<sup>4,5</sup> evidence for some reservoir fluids that phase behavior in condensing- gas drives departs substantially from traditional three-component fluid concepts. Experimental observations and equation-of-state analysis indicate existence of combined condensing/vaporizing drive mechanism rather than condensing-drive mechanism in the reservoir.

The easiest method for understanding the condensing-vaporizing drive mechanism is based on four-component<sup>4</sup> group model for gas-oil systems. Lean components, and light intermediate components such as ethane, propane and butane present in the injection gas, are categorized in the first and second groups. The third group contains the middle intermediates that can be vaporized from the oil. The lightest component in this model ranges from butane to decane, depending on the injection gas composition. The fourth group components are those of  $C_{30+}$  fraction of the oil which are difficult to vaporize.

When the enriched gas contacts the reservoir fluid, the light intermediates of the gas condense into the oil and middle intermediates are being stripped from the oil

into the gas. The oil continues to lose the middle intermediates and become saturated with the light intermediates with a few contacts between the injection gas and the oil. The light intermediates of the injection gas can not substitute for the middle intermediates the oil is using. This net condensation of intermediates makes the oil to become lighter. Subsequent contacts of oil and injection gas makes the oil heavier by net vaporization of the intermediates.

Significant residual oil would remain undisplaced if mechanism stopped at this stage. However, there are further steps to be followed in this mechanism. The first gas comes into contact with the reservoir fluid slightly downstream from the injection point, will be the injection gas that has lost most of its light intermediates and took up small portion of middle intermediates from the upstream oil. There will be reduced mass transfer between this gas and fresh oil. The gas that follows will be richer since it has passed over the oil that was saturated with light intermediates. This gas contains the same amount of light intermediates as the injection gas but it carries part of the middle intermediates of the oil over which it passed. The downstream oil which contact this gas, will receive slightly more condensable intermediates and become lighter than the upstream oil before oil vaporization takes place.

The process mechanism switches to kind of vaporizing drive mechanism in the farther downstream. However, there is an important difference with vaporizing-drive mechanism<sup>4</sup>. The original oil does not need to be rich or undersaturated in intermediates, both of which are basic conditions for developing vaporizing-drive miscibility. Instead, the gas develops only enough richness by the oil vaporization so that it nearly generates a condensing-drive mechanism. Then, condensation develops like the mechanism occurring in condensing-drive mechanism.

A sharp near-miscible transition zone develops before the condensation process switches to the vaporizing mechanism. Upstream of this transition zone is vaporizing region and the condensing region is the leading edge of this region. The near-miscible fluid is richer in middle intermediates. Those components were vaporized from the residual saturation upstream and recondensed in the transition

zone. The development and propagation of two-phase transition zone results in a very efficient displacement even though miscibility is not actually developed. The sharpness of the transition zone deteriorates as either the pressure or enrichment of the injection gas falls below some critical value.

### **2.2.5 The CO<sub>2</sub> Miscible Process**

Displacement experiments<sup>6-10</sup> indicate possibility of dynamic miscibility at pressures above the MMP. The major advantage of CO<sub>2</sub> flooding is the attainable MMP pressure in large spectrum of reservoirs. CO<sub>2</sub> achieves dynamic miscibility at lower pressures compare with lean hydrocarbon gases by extracting hydrocarbons from gasoline and gas/oil fractions of the crude<sup>6,9</sup> as well as intermediate molecular weight hydrocarbons such as C<sub>5</sub> through C<sub>30</sub><sup>6,9</sup>.

The complicated phase behavior of CO<sub>2</sub> and reservoir fluid, and the transition-zone compositions over which dynamic miscibility occurs could rarely be represented in simplified ternary diagrams.

## **2.3 Experimental Methods For Determining MMP**

### **2.3.1 Slim-tube Experiments**

The first slim-tube apparatus was recommended by Yellig and Metcalfe<sup>8</sup> for measuring minimum miscibility pressure. The slim-tube is illustrated schematically in **Fig. 2.7**. This apparatus consists of a 40-ft-long, 1/4-inch diameter coiled stainless steel tube packed with 160 to 200-mesh Ottawa sand. The sandpack is initially saturated with oil at desired temperature and pressure before the solvent is injected into the sandpack with a positive displacement pump. The slim-tube, back-pressure regulator, sightglass, injection cell and differential pressure transducer are all contained in a constant-temperature air bath.

The breakover point in the oil recovery curve versus a series of displacement pressures is recommended as a criterion to determine the pressure or fluid compositions where dynamic miscibility occurs. In this experiment, as the pressure is increased, the recovery increases dramatically, till it reaches the point of

discontinuity. For high pressures much above that discontinuity, there is small incremental advantage from recovery perspective.

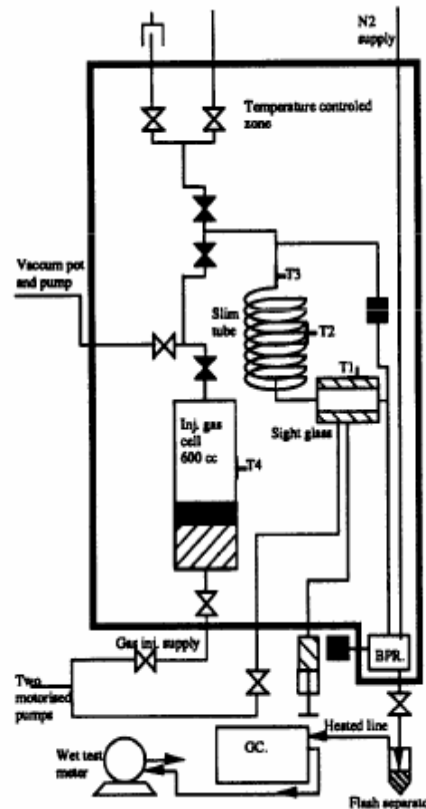


Fig. 2.7—Schematic diagram of the slim-tube apparatus<sup>10</sup>

Oil recovery is determined by direct measurement of produced oil and solvent extraction of the sandpack after 1.2 pore volume of solvent injection. Yellig and Metcalfe<sup>11</sup> reported that level of oil recovery and sharpness of the break in the recovery curve depends on the temperature, oil and injection gas composition, slim-tube dimension and operating conditions.

An ideal tube should provide a one dimensional dispersion free displacement of oil by injection gas. This is not accordant with conditions in a real reservoir. It is merely a well controlled experiment, with valuable results for simulating

compositional changes resulting from continuous contacts between the reservoir fluid and injection gas. In this experiment, flow effects such as viscous fingering, gravity override, dispersion, heterogeneity, etc. are kept at a minimum. The flow in a slim-tube is described by relative permeability which depends on fluid saturation and interfacial tension (IFT) between phases.

In spite of increasing knowledge and investigation<sup>11-12</sup> concerning the validity of slim-tube results, the slim-tube technique may not be as trustworthy as it was once thought to be. Dependence<sup>13</sup> of relative permeability data to the interfacial tension ratio suggests that the response of a slim tube is dominated by IFT effects, and there is very little influence of viscosity ratio in the slim tube.

### 2.3.2 Rising Bubble Apparatus

Rising bubble apparatus (RBA), first proposed by Christiansen and Kim<sup>14</sup> was an alternative and much quicker apparatus in determining MMP.

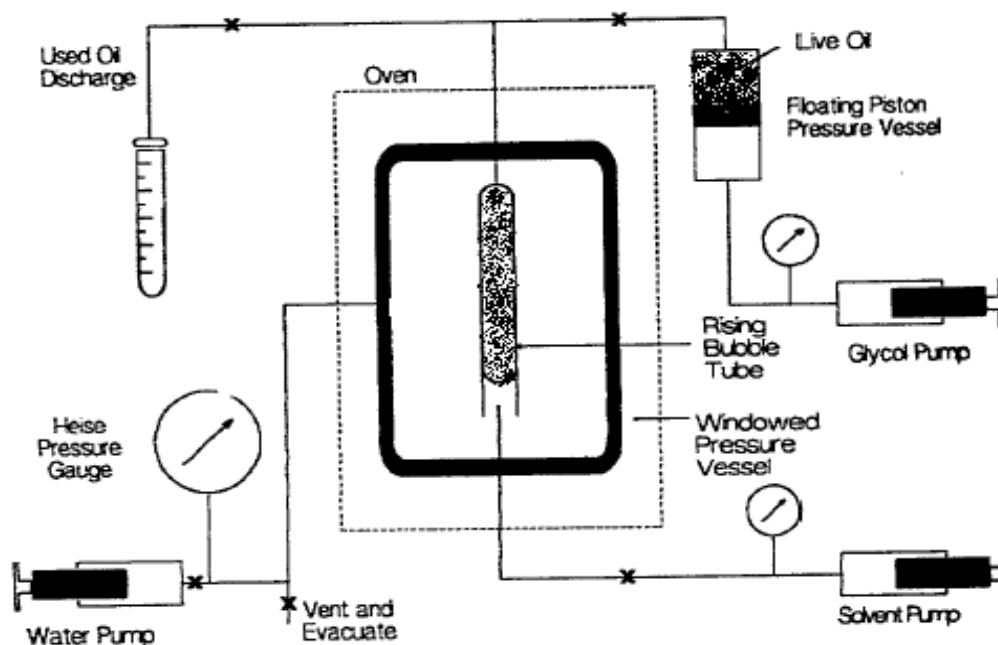


Fig. 2.8— A typical diagram of rising bubble apparatus<sup>15</sup>

**Fig. 2.8** shows a typical diagram of the RBA. Oil is confined in a slim glass tube inside a double-windowed pressure vessel. A solvent-gas bubble is released into the water inside the tube below the oil. This bubble rises through the water-oil interface into the oil. The solvent bubble continually contacts the oil through its upward movement which results either in reaching equilibrium with the original oil, or achieving miscibility depending on the operating pressure. This method is suitable only for the vaporizing-gas drive mechanism, where the enrichment of the advanced gas creates the miscible fluid. A series of experiments are conducted at different pressures, and the bubble shape is monitored as it rises through the oil column.

The bubble will exhibit three distinctive behaviors dependent on how close the pressure is to the MMP value. At pressures lower than MMP the bubble rises through the oil column. As pressure increased to values close to the MMP, the new bubble released into the water is too large to become stable in the oil. Since at pressures close to MMP the interfacial tension between the solvent and oil becomes very low, the large bubble at some point in the oil column breaks into smaller bubbles. The larger bubble of these new formed smaller bubbles dissolve into the oil and the smallest bubbles rise on through the oil.

At pressures equal to, or above the MMP, the solvent bubble rises through the water-oil contact and immediately bursts into several smaller bubbles. These smaller bubbles progress a short distance higher and no tiny bubbles continue upward in the oil.

For reservoir fluids, the MMP measured by RBA appears to be higher<sup>15</sup> and more conservative than measured MMP by slim tube for the same system. The distinct change in bubble behavior observed for a small change in pressure indicates a rapid decrease in interfacial tension. Such changes only occur in the vicinity of the critical point or when first contact miscibility may be achieved.

## **2.4 Minimum Miscibility Pressure Correlations**

Multiple contact miscible floods have proven to be one of the most effective enhanced oil recovery methods currently available. The available



displacement experimental procedures for determining the optimal flood pressure, defined as the minimum miscibility pressure, are both costly and time consuming. Therefore, use of reliable correlations that were developed from reliable experimental data would be of great interest. The results of these correlations however would only be for the preliminary screening studies that would be conducted over a wide range of conditions.

The earliest attempt for estimation of MMPs is based on Benham<sup>16</sup> investigation. He indicated that a pseudo-ternary representation of reservoir fluids could be used to illustrate the mechanism for obtaining miscibility conditions. Based on his assumption, he proposed a method for determining the composition requirement of the injection gas. The derived MMP correlation was based on mixture critical properties using a modified Kurata-Katz<sup>17</sup> method.

Metcalfe<sup>18</sup> *et al.* continued the work of Cook<sup>19</sup> *et al.* which was the study of gas cycling rather than miscibility condition. A series of constant pressure and temperature cells were used to simulate the flow of fluid into the reservoir. It was assumed that vapor and liquid of each cell are in equilibrium contacts. In the first cell gas is mixed with the liquid and flashed. The excess volume of liquid and vapor is transferred to the next cell. In his experiment MMP is defined as the pressure which causes formation of near critical composition of the fluids.

Using the Peng-Robinson equation of state, Kue<sup>20</sup> developed a correlation for condensing drive mechanisms which was applicable for wider range of temperature, pressure and fluid compositions. In his approach, at a specified pressure and temperature injection gas is mixed with the reservoir fluid and flash calculation is performed on two phase mixture. The flashed liquid is mixed with the injection gas and flashed calculation is repeated till the liquid fraction composition and the vapor composition are the same. This point is indicative of the plait point and the pressure of the performed flash calculations is the MMP. Kue's correlation showed better results compared to Benham correlation.

Similar to Kue's method, Turek<sup>21</sup> *et al.* proposed a new algorithm for calculating MMP of condensing and vaporizing mechanisms. Their method is based on forward and backward contact experiments of the single mixing cell.

In Flock<sup>22</sup> *et al.* approach MMP was defined as the pressure at which the injection gas composition for condensing drive, and the oil composition for the vaporizing drive, was intersected with the critical tie line (the tie line passing through plait point)

Later investigations by Zick<sup>4</sup> and Stalkup<sup>5</sup> indicated the possibility of the combined vaporizing-condensing mechanism drives in the reservoir. They demonstrated that MMP is predictable by conducting compositional simulation but sufficient care should be taken to account for numerical dispersion. Shelton and Yalborough<sup>23</sup> also showed some multi contact experiments which seem to have exhibited the combined mechanism.

Jensen and Michelson<sup>24</sup> illustrated that the calculated MMP from extension of critical tie line, may exceed the FCMP. They concluded that the extended tie line criterion is not adequate in predicting MMPs. Instead, they proposed a single cell technique to simulate miscibility process.

Later studies by several authors investigated the reliability of single cell and critical tie line methods by the analytical solution of one-dimensional flow.

In 1990 Monroe<sup>25</sup> established existence of the third critical tie line, named as "cross-over tie line", which influences miscibility process.

Johns<sup>26</sup> *et al.* presented analytical solution for dispersion-free, one dimensional flow of four component hydrocarbon system and confirmed the existence of combined vaporizing-condensing drive mechanism. In their study they stated that cross-over tie line is responsible in this kind of drive mechanism.

The work of John and Orr<sup>27</sup> extended the four-component displacement theory in single component gas injection of multi component reservoir fluid. Wang and Orr<sup>28</sup> extended the work of John<sup>29</sup> *et al.* for displacement of oil with arbitrary

number of gas components. In their method the Analytical solution for calculating MMPs relies on the solution of the tie line intersection equations.

In this study a review of the literature of several MMP correlations of vaporizing gas drive (VGD) and condensing gas drive (CGD) mechanisms is investigated. An early correlation was presented by Benham<sup>16</sup> *et al.* where the required gas enrichment for condensing drive mechanism was correlated as a function of temperature, pressure, gas intermediate and heavy fractions of the oil molecular weights.

Glasø<sup>31</sup> proposed a correlation which was the extension of Benham<sup>16</sup> *et al.* study, and gives the MMP for VGD, CGD, CO<sub>2</sub>, and N<sub>2</sub> systems. The input parameters for this correlation are temperature, Mole percent of the methane in the injection gas, Molecular weight of C<sub>2</sub>-C<sub>6</sub> intermediates in the injection gas and the molecular weight of heptane- plus fraction of the oil. A new parameter called, paraffinicity characterization factor (k), was defined to account for oil composition effect on MMP.

In 1985 Kue<sup>20</sup> presented a Peng-Robinson equation of state based equation which simulated the backward multiple contact experiment for predicting MMPs of rich gas systems. A comparative study by Yurkiv<sup>32</sup> *et al.* demonstrated the reliability of this correlation compared with those of Glasø<sup>31</sup> and Benham<sup>16</sup> *et al.* but as stated before<sup>24</sup> the accuracy of these three correlations based on injection gas key tie line is suspicious.

A correlation developed by Sebastian<sup>33</sup> *et al.* gives the MMP for CO<sub>2</sub>-rich gas injection. This study takes into account the effects of impurities (up to 55% mole percent) in the injection gas. The new correlating parameter of this correlation is the pseudocritical molar average temperature of the injection gas. Alston<sup>34</sup> *et al.* had investigated the effect of CO<sub>2</sub> impurities on MMP with a similar correlation with weight average critical temperature as a correlating parameter.

In 1986 Firoozabadi and Aziz<sup>35</sup> modeled the VGD with the Peng-Robinson equation of state and a compositional simulator. They proposed a simple correlation

for the estimation of MMP of Nitrogen and lean-gas systems. The MMP was correlated as a function of molecular weights of heavy fractions of the oil, temperature and the molar concentration of intermediates in the oil.

Eakin and Mitch<sup>36</sup> produced a general equation using 102 rising bubble apparatus (RBA) experiment data. The input parameters are heptane plus fraction molecular weight, solvent composition and the pseudoreduced temperature.

Pedrood<sup>37</sup> simulated the miscibility process of rich gas systems by one dimensional compositional model.

Many available MMP correlations in the literature are developed for CO<sub>2</sub> or impure CO<sub>2</sub> flooding. The evaluated MMP correlations in this study are suitable for hydrocarbon flooding. The reliability of each individual correlation was evaluated by determining, how close the predictive MMPs are to the simulation results. A comparative evaluation of MMP correlations is one of the objectives of this investigation. The following MMP correlations will be evaluated in the present study.

#### 2.4.1 Glasø Correlation

Glasø<sup>31</sup> proposed a correlation for predicting minimum miscibility pressure of multicontact miscible displacement of reservoir fluid by hydrocarbon gases, N<sub>2</sub> and CO<sub>2</sub>. These equations are the equation form of the Benham<sup>16</sup> *et al.* correlation. These equations give the MMP as a function of reservoir temperature, molecular weight of C<sub>7+</sub>, mole percent ethane in the injection gas and the molecular weight of the intermediates (C<sub>2</sub> through C<sub>6</sub>) in the gas.

The proposed equations by Glasø are as follows:

$$(MMP)_{x=34} = 6,329 - 25.410 \times y - (46.475 - 0.185 \times y) \times z \\ + (1.127 \times 10^{-12} \times y^{5.258} \times e^{319.8zy^{-1.703}}) \times T. \dots\dots\dots(2)$$

$$(MMP)_{x=44} = 5,503 - 19.238 \times y - (80.913 - 0.273 \times y) \times z \\ + (1.7 \times 10^{-9} \times y^{3.730} \times e^{13.567zy^{-1.508}}) \times T. \dots\dots\dots (3)$$

$$(MMP)_{x=54} = 7,437 - 25.703 \times y - (73.515 - 0.214 \times y) \times z \\ + (4.920 \times 10^{-14} \times y^{5.520} \times e^{21.706zy^{-1.109}}) \times T. \dots\dots\dots (4)$$

Where,

$x$ = is the molecular weight of  $C_2$  through  $C_6$  components in injection gas, in lbm/mol,

$y$ = is corrected molecular weight of  $C_{7+}$  in the stock-tank oil in lbm/mole and is equal to:

$$y = \left( \frac{2.622}{\gamma_{o,c_{7+}}^{-0.846}} \right)^{6.558}$$

$\gamma_{o,c_{7+}}$  =specific gravity of heptane-plus fraction, and

$z$ = mole percent methane in injection gas

Prediction of the MMP for  $x$  values other than those specified by the mentioned equations should be obtained by interpolation.

The accuracy of the MMP predicted from the three mentioned equations is related to the accuracy of the mole percent methane in the injection gas and the molecular weight of  $C_{7+}$  in the stock tank oil. The corrected molecular weight of the stock tank oil ( $y$ ) indicates the paraffinicity of the oil which affects the MMP. The paraffinicity of the oil influences the solubility of hydrocarbon gas in the oil<sup>38</sup>. Oil with paraffinicity characterization factor (**Eq. 5**) less than 11.95 represents oil with a

relatively high content of aromatic components and consequently has corresponding higher MMPs.

Eqs. 2 though 4 are developed for reservoir oils with a calculated  $K$  factor (paraffinicity characterization factor as a function of,  $f_{Vi}$ , volume fraction of oil components,  $T_{bi}$ , boiling-point temperature of component  $i$ , and  $\gamma_o$ , oil specific gravity.  $K$  factor is defines as :

$$\left( \sum_{i=1}^n f_{Vi} T_{Bi}^{1/3} \right) \frac{1}{\gamma_o} \text{ of } 11.95.$$

The Molecular weight of  $C_{7+}$  for oil not characterized with a  $K$  factor of 11.95 should be corrected by using equation 5 reported by Whitson<sup>19</sup>.

$$K_{c_{7+}} = 4.5579 \times M_{c_{7+}}^{0.15178} \times \gamma_{c_{7+}}^{-0.84573} \quad \dots\dots\dots (5)$$

Using CO<sub>2</sub> as the injection gas, Glasø proposed the following equation.

$$\begin{aligned} (MMP) = & 810 - 3.404 \times M_{C_{7+}} \\ & + (1.7 \times 10^{-9} \times M_{c_{7+}}^{3.730} \times e^{786.8 M_{c_{7+}}^{-1.058}}) T. \quad \dots\dots\dots (6) \end{aligned}$$

Using the conducted displacement tests, Glasø found that the solubility of CO<sub>2</sub> in hydrocarbon is equivalent to a mixture of 58 mole % methane and 42 mole % propane in hydrocarbon. It was his main assumption in developing Eq. 6 which is used in predicting MMP of CO<sub>2</sub>/oil systems.

Since this correlation is developed from fluid properties data of North Sea gas/oil system, Glasø correlation should be used with great precaution.

#### 2.4.2 Firoozabadi *et al.* Correlation

A simple correlation proposed by Firoozabadi<sup>35</sup> *et al.* predicts MMP of reservoir fluids using lean natural gas or N<sub>2</sub> for injection. Three parameters account the effect of multiple-contact miscibility of a reservoir fluid under N<sub>2</sub> or lean gas flooding: The concentration of intermediates, the volatility, and the temperature.

The correlating parameter includes the ratio of the intermediates (mole percent) divided by molecular weight of the  $C_{7+}$  fraction. Intermediates contents of a reservoir fluid are usually attributed to the presence of  $C_2$  through  $C_6$ ,  $CO_2$ , and  $H_2S$ . Firoozabadi *et al.* observed that exclusion of  $C_6$  from intermediates improves the correlation of the MMP. Therefore, intermediates in this study are defined by  $C_2$  through  $C_5$  and  $CO_2$  components. The heptane plus molecular weight provides an indication of the oil volatility. The equation is as follows:

$$MMP = 9,433 - 188 \times 10^3 \times \left( \frac{x_{\text{int}}}{M_{c_{7+}} \times T^{0.25}} \right) + 1430 \times 10^3 \times \left( \frac{x_{\text{int}}}{M_{c_{7+}} \times T^{0.25}} \right)^2 \cdot \dots \dots (7)$$

Where

MMP=Minimum Miscibility pressure, psi

$$x_{\text{int}} = x_{co_2} + \sum_{i=2}^{i=5} x_i = \text{mole percent intermediates in the oil,}$$

and,

$M_{c_{7+}}$  =molecular weight of heptane plus.

It should be noted that Peng-Robinson equation-of-state (PR-EOS) based correlation proposed in this method is primary for estimating MMPs of VGD mechanisms by  $N_2$  or lean hydrocarbon gases. The dependency of MMP on reservoir temperature is not well presented in this equation. More data are required to improve this temperature dependency<sup>35</sup>.

#### 2.4.3 Eakin *et al.* Correlation

The MMP data of combinations of oils, temperatures and solvents observed by Rising Bubble Apparatus (RBA) were represented by Eakin<sup>36</sup> *et al.* correlation. Input variables for this equation are solvent composition,  $C_{7+}$  molecular weight, and the

pseudoreduced temperature of the reservoir fluid. The base solvents used in their study were nitrogen, flue gas, carbon dioxide, and rich and lean natural gases.

RBA is an alternative and much quicker apparatus for determining MMP but the obtained MMP is usually higher than the measured MMP by a slim-tube apparatus.

Kay's<sup>39</sup> rules were used to calculate pseudocritical temperature,  $T_{pc}$ , and pseudocritical pressure,  $P_{pc}$ , of the oil. The pseudoreduced temperature and pressure were defined by:

$$T_{pr} = T / T_{pc} \dots\dots\dots (9)$$

and,

$$\ln p_{pr} = \ln (MMP / p_{pc}) = \sum_{i=1}^n \left( A_i + \frac{B_i}{T_r} \right) y_i \dots\dots\dots (10)$$

Where,

$A_i$  and  $B_i$  = constants characteristic for every component (**Table 2.1**),

$y_i$  = mole fraction of component  $i$  in the solvent,

$n$  = number of components in the solvent,

$$T_{pc} = \sum_{i=1}^n x_i T_{ci}, \text{ } ^\circ\text{R, and}$$

$$P_{pc} = \sum_{i=1}^n x_i P_{ci}, \text{ } ^\circ\text{R.}$$

The general proposed correlation by Eakin *et al.* was:



$$\begin{aligned}
\ln p_{pr} = \ln(MMP / P_{pc}) = & (0.1697 - 0.06912 / T_{pr}) \times y_{c1} \times (M_{c7+})^{0.5} \\
& + (2.3865 - 0.005955 \times \frac{M_{c7+}}{T_{pr}}) \times y_{c2+} \\
& + (0.01221 \times M_{c7+} - 0.0005899 \times \frac{M_{c7+}^{1.5}}{T_{pr}}) \times y_{co_2} \dots\dots\dots(11)
\end{aligned}$$

**Table 2.1—Constant parameters of reduced temperature equation**

Component	<u>Light Oil</u>		<u>Medium Oil</u>	
	A	B	A	B
CH4	2.4458	-1.1016	2.9173	-1.2593
N2	2.7068	-0.4804	-	-
CO2	2.8016	-2.0966	3.6476	-3.0287
C2H6	2.8836	-1.8302	2.9943	-2.4702

This correlation has a standard deviation factor of 4.8% from the measured MMP values. The measured MMPs are only for two recombined sample of reservoir fluids with API gravities of 36.8 and 25.4, at 180 and 240°F.

## 2.5 Thermodynamic Method

In this method, selected EOS is calibrated to experimental PVT data including swelling and slim-tube measurements. Using of reliable experimental data in tuning EOS makes EOS (thermodynamic) methods the most reliable prediction methods.

In this method minimum miscibility pressure is explained traditionally by ternary diagrams. The limiting tie line is the extension of the tie line passing through the composition of the original oil and the tie line which passes through the critical point of the ternary diagram is called critical tie line. Monroe<sup>25</sup> *et al.* showed three key tie lines which control displacement behavior in the reservoir: The tie lines that extends through injection gas composition, the tie line passing through the oil

composition, and the third tie line called "the crossover tie line". Multi contact miscibility occurs if any of these tie lines correspond to the critical tie line.

In vaporizing gas drive mechanisms miscibility is controlled only by the limiting tie line passing through the oil composition and is not dependent on injection gas composition. The gas phase composition varies along the dew-point phase boundary expressed at constant pressure and temperature in a pseudoternary diagrams towards the critical point composition.

In condensing drive mechanisms the key tie line passing through the injection gas composition controls the development of miscibility. In this displacement mechanism miscibility is obtained at the site of injection. The intermediate components are condensed from the injection gas to the reservoir oil and miscibility develops as the tie line passing through the injection gas composition becomes the critical tie line expressed in ternary diagram model.

Orr *et al.*<sup>40</sup> and Johns *et al.*<sup>26</sup> showed that crossover tie line controls the development of miscibility in combined vaporizing-condensing mechanisms.

## 2.6 Simulator Eclipse

Black oil miscible option is an implementation of the empirical correlation suggested by Todd<sup>41</sup> *et al.*

Eclipse compositional model deals with miscibility naturally since phase equilibrium is completed in every grid. An additional accounting of miscibility must be taken by modifying the relative permeability curves. Since IFT between fluids will change the residual oil saturation and consequently relative permeability curve will be modified. The scaled relative permeability curve is evaluated as a weighted average of miscible and immiscible relative permeability curves. Calculation of surface tension, using Macleod-Sugden<sup>42</sup> correlation, and weighted average of relative permeability curves are as follows.

$$\sigma = \left\{ \sum_{i=1}^{N_c} \sigma_i \times (x_i \times \rho_L^m - y_i \times \rho_V^m) \right\}^4 \dots\dots\dots (12)$$

where,

$x_i$ , liquid mole fraction of component  $i$ ,

$y_i$ , vapor mole fraction of component  $i$ ,

$\sigma_i$ , component surface tension, dyne/cm,

$\rho_L^m$ , liquid phase molar density, g-mole/cc,

and,

$\rho_V^m$ , is the vapor phase molar density with unit of g-mole/cc.

Calculated surface tension by this correlation becomes zero at critical point where the phase compositions and densities are the same and two phases become fully miscible. An interpolation factor,  $F$  is defined:

$$F = \left( \frac{\sigma}{\sigma_0} \right)^N \dots\dots\dots (13)$$

Where  $\sigma_0$  is a reference arbitrary surface tension value. Maximum value of 1 is attributed to the dominant immiscible flow whereas the zero value of  $F$  is indicative of a miscible displacement mechanism.

This interpolation factor is used in obtaining a weighted average of immiscible (entered saturation data curves) and miscible (straight line) relative permeability curves.

$$K_{ro} = FK_{ro}^{imm} + (1 - F)K_{ro}^{mis} \dots\dots\dots (14)$$

The critical immiscible saturation  $S_{cr}^{imm}$  is obtained from the user-defined saturation curves (from third column of Fig. 4.2 which corresponds to the oil relative permeability when only oil, gas and connate water are present), whereas the critical

miscible saturation is usually zero. The interpolation factor is used in scaling of these two permeabilities to result in the same critical saturation.

$$S_{cr} = FS_{cr}^{immis} + (1 - F)S_{cr}^{mis} \dots\dots\dots (15)$$

So, both of the scaled relative permeabilities have the same endpoint critical saturation,  $S_{cr}$ . The scaled miscible relative permeability is a straight line with critical saturation of  $S_{cr}$ .  $K_{ro}^{mis}$  becomes the dominate contribution (straight line) with a zero critical saturation as F approaches to zero.

### 3. RESULTS

#### 3.1 Comparative Investigation of MMP Correlations

Multiple contact miscibility achieved by injection of lean hydrocarbon or flue gas into the reservoir is one of the most economical and widely used oil recovery methods in the oil industry. The economic success of gas injection project can be improved by operating at pressures close to MMP. However, this requires accurate experimental measurements of MMP. The current proposed MMP correlations may be good substitute for both costly and time consuming experimental measurements. Unfortunately, most of the MMP correlations are not flexible to represent a variety of solvent/oil combinations and care must be taken when selecting one of them. Reliable MMP correlations should be used for preliminary screening or feasibility studies, but should not be relied upon. The first part of this study provides an evaluation of the existing lean hydrocarbon or impure CO<sub>2</sub>-stream MMP correlations published in the literature.

**Table 3.1—Reservoir oil compositions (reported by Core Laboratories, INC.)**

Component	Oil A, mole%	Oil B, mole %
N <sub>2</sub>	0.03	1.85
CO <sub>2</sub>	0.05	0.26
C <sub>1</sub>	28.24	38.85
C <sub>2</sub>	0.6	10.85
C <sub>3</sub>	1.23	7.28
iC <sub>4</sub>	0.47	2.81
nC <sub>4</sub>	1.38	3.44
iC <sub>5</sub>	0.86	2.33
nC <sub>5</sub>	1.06	1.52
C <sub>6</sub>	1.39	3.29
C <sub>7+</sub>	64.69	27.52
<b>C<sub>7+</sub> properties:</b>		
Molecular Weight	308	175
Density, lb/ft <sup>3</sup>	58.59	51.17
Oil gravity, API	20.8	44.5
<b>Calculated critical properties:</b>		
T <sub>c</sub> , F	1089.54	552.46
P <sub>c</sub> , psi	1468	2732.63

**Table 3.2—Bubble point pressures of the reservoir fluids**

T, °F	P <sub>b</sub> , psi	
	Oil A	Oil B
100	1,209	1,959
200	1,586	2,505
300	1,840	2,830

### 3.1.1 Reservoir Fluid Composition

To investigate the effect of oil composition on estimated minimum miscibility pressure, two different oil samples (reported by Core Laboratories, INC.) with API gravities of 20.8 and 44.5 have been considered. **Tables 3.1** and **3.2** provide composition data and bubblepoint pressures of these reservoir fluids respectively. Mole percent of heptanes plus fraction (greater than 20%) and high critical point temperature compare to typical reservoir temperature, are indicative of black oil system (**Fig. 3.1**). The reported simulation results in this chapter are the result of using PVTsim in modeling phase behavior of reservoir fluids.

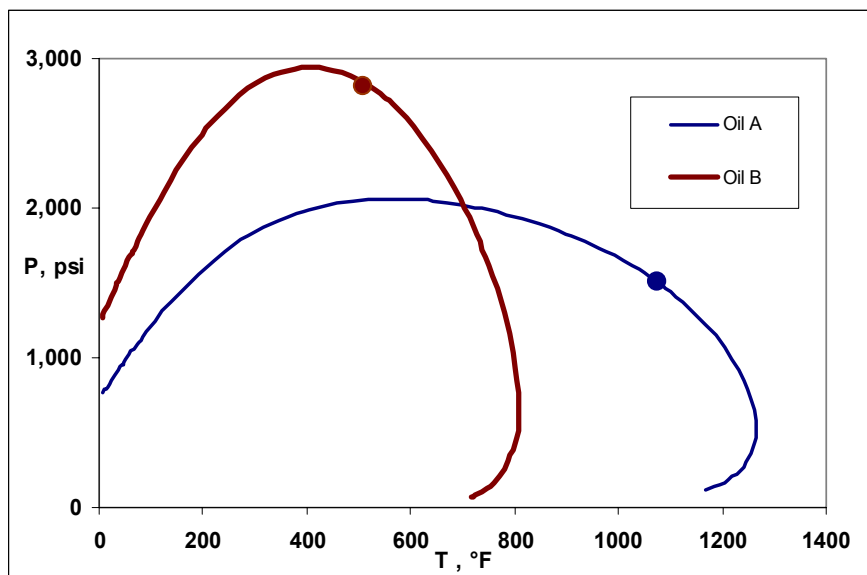


**Fig. 3.1— Phase envelope of reservoir fluids (using PVTsim). Higher API gravities cause extension of the phase envelope toward higher temperatures**

### 3.1.2 Injection Gas Composition

It is most economical to reinject all or part of the produced dry gas back into the reservoir. Produced gas of the reservoir is an alternative source for gas injection and pressure maintenance processes. To achieve this purpose, the compositions of the injection gases are close to the equilibrium gas with the reservoir fluid. For each reservoir fluid, flash calculations at different temperatures (100, 200 and 300 °F) and at pressures, below the corresponding bubble point pressure of the oil at that temperature (Table 3.2), were made and the separator gas as a result of flash process, has been considered as the injection gas. **Tables 3.3** and **3.4** indicate the injection gas compositions and flash conditions.

**Table 3.3—Injection gas composition (mole %) for oil A**

Component	Gas A1	Gas A2	Gas A3
N <sub>2</sub>	0.289	0.216	0.188
CO <sub>2</sub>	0.079	0.101	0.115
C <sub>1</sub>	98.038	96.482	94.209
C <sub>2</sub>	0.556	0.779	0.938
C <sub>3</sub>	0.457	0.805	1.131
iC <sub>4</sub>	0.096	0.195	0.301
nC <sub>4</sub>	0.21	0.458	0.748
iC <sub>5</sub>	0.069	0.176	0.321
nC <sub>5</sub>	0.069	0.187	0.355
C <sub>6</sub>	0.041	0.136	0.296
C <sub>7</sub>	0.049	0.199	0.507
C <sub>8</sub>	0.027	0.125	0.351
C <sub>9</sub>	0.013	0.071	0.226
C <sub>10+</sub>	0.007	0.07	0.312
<b>C<sub>10+</sub> properties:</b>			
Molecular weight	162.7061	164.7383	168.4278
Density, lb/ft <sup>3</sup>	51.4757	51.70899	52.13655
<b>Injection gas properties:</b>			
Gas A1: Flash of oil A @ T=100 °F & P=1200 psi			
Gas A2: Flash of oil A @ T=200 °F & P=1500 psi			
Gas A3: Flash of oil A @ T=300 °F & P=1800 psi			

**Table 3.4—Injection gas composition (mole %) for oil B**

Component	Gas B1	Gas B2	Gas B3
N <sub>2</sub>	7.401	5.366	4.1
CO <sub>2</sub>	0.307	0.35	0.355
C <sub>1</sub>	77.582	71.203	63.337
C <sub>2</sub>	8.763	11.163	12.321
C <sub>3</sub>	3.128	4.99	6.43
iC <sub>4</sub>	0.802	1.471	2.096
nC <sub>4</sub>	0.798	1.577	2.368
iC <sub>5</sub>	0.349	0.803	1.347
nC <sub>5</sub>	0.196	0.478	0.834
C <sub>6</sub>	0.248	0.731	1.462
C <sub>7</sub>	0.188	0.66	1.493
C <sub>8</sub>	0.11	0.443	1.106
C <sub>9</sub>	0.059	0.281	0.792
C <sub>10+</sub>	0.069	0.484	1.959
C <sub>10+</sub>	0.069	0.484	1.959
<b>C<sub>10+</sub> properties:</b>			
Mw	150.1565	157.2903	167.6555
Density, lb/ft <sup>3</sup>	50.6657	51.45875	52.65102
<b>injection gas properties:</b>			
Gas B1: Flash of oil B @ T=100 °F & P=1900 psi			
Gas B2: Flash of oil B @ T=200 °F & P=2400 psi			
Gas B3: Flash of oil B @ T=300 °F & P=2800 psi			

As it is clear from these tables, the higher the temperature of the flash condition, the richer the gas is in intermediate components.

### 3.1.3 Correlation Results

There are only a few correlations applicable for this investigation. Most of the proposed MMP correlations are presented for CO<sub>2</sub> flooding rather than hydrocarbon flooding which is a general case. Among the MMP correlations mentioned above, Firoozabadi<sup>35</sup> *et al.* are correlations that are not dependent on injection gas composition. Eakins and Glasø correlations consider effects of gas and oil compositions in predicting MMPs.

Two different oil samples along with three injection gas compositions for each specific oil gravity cause various combination of gas flooding processes. Tables



3.5 through 3.7 indicate the predicted MMP's using different correlations described above.

As we know the heavier the reservoir fluid, the higher MMP is required to achieve miscibility. Reservoir fluid with API gravity of 20.8 (oil A) requires the highest MMPs. The injection gas with higher quantity of intermediate components causes smaller MMPs for a specified oil reservoir. Therefore, the required MMP to achieve dynamic miscibility for oil A, is highest for injection gas A1 and lowest for injection gas A3.

As mentioned before, the injection gases used in this study are the separator gases which are the result of flash calculations. The separator gas with higher flash temperature contains more intermediate components and is most desirable in gas injection processes.

**Table 3.5** represents the predicted results using Eakin<sup>36</sup> *et al.* correlation. Estimated MMP results are provided at reservoir temperatures of 100, 200 and 300 °F. Higher MMP for oil A and injection gases A1, A2 and A3 is predictable.

**Table 3.5—Predicted MMP using Eakin *et al.* correlation. This correlation accounts for effect of CO<sub>2</sub> in decreasing miscibility pressure**

Reservoir Temperature, °F	Oil A			Oil B		
	Gas A1	Gas A2	Gas A3	Gas B1	Gas B2	Gas B3
100	6,067	5,856	5,532	3,511	3,263	2,936
200	6,808	6,594	6,265	3,840	3,610	3,295
300	7,411	7,197	6,866	4,102	3,889	3,587

**Table 3.6— Predicted MMP's by Firoozabadi *et al.* correlation. This correlation like majority of lean gas MMP correlations ignores the effect of injection gas composition**

Reservoir Temperature, °F	Oil A	Oil B
	Injection gases:A1, A2, A3	Injection gases:B1, B2, B3
100	8,399	3,564
200	8,557	4,000
300	8,639	4,294

**Table 3.7— Predicted MMP using Glasø correlation. This correlation predicts unreliable MMP's for oil A (order of plots from top to bottom: A2, A1 order instead of A1, A2) and very low values for injection gas B2**

Reservoir temperature, °F	Oil A		Oil B	
	Gas A1	Gas A2	Gas B1	Gas B2
100	3,640	8,716	1,682	540
200	6,966	18,025	3,204	1,077
300	10,313	27,334	4,726	1,612

The only parameters in Firoozabadi<sup>35</sup> *et al.* correlation for vaporizing-drive mechanism are the amount of intermediates, the oil volatility, and reservoir temperature. This correlation doesn't account for varying injection gas compositions and the estimated MMPs for light oil is relatively not dependent on injection gas composition. Predicted MMP results for reservoir fluids A and B are presented in Table 3.6.

Table 3.7 indicates the correlation results using Glasø<sup>31</sup> correlation. Unlike the previous correlation this correlation estimates the MMP of fluid with API gravity of 20.8 much higher than the other reservoir fluid but the effect of injection gas composition seems to be negligible. Gas A1 should have the greatest MMPs due to low quantities of its intermediate components compare to A2 but the results are anomalous. Low estimated MMP values for injection gas B2 is abnormal.

The discrepancy among these correlations makes the selection impossible unless there is evidence that correlation was adequate for an oil/solvent with similar characteristics.

### 3.1.4 Comparison of Simulation and Correlation Results

Since the reservoir fluid A is too heavy the required MMP to achieve miscibility with injection gases A1, A2, and A3 are too high. Therefore, only reservoir fluid B with higher API gravity is appropriate for this part of study. **Table 3.8** indicates the comparison of MMP and simulation results for oil B/Gas B1 system. Among these correlations Glasø *et al.* correlation is strongly dependent on reservoir temperature. It can be clearly seen in this correlations that MMP values

increase rapidly as temperature increases. Other correlations except for Glasø approach, seems to represent parallel slopes and closer MMP values to each other.

**Table 3.8— Comparison of simulation and correlation results for fluid B/injection gas  
B1 system**

<b>T, °F</b>	<b>Simulation</b>	<b>Eakin</b>	<b>Glasø</b>	<b>Firoozabadi</b>
<b>100</b>	4,354	3,511	1,682	3,564
<b>200</b>	4,372	3,840	3,204	4,000
<b>300</b>	3,964	4,102	4,726	4,294

Evaluation of the accuracy of each MMP correlation illustrates that Firoozabadi *et al* and Eakin *et al.* methods are found to be the most reliable correlations among the other ones. These correlations are EOS and statistic based models and the good agreement with simulation results could be attributed to this concept. As was mentioned before, simulation approach in calculating MMPs for different injection gas/oil systems is based on equation of state (EOS) model. It should be added that MMP data or other types of PVT data must be used to calibrate the EOS. The advantage of using EOS is that it is a self consistent method and can be easily tuned to available experimental data.

The large inaccuracy of the Glasø correlation in predicting the vaporizing-gas drive MMPs is related to the limited slim tube experiments. This correlation was mostly developed from experimental slim tube MMP data of North Sea gas/oil system and special care should be paid to predict MMPs of other reservoir fluids.

As a general case, the evaluated MMP correlations in this study are not sufficiently accurate and they should be applied with great care in particular situations even for preliminary MMP calculations and screening processes.

### **3.2 Evaluation of Parameters on Miscible and Immiscible Gas-Injection Processes**

Injection of cost-effective lean hydrocarbon gas or flue gases could be employed in reservoirs where a favorable combination of pressure, reservoir

characteristics and fluid properties make the gas injection project a competitive process compare to other secondary oil recovery methods. However, for a gas injection project, to be competitive several conditions should be satisfied. The incremental oil recovery is largely dependent on injection pressure, reservoir characteristics and fluid properties such as heterogeneity, relative permeability, viscous fingering, fluid mobility, gravity segregation, etc.

In this chapter, a parametric study is done, using a 3D, compositional simulator to analyze the effect of such important parameters in miscible or immiscible performance recovery from the reservoir.

### 3.2.1 Field Description

The specification of the reservoir model is given in the **Table 3.9**. Adaptive implicit solution avoids the time step restrictions imposed by small blocks and minimizes the computational expense of a fully implicit solution. The two layers are homogenous and of constant porosity, permeability, and thickness. Saturation and PVT data of the reservoir fluid including the injection gas composition are provided in **Tables 3.10** through **3.12** and in PROPS section of the presented simulation data file in **Appendix A**.

Reservoir fluid is initially undersaturated. The initial reservoir pressure is 4,200 psi and the saturation pressure of the reservoir fluid at 217 °F is 2,931 psi. The reservoir oil gravity is 47 °API with a viscosity of 0.18 cp at initial reservoir conditions. Low water viscosity in the reservoir, 0.3 cp, giving rise to the low gas to oil mobility ratio. Setting the initial condition for the location of water/oil contact to 8,500 ft (80 ft below the oil zone), and setting the oil/water capillary pressure to zero could eliminate the transition zone between oil and water phases. The very small compressibility and volume of the water; however, makes water rather insignificant in this problem. Initial oil and water saturations are 0.78 and 0.22. Estimated initial oil in place oil is 10.068 MMRB.

**Fig. 3.2** shows the injection and production well location. Injection well is perforated in the first layer whereas the production well is completed in the second

layer and produced on deliverability against a 1,000 psi flowing bottomhole pressure and maximum gas production rate constraint of 30,000 Mscf/day. Lean gas with similar composition of the vapor phase in equilibrium with the reservoir fluid at reservoir temperature and pressure slightly below the bubble point, is injected continuously into the first layer of the reservoir with average thickness of 40 ft.

**Table 3.9—Reservoir grid data and water properties**

<b>Reservoir grid data</b>				
NX=NY=9, NZ=2				
DX=DY=293.3 ft				
Porosity	0.13			
Datum (subsurface), ft	8,420			
Oil/water contact, ft	8,500			
Capillary pressure at contact, psi	0			
Initial pressure, psi	4,200			
Reservoir temperature, °F	217			
<u>Layer</u>	<u>Horizontal permeability</u>	<u>Vertical Permeability</u>	<u>Thickness, ft</u>	<u>Depth to top (ft)</u>
1	90	9	40	8,340
2	90	9	40	8,380
<b>Water properties</b>				
compressibility, psi <sup>-1</sup>	3 × 10 <sup>-6</sup>			
density, lbm/ft <sup>3</sup>	63			
Rock compressibility, psi <sup>-1</sup>	4 × 10 <sup>-6</sup>			
viscosity, cp	0.3			

Constant injection pressure for the injection well is the only constraint applied to the injection well. Further information of the reservoir model and fluid characterization are provided in the Appendix A.

<b>Table 3.10—gas relative permeability data</b>	
<b><math>S_g</math></b>	<b><math>K_{rg}</math></b>
0	0
0.04	0
0.1	0.022
0.2	0.1
0.3	0.24
0.4	0.34
0.5	0.42
0.6	0.5
0.7	0.8125
0.78	1

<b>Table 3.11—Three phase saturation data</b>		
<b><math>S_o</math></b>	<b><math>K_r(o,w)</math></b>	<b><math>K_r(3 \text{ phase})</math></b>
0	0	0
0.15	0	0
0.38	0.00432	0
0.4	0.0048	0.004
0.48	0.05288	0.02
0.5	0.0649	0.036
0.58	0.11298	0.1
0.6	0.125	0.146
0.68	0.345	0.33
0.7	0.4	0.42
0.74	0.7	0.6
0.78	1	1

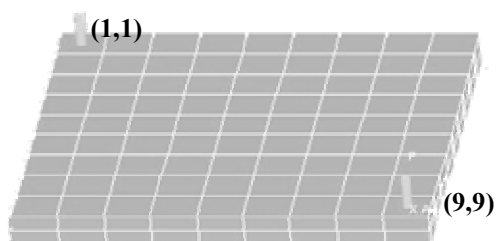


**Fig. 3.2—Three-dimensional grid configuration. Injection and production wells are located on the (1,1) and (9,9) coordinates of the X-Y plane**

**Table 3.12—Reservoir fluid and injection gas composition**

<b>Component</b>	<b>Reservoir fluid, mole %</b>	<b>Injection gas, Mole %</b>
N <sub>2</sub>	0.92	0
CO <sub>2</sub>	0.32	0.877
C <sub>1</sub>	41.25	87.526
C <sub>2</sub>	8.68	6.36
C <sub>3</sub>	7.27	3.906
C <sub>4</sub>	4.9	1.331
C <sub>5</sub>	2.89	0
C <sub>6</sub>	4.29	0
C <sub>7+</sub>	29.48	0
<b>Heptanes plus properties:</b>		
<b>Molecular weight</b>		202
<b>Specific gravity</b>		0.86

### 3.2.2 Relative Permeability Effect

The term miscible recovery is defined as any oil recovery displacement mechanism, where the phase boundary or interfacial tension between the displaced and displacing fluids is negligible. In this situation the capillary number becomes infinite and the residual oil saturation can be reduced to the lowest possible value because there is no interfacial tension (IFT) between the fluids.

Setting the reference surface tension defines the interpolation factor (Eq. 13),  $F$  and consequently the appropriate relative permeability curve dependent on dominant flow will be used.

In this section, miscibility option is imposed by setting the reference surface tension. This is the surface tension value at which immiscible relative permeability curves are measured. The adopted arbitrary reference surface tension (based on mixing option of the fluids at initial reservoir conditions) is 90 dyne/cm. Eclipse assigns this value for gridblocks containing a single phase. Therefore, immiscibility factor,  $F$ , equals to unity (using Eq. 13). The immiscibility factor approaches to zero for gridblocks containing two phases. It becomes zero when two phases form a single phase and become fully miscible.

Simulation runs conducted at injection pressure of 4,800 psi (This is the estimated MMP value determined for injection gas/reservoir fluid system at reservoir

temperature of 217 °F) for two cases of miscible (straight line) and immiscible (input saturation data) option. Following are the simulation results concerning the effect of relative permeability on recovery performance of the reservoir. Difference in fluid saturation profiles, variation in reservoir pressure, and injection rates are also part of comparison between two displacement mechanisms.

### 3.2.2.1 Fluid Saturation Profiles

**Figs. 3.3** and **3.4** indicate oil saturation profiles of the various diagonal gridblocks for immiscible displacement of the reservoir fluid. According to these figures, three different zones in saturation profiles of the first and second layers could be demonstrated. As injection gas enters the gridblock, the oil saturation starts decreasing very rapidly till the saturation reduces approximately to the residual oil saturation provided in relative permeability curve. This first zone is common for both layers of reservoir.

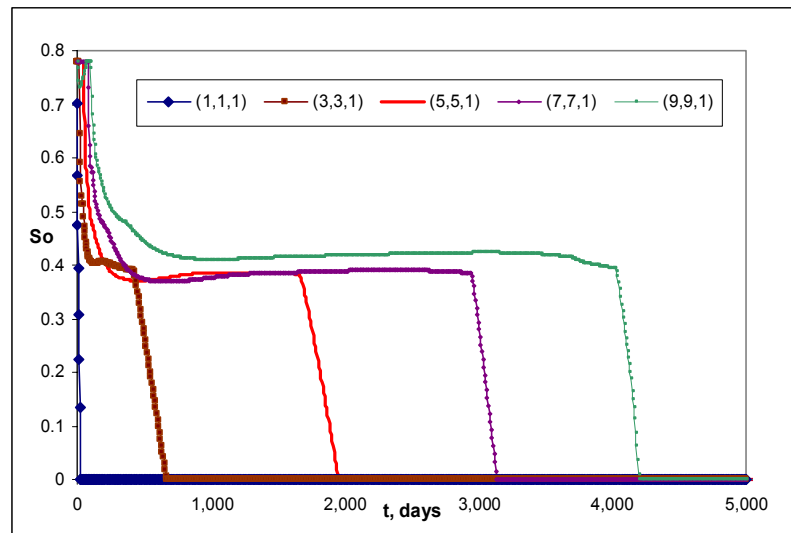


**Fig. 3.3—Variation in oil saturation during gas injection of the first layer (for immiscible relative permeability curve)**

It seems that injection gas which swept most of the oil content of the first layer tends to flood the second layer to a higher degree at this time. The stable oil saturation of the first layer (horizontal line) represents second zone. The third zone is



when the injection gas vaporizes all the oil rapidly and the oil saturation of the cell becomes zero. The oil saturation of the second layer, represented in Fig. 3.4, is not as steady as the first layer. After the period of nearly unchanged oil saturation, injected gas sweeps the remaining oil completely. Time of thorough oil sweepout for the grids (1,1,1), (3,3,1), (5,5,1), (7,7,1), and (9,9,1) are 35, 681, 1,963, 3,144, and 4,240 days respectively. The corresponding values for the second layers are 93, 952, 2,425, 3,778, and 4,320 days. Since the injection well is completed in the first layer and vertical permeability between two layers is a low fraction of horizontal permeability, earlier oil sweepout occurs in this layer. It should be noted that in spite of immiscible displacement the oil saturation take values less than residual oil saturation. This improvement in oil sweepout is the result of vaporization of the residual oil even when miscibility is not achieved. Estimated immiscible residual oil saturation using Table 3.11 is around 0.38. Swelling or expansion of the undersaturated oil resulting from addition of dissolved gas may be the other reason.

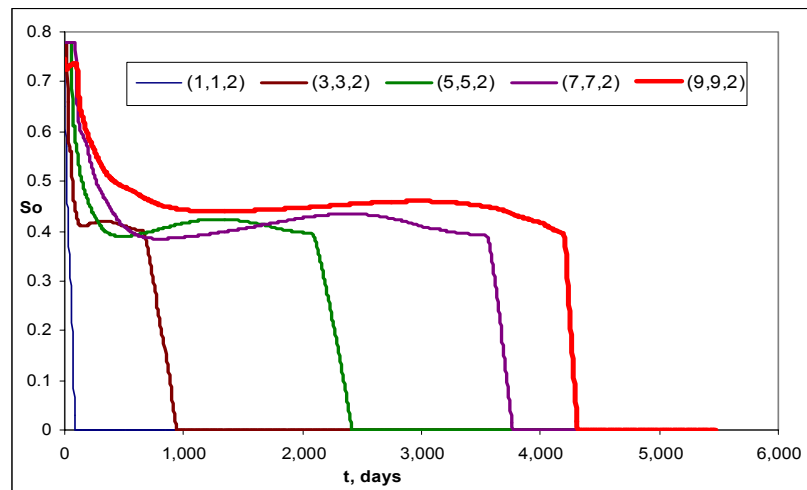


**Fig. 3.4—Variation in oil saturation of the second layer (using immiscible relative permeability curve)**

**Figs. 3.5 and 3.6** indicate variation in oil saturation of individual layers when miscible relative permeability curves are used. Same trend of Fig. 3.3 is observed in Fig. 3.5. The second plateau trend in Fig. 3.5 is around 0.11. This is much lower than

residual oil saturation using immiscible  $k_r$  curve which is 0.39. Earlier oil sweepout occurs in displacements using miscible  $k_r$  compare with immiscible  $k_r$ . The corresponding sweepout time values for the particular grids are 17, 196, 590, 1,028, 1,396 days for the first layer, and 39, 305, 886, 1,493, and 1,744 days for the second layer. The saturation profile of the second layer doesn't exhibit the second trend and the oil saturation keeps decreasing during the production life of the reservoir.

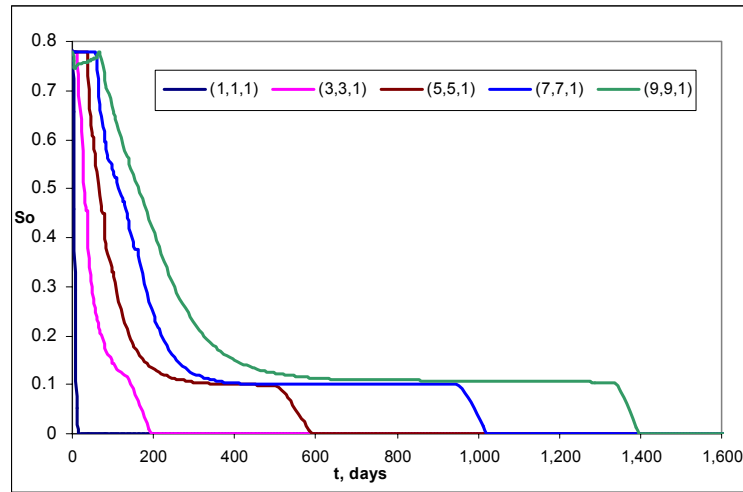


**Fig. 3.5—Variation in oil saturation of the first layer (miscible  $k_r$ )**

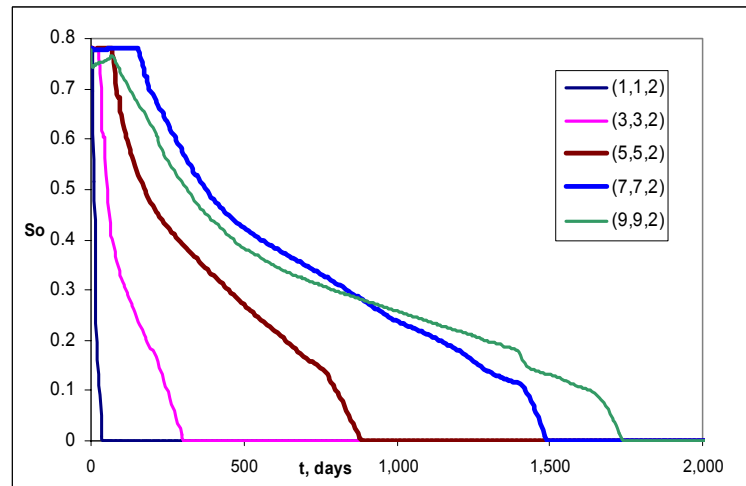


**Fig. 3.6—Variation in oil saturation of the second layer (miscible  $k_r$ )**

**Fig. 3.7** compares the oil saturation of grids (5,5,1) and (5,5,2) when using miscible and immiscible relative permeability curves. Results indicate the importance of miscible relative permeability in high sweep efficiency of the reservoir. In all these cases the sweep efficiency is higher when using miscible  $k_r$ . As miscibility develops, the gas front into the cell sweeps the oil content of the grid in earlier time.

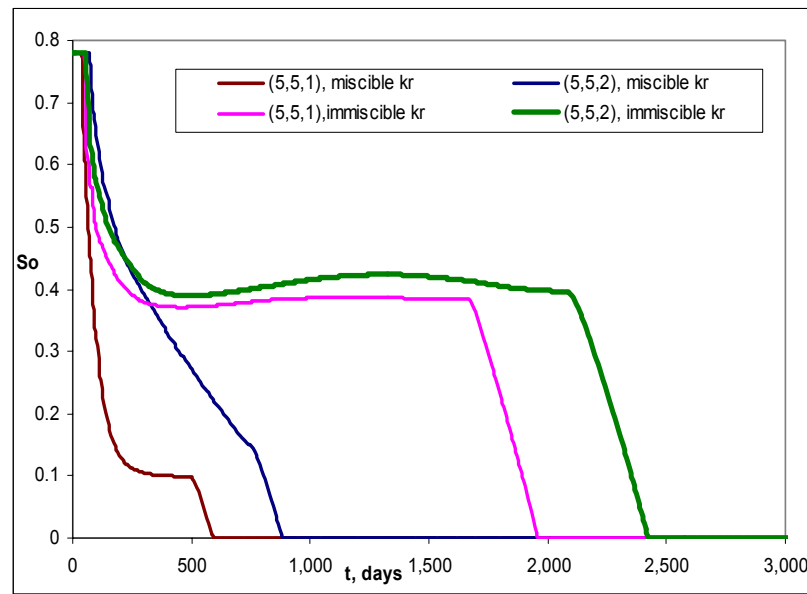


**Fig. 3.7—Higher oil saturation for bottom layer using immiscible  $k_r$**

The initial water saturation value, 0.22 is the connate water accumulated in the reservoir. In the absence of mobile water the injection gas will only displace the undersaturated oil of the reservoir and the gas saturation profile, shown in **Fig. 3.8**, is predictable.

#### **3.2.2.2 Reservoir Performance**

**Fig. 3.9** compares the production-well gas/oil ratio (GOR) for gas injection projects using miscible and relative permeability curves and at constant injection pressure of 4,800 psi. Calculated GOR using immiscible relative permeability curve, increases gradually up to 182 Mscf/bbl value at the end of the project life. This is considerably lower than correspondent GOR values when using miscible  $k_r$ .

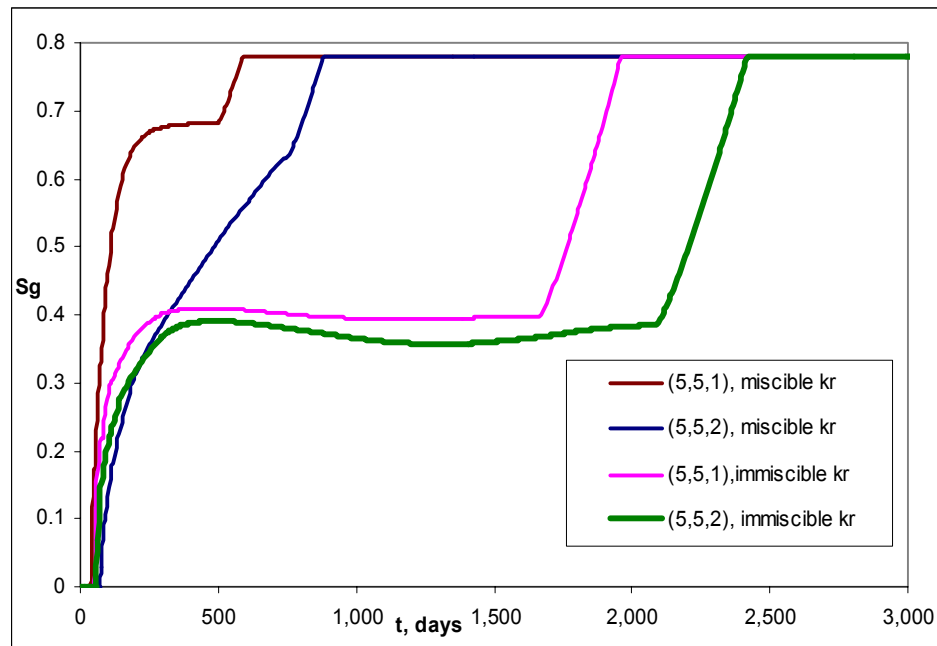


Fig. 3.8—Comparison of average gas saturation using miscible and immiscible  $k_r$

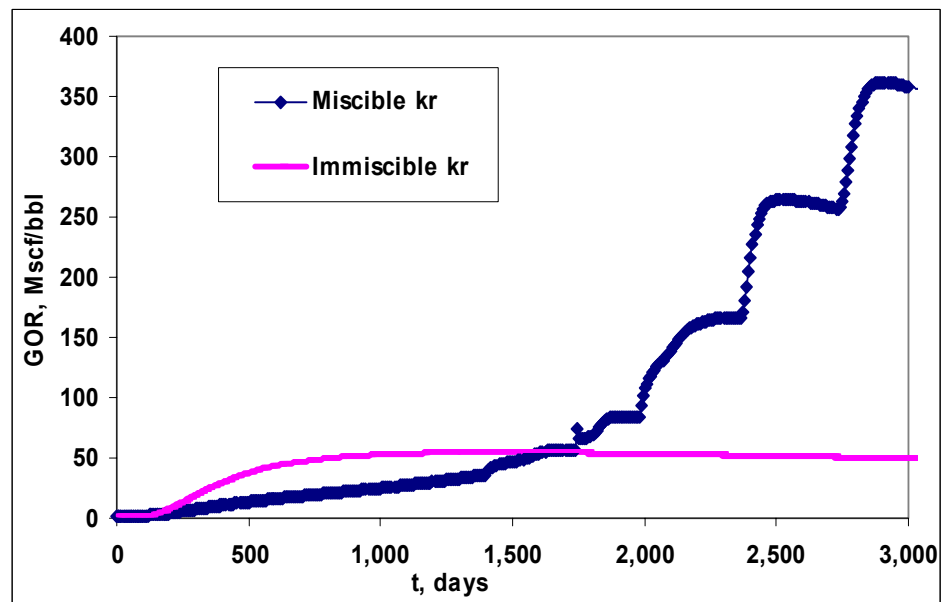


Fig. 3.9—Comparison of production well gas/oil ratio using different relative permeability curves

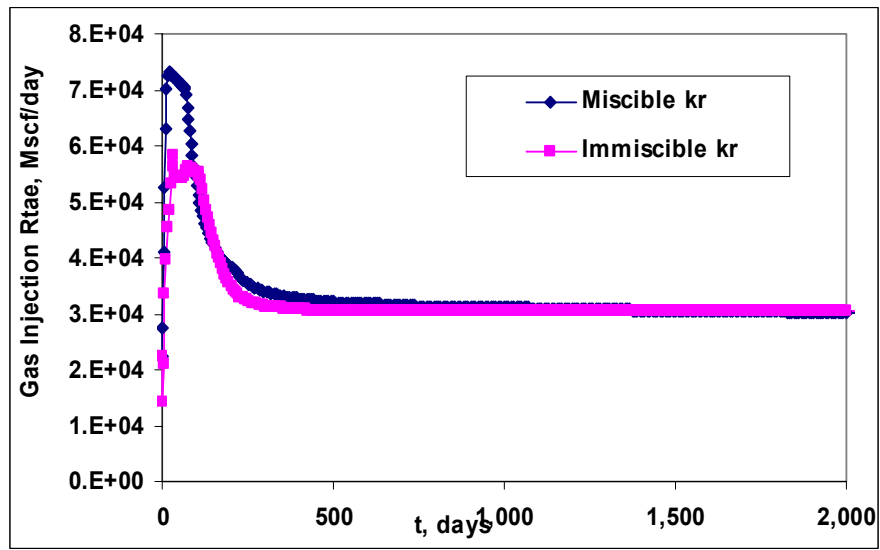


Fig. 3.10— Pressure disturbance in the reservoir at the early days of production causes unsteady gas injection rate

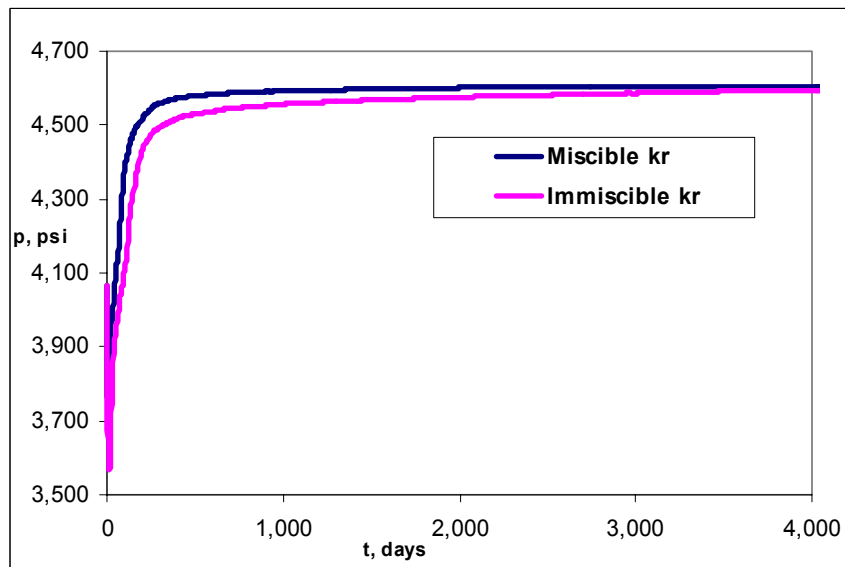
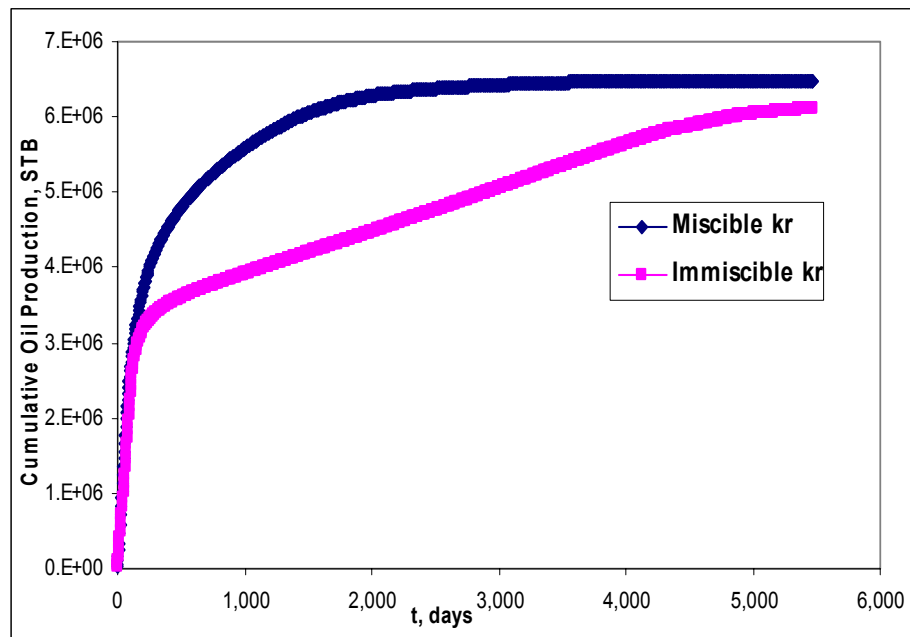


Fig. 3.11— Higher injection rates (using miscible  $k_r$ ) cause greater average reservoir pressure in this displacement.

Higher average reservoir pressure and injection-gas rates when using miscible  $k_r$  in comparison with immiscible  $k_r$  is observed in the Figs. 3.10 and 3.11..

Both, injection rates and reservoir pressure become stable towards the end of the project.

Cumulative oil production and predicted recovery vs. pore volume of injection gas is provided in **Figs. 3.12** and **3.13**. Distinct recovery trends are estimated for different miscible and immiscible relative permeabilities. The calculated oil recoveries at 1.2 pore volume of injected gas for miscible  $k_r$  and immiscible  $k_r$  are 73.5% and 55.4% of OOIP. In other word, 18.1 %OOIP is the incremental oil recovery using miscible  $k_r$  for the same injection pressure and pore volumes of injection gas as those of immiscible ones. Moreover, the revenue from additional oil recovery is concentrated in the early life of the project and the rate of return of investment using miscible  $k_r$  is higher compare with that of immiscible  $k_r$ . Considerable amount of recoverable oil is produces up to nearly seven years of gas injection for miscible  $k_r$ . Therefore it is most beneficial to stop flooding at this time, since only a maximum of 0.1% OOIP incremental oil recovery is predicted at the end of the project which is at 15 years of injection.



**Fig. 3.12—Comparison of cumulative oil production for two relative permeabilities.**

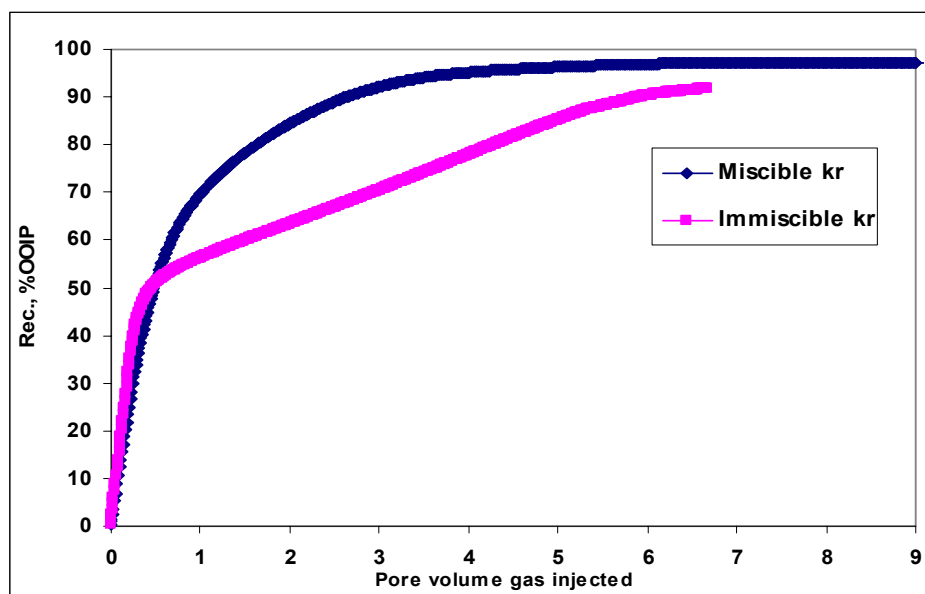


Fig. 3.13—Significant incremental oil recovery using miscible  $k_r$

It should be noted that for highly undersaturated reservoirs with high-gravity crude oils, which is this case study, recovery increases significantly by initiating gas injection project at the highest pressure possible, even though miscibility is not developed. The improvement in recovery efficiency is mainly the result of reduction in oil viscosity, oil swelling, and vaporization of the residual oil. Recovery in miscible displacement is strongly sensitive to changes in fluid properties and reduction in interfacial tension, resulting in variation of the relative permeability endpoints.

### 3.2.3 Injection Pressure Effect

In this part of the study, the effect of injection pressure on the oil recovery from the entire symmetrical grid model has been investigated. Injection and production wells are completed in the first and second layer, respectively. Estimated MMP based on equation of state analytical method is approximately 4,800 psi. Numerous simulation runs have been conducted at pressures below, equal and greater than this pressure. Since in vaporizing drive mechanisms, the pressure at miscible front should be greater than the predicted miscible pressure, injection of

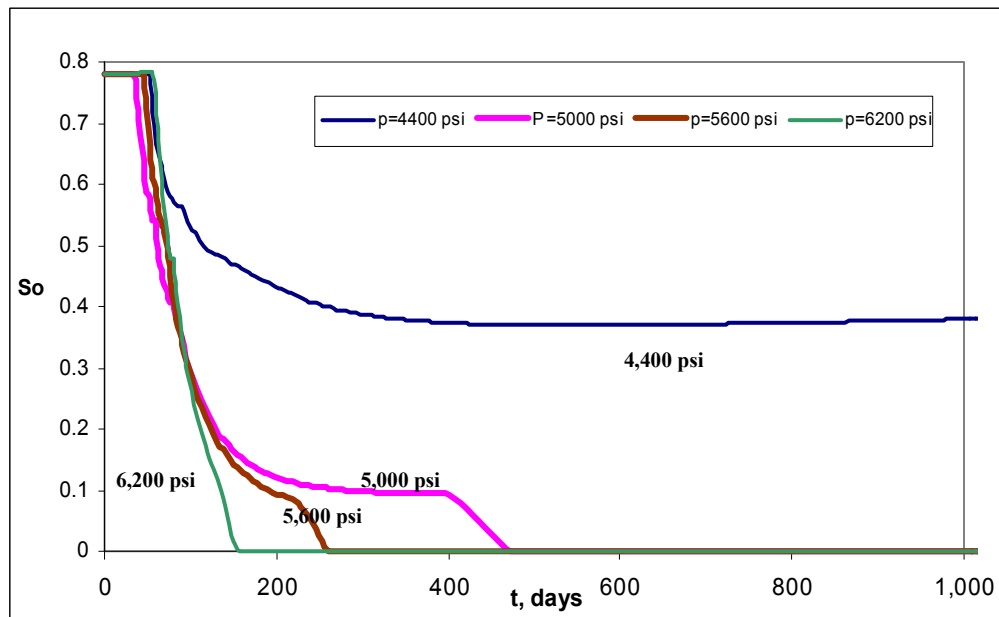
gas at 5,000 psi will raise the average reservoir pressure from initial pressure of 4,200 psi to the miscibility pressure of 4,800 psi. Therefore, the injection pressure of 5,000 psi seems to be the best candidate for representing MMP in simulation model. Following are the comparison results by compositional simulation.

### 3.2.3.1 Saturation Profiles

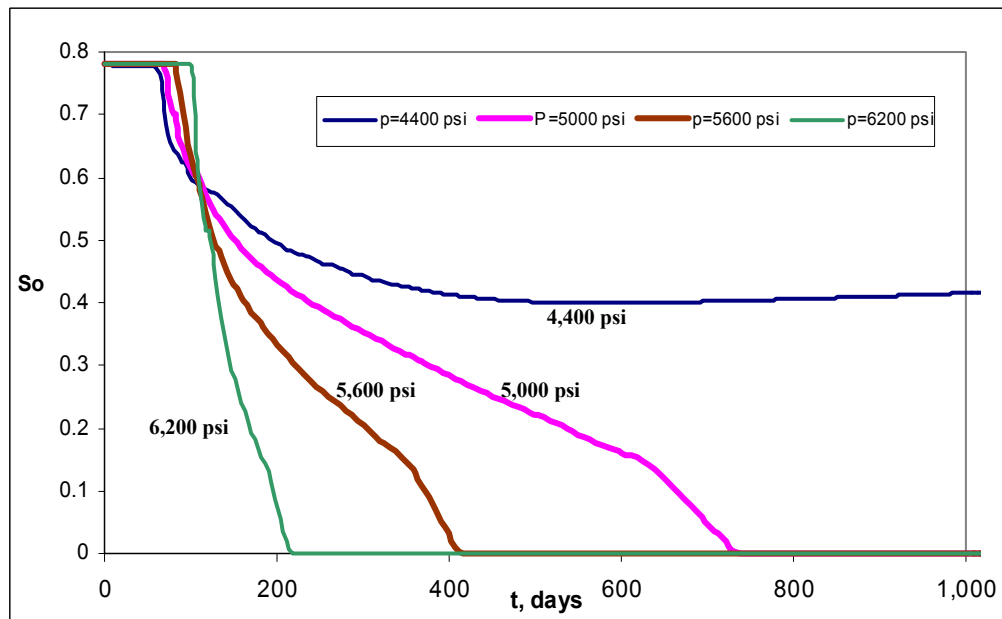
In this step, the variation in oil saturation of particular gridblocks under gas injection is investigated. **Fig. 3.14** indicates the saturation values for typical reservoir grids (5,5,1) and (5,5,2). These are the mediate grids of the reservoir which are located on the first and second layers. Time of gas breakthrough into grid (5,5,1) is 38, 39, 49, and 63 days after injection of gas at 4,400, 5,000, 5,600, and 6,200 psi, respectively. Greater breakthrough times are observed for the second layer (grid (5,5,2)) which are 64, 77, 86, and 101 days. Comparison of these values results in the following conclusions

- The higher the injection pressure, the greater the breakthrough time of the gas into the gridblock is. Since the gas tends to flow through the shortest distance between the wells in this 5-spot pattern, and injection at higher pressures cause greater front velocities, most of the injected gas at higher pressures sweeps the diagonal grids rather than marginal ones (**Fig. 3.15**). Gas velocities along the marginal streamlines are the lowest value since the pressure gradient is lower than that of diagonal grids.
- Since the injection well is perforated in the first layer, and the vertical permeability is a small fraction of the horizontal one, sweep efficiency is higher in gridblock (5,5,1) than (5,5,2) and earlier gas breakthrough is observed in this grid. The difference in breakthrough times of second-layer grid increases with increasing pressure, i.e. 77 and 101 days for pressures of 5,000 and 6,200 psi. Zero oil saturation is observed at 480, 259, and 157 days for grid (5,5,1), and after 745, 415, and 217 days of miscible injection for grid (5,5,2) at pressures of 5,000, 5,600 and 6,200 psi, respectively.





a) Low sweep efficiency in grid (5,5,1) at injection pressure of 4,400 psi



b) Earlier oil sweepout, shorter gas breakthrough time in grid (5,5,2) at higher pressures.

Fig. 3.14—Variation in oil saturation of grids (5,5,1) and (5,5,2)

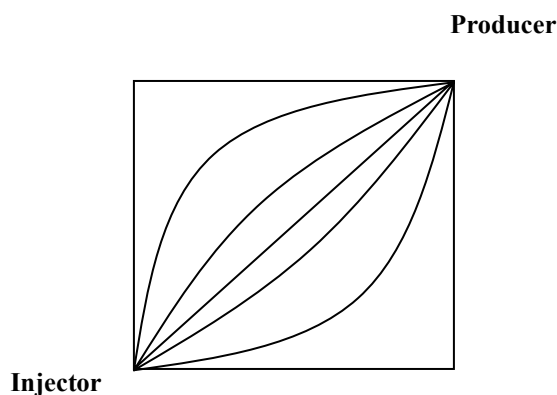


**Fig. 3.15—Higher pressure gradient along the diagonal streamlines located on the shortest distance between wells makes sweep efficiency of this region higher.**

**Figs. 3.16 through 3.18** show the variation in oil saturation of diagonal gridblocks located on the shortest distance between the injection and production wells. These saturation profiles compare the extent of oil sweepout of individual layers and location of the gas front at different time steps and for injection pressures below, equal to and greater than miscibility pressure.

It is clearly seen that the injection gas tends to flow through the first layer and reduces the oil saturation of that layer to a certain value. This value is the critical oil saturation in miscible relative permeability curve. Then, injected gas starts sweeping of the oil of the bottom layer for a particular time period depending upon injection rate. The higher the injection pressure, the sooner the gas sweeps the oil content of the grids.

### **3.2.3.2 Reservoir Performance**

**Fig. 3.19** indicates the variation in average reservoir pressure for different injection pressures. At very early days of production and for injection pressures of 4,400 and 5,000 psi, a reduction in reservoir pressure is observed because of the decrease in gas injection rate. And next it keeps increasing towards the end of project. It is clearly seen in Fig. 3.19 that gas injection raises the average reservoir pressure from initial value of 4,200 psi to pressure value around 200 psi below the injection pressure.

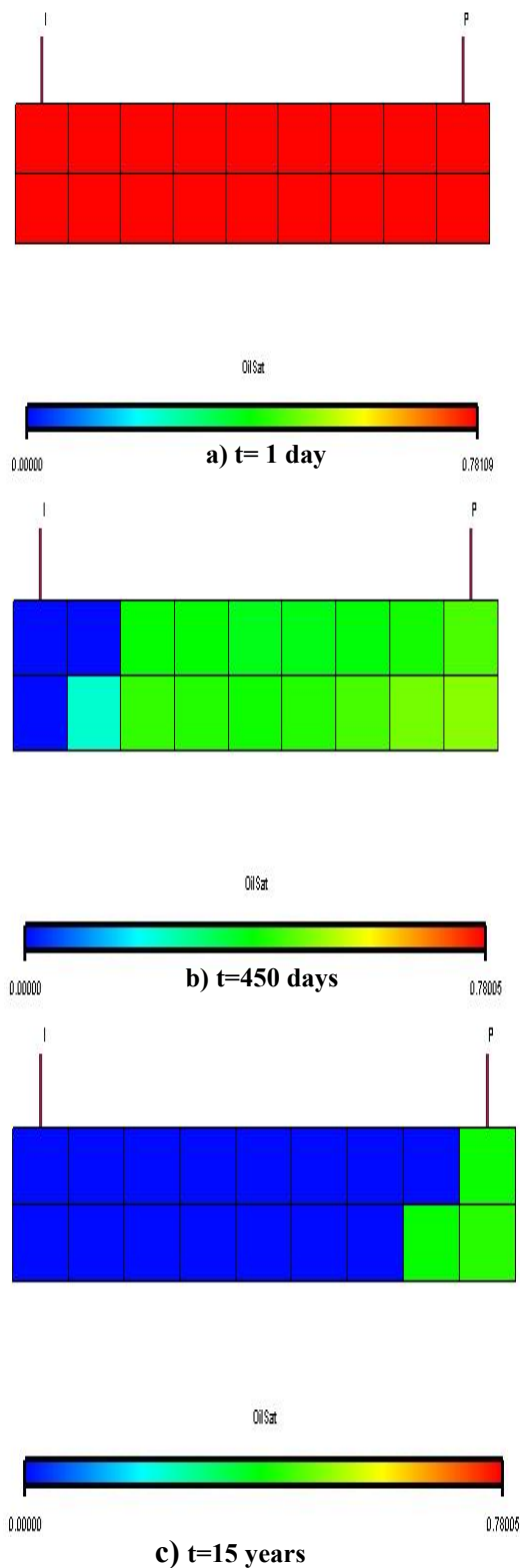


**Fig. 3.16—Saturation profiles at 4,400 psi**

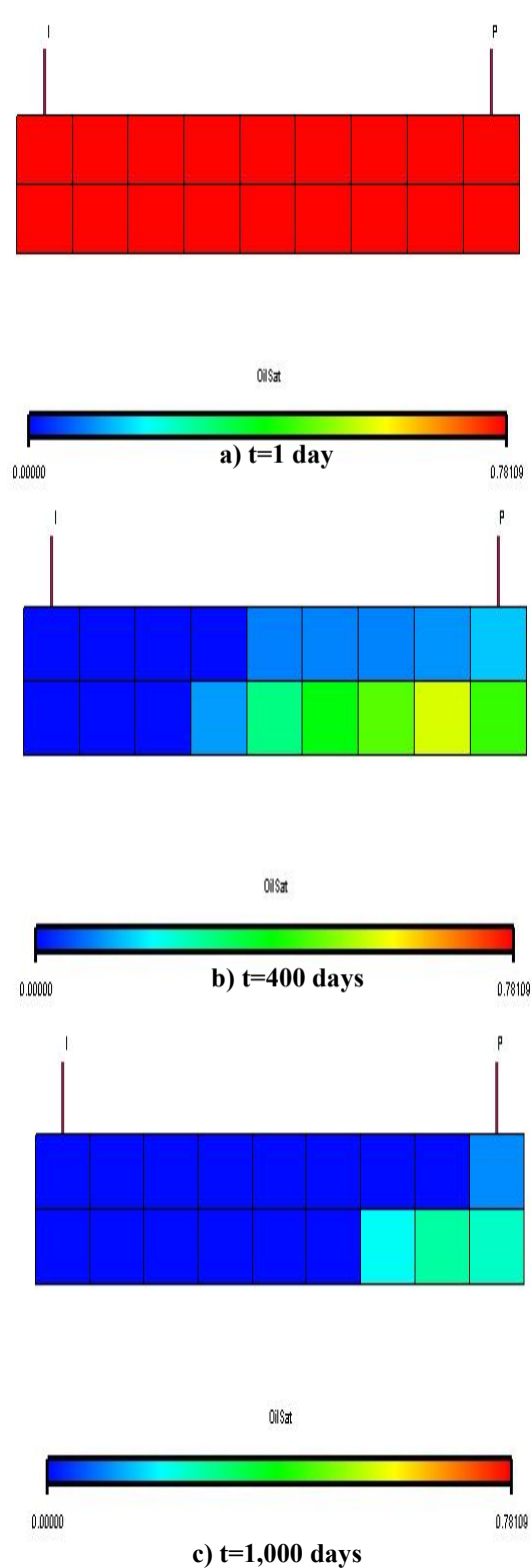


**Fig. 3.17—Saturation profiles at MMP=5,000**

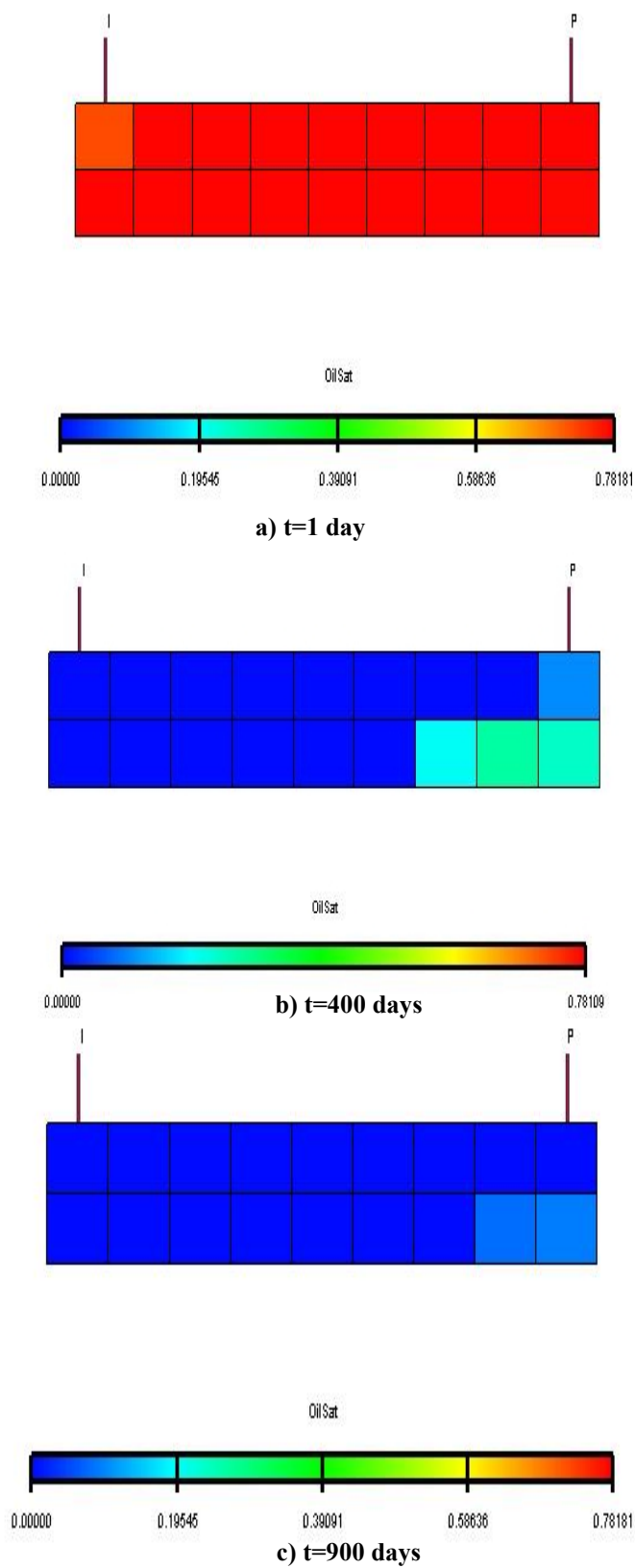


**Fig. 3.18— Saturation profiles at 5,600 psi ( $P > \text{MMP}$ )**

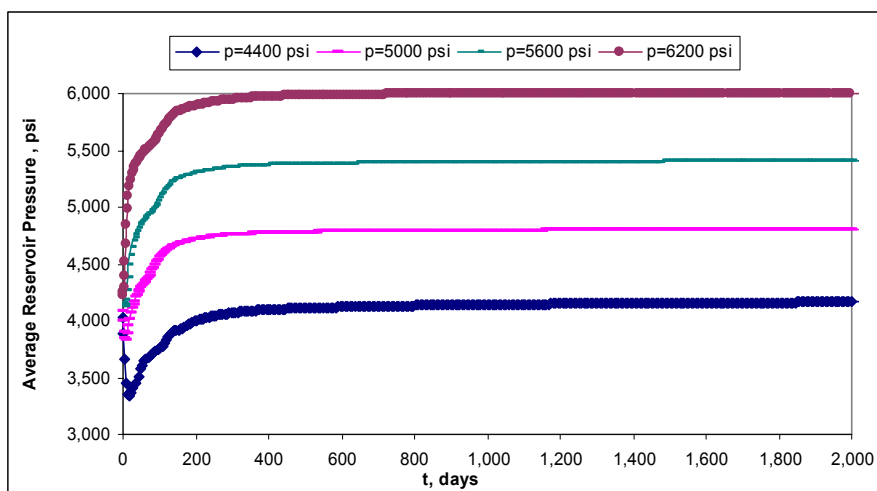


**Fig. 3.19—Variation in reservoir pressure during gas injection at different injection pressures**

Predicted oil recoveries, provided in **Figs. 3.20** and **3.21**, (increasing order in injection pressure) after 8.9, 9.11, 9.18 and 9.25 pore volumes of injection gas at the end of project are 82.25, 97.24, 97.5, and 97.65 %OOIP, respectively. Total recoverable reservoir oil is produced after 4,487, 3,882, and 3,665 days of miscible injection at 5,000, 5,600, and 6,200 psi, respectively.

Gas formation volume factor was used in recovery calculations to convert cumulative injection gas to the number of injected gas pore volumes. Gas formation volume factor can be calculated easily by knowing average reservoir pressure and injection gas composition.

Estimated recoveries at 1.2 pore volume of injected gas are about 50.9, 75.2, 79.6, and 82.6 %OOIP which are attainable after 677, 537, 486, and 444 days of continuous gas injection, respectively. It is clearly seen that incremental oil recovery due to miscible injection is paramount; however the marginal increase in oil recovery as the result of injection at pressures higher than MMP may not compensate for additional equipment and operating costs at greater pressures. Oil recoveries are usually greatest when the gas injection process is operated under miscible conditions. Miscibility can be achieved by managing the reservoir pressure. Under appropriate condition of achieving miscibility, MMP will be the optimum injection pressure.

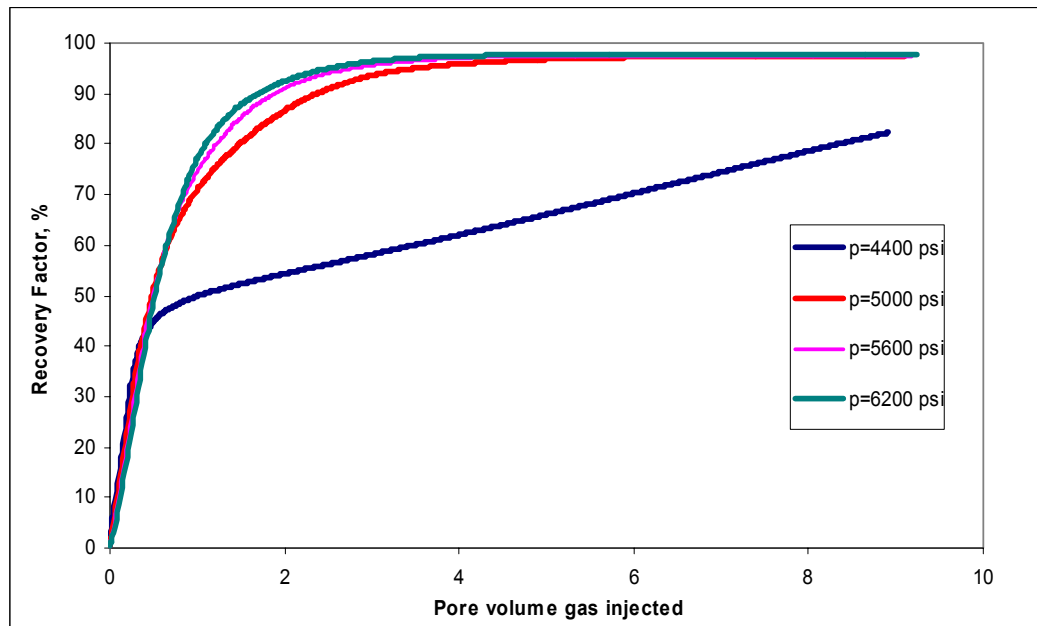


**Fig. 3.20—Incremental oil recovery after around 4 pore volume of injected gas is marginal at pressures above MMP**

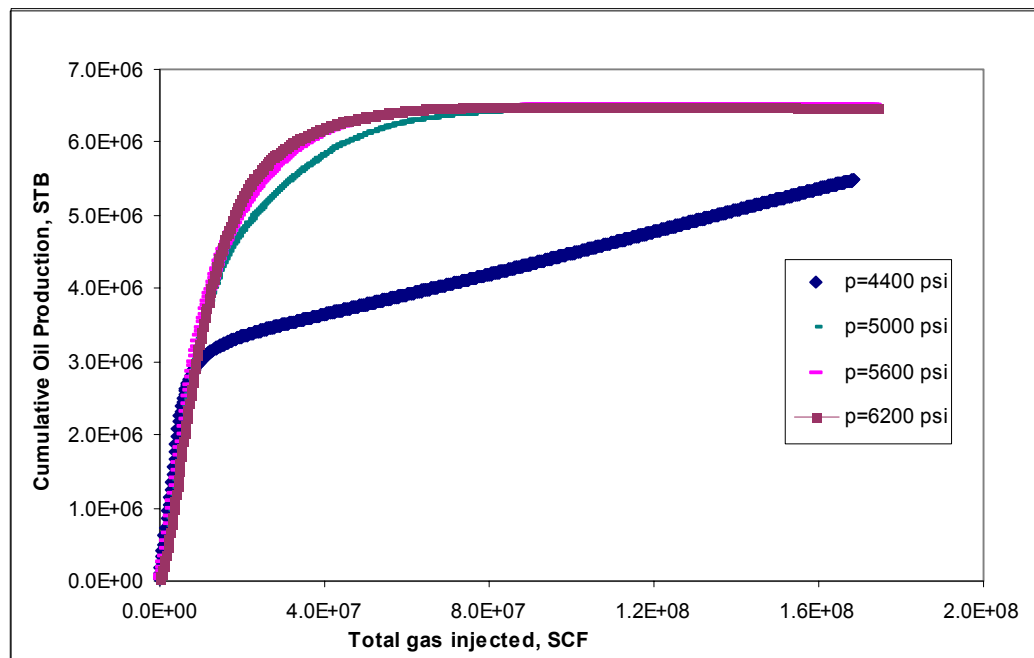
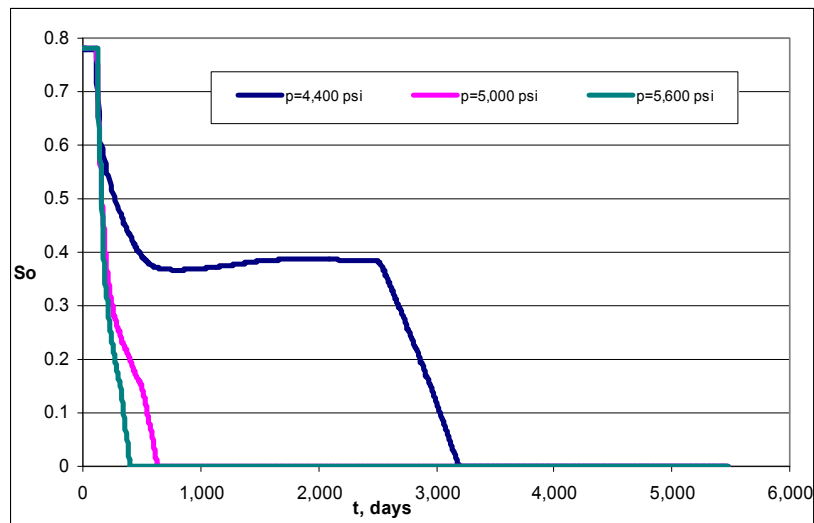


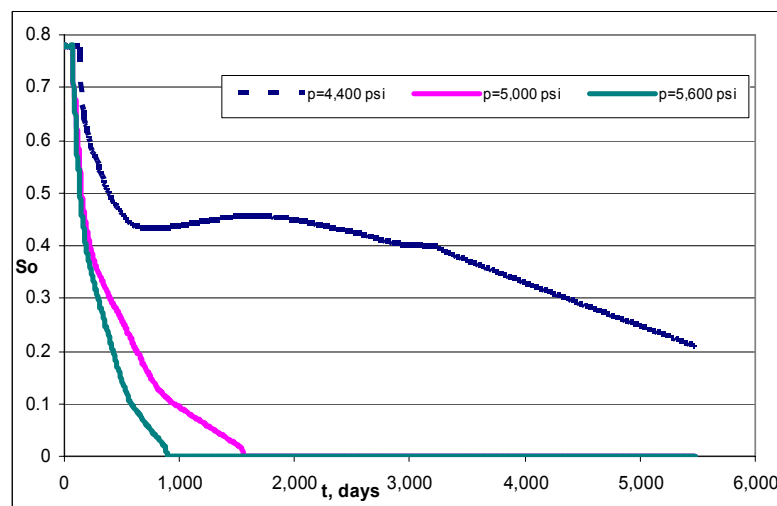
**Fig. 3.21—Cumulative oil production at above MMP and below the MMP injection pressures**

### 3.2.4 Vertical Permeability Effect

Setting the  $k_v/k_h$  ratio, from base value of  $10^{-1}$  to  $10^{-4}$  cause some changes in reservoir performance and calculated oil recovery from the reservoir because the



a) grid (5,5,1)



b) grid (5,5,2)

Fig. 3.22—Oil saturation profile of grid (5,5,1) and (5,5,2) for vertical permeability of 0.009 and different injection pressures

vertical communication is reduced. This is for the case which the injection and production constraints remain the same.

**Figs. 3.22** shows the variation in oil saturation of the gridblocks (5,5,1) and (5,5,2). Summary of comparison results with Figs. 3.14 and 3.15 for different vertical to horizontal permeability ratios are provided in **Table 3.13**.

The results indicate that gas breakthrough time increases as vertical permeability decreases. At lower vertical permeability values, thorough oil sweepout of the particular grids occurs at later times due to poorer vertical sweepout efficiency.

**Table 3.13—Comparison of oil saturation profiles for different  $k_v/k_h$  ratio**

P, psi	Time of gas breakthrough into grid (5,5,1), days		Time of gas breakthrough into grid (5,5,2), days		Time of oil sweepout for grid (5,5,1), days		Time of oil sweepout for Grid (5,5,2), days	
	$K_v=9$ md	$K_v=0.009$ md	$K_v=9$ md	$K_v=0.009$ md	$K_v=9$ md	$K_v=0.009$ md	$K_v=9$ md	$K_v=0.009$ md
4,400	38	118	64	138	2,847	3,193	3,471	>5,475
5,000	39	123	77	74	480	1,076	745	1,568
5,600	49	127	86	73	259	407	415	903

**Fig. 3.23** indicates the average reservoir pressure during 15 years of injection. After initial instability, reservoir pressure increases gradually till it becomes steady at pressures, around 400 psi below the injection pressures. The reduction in average reservoir pressure is 200 psi greater than reservoir pressure with vertical permeability of 9 md (Fig. 3.19).

**Table 3.14** compares the estimated oil recoveries of reservoirs with different vertical permeabilities and oil zone height of 80 ft. The predicted recoveries are tabulated at 1.2 pore volumes of injected gas at different injection pressures and after 15 years of injection. It can be observed that the number of pore volumes injected increases as the injection pressure increases and so does the recoveries although the incremental change is not substantial. Additionally, lower vertical permeabilities cause lower oil recoveries due to lower vertical communication between two layers.

Lower vertical permeability not only decreases the recovery efficiency of the reservoir but also it lowers the gas injectivity. This is valid for both miscible and



immiscible displacement mechanism. It takes longer time to inject same amount of gas in to the reservoir with lower vertical permeability.

It should be noticed that in reservoirs with pay zone extends vertically, the low ratio of vertical to horizontal permeabilities can minimize the segregation of the gas and displaced fluid and improve the oil recovery but this not the case for this study.

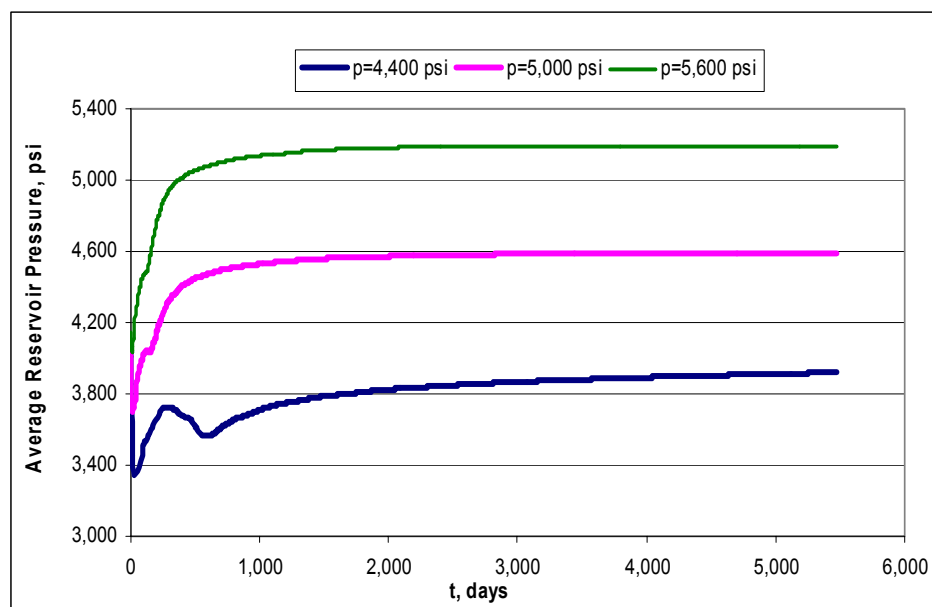


**Fig. 3.23—Lower vertical permeability ( $k_v=0.009$  md) decreases the average reservoir pressure 200 psi greater than that of reservoir with  $K_v=9$  md**

**Table 3.14—Effect of  $k_v/k_h$  ratio on calculated oil recovery**

P, psi	Calculated oil recovery at 1.2 pore volume injection				Calculated oil recovery after 15 years of injection			
	$k_v=9$ md		$k_v=0.009$ md		$k_v=9$ md		$k_v=0.009$ md	
	t, days	Recovery factor, %	t, days	Recovery factor, %	Pore volume injected	Recovery factor, %	Pore volume injected	Recovery factor, %
4,400	677	50.9	933	45.6	8.9	82.2	8.5	70.32
5,000	537	75.2	632	67.1	9.11	97.2	8.98	96.36
5,600	444	79.6	573	69.9	9.18	97.5	9.08	96.58

### 3.2.5 Effect of Well Completion on Recovery Efficiency

This part of the study considers the effect of well completion on performance recovery from the homogeneous or heterogeneous reservoirs. In the homogeneous case, different vertical permeabilities (9 & 0.009 md) were investigated. For the heterogeneous reservoir, the effect of permeability stratification of two layers of the reservoir is the subject of the study. Layer permeability can take values of 9 and 0.009 md.

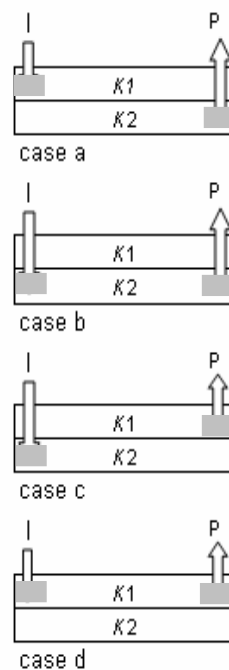


**Fig. 3.24—Different completion patterns**

Four different completion patterns were investigated. These are provided in **Fig. 3.24**. Injection to the 1st and production from the 2nd layer (case a), Injection and production from the second layer (case b), injection to the second and production from the first layer (case c), and injection and production from the first layer, cause a variety of completion patterns that may occur in the reservoir.

### 3.2.5.1 Recovery Performance

**Table 3.15** summarizes the result of several simulation runs for the homogeneous reservoir. Simulation results indicate that reservoir performance for completion patterns a and c are so close. Similar performance was also predicted for patterns b and d. As this table indicates, higher oil recovery is predicted for case a where the injection well is perforated on the first layer. This is valid for miscible or immiscible displacement of the oil. The differences in calculated recoveries at 1.2 pore volume of injected gas for case a and b with vertical permeability 0.009 md and at injection pressures of 4,400 and 5,600 psi, are 13.03 and 20.77 %OOIP. This demonstrates that recovery efficiency even in miscible displacement mechanism and at injection pressures above the MMP is considerably dependent on injection-well completion pattern. The effect of injection- well completion on the calculated oil recovery between two cases is more significant in the homogeneous reservoirs with low vertical permeability values. The influence of injection well completion on the recovery performance is more significant in reservoirs with thick pay zones. Lower GOR and consequently produced gas from the reservoir after 1.2 pore volume of miscible gas injection in addition of the higher oil recovery, could be accounted as efficient miscible displacement characteristics.

The next section is dedicated to the effect of well completion on the oil recovery from a heterogeneous reservoir. Four completion patterns for each injection pressure along with location of the permeable layer (upper or lower layer) generate 16 combinations of injection patterns. **Table 3.16** provides the summarized simulation data at 1.2 pore volume of injected gas into a stratified reservoir with vertical permeability of 9 and 0.009 mD for the first and second layers. The areal permeability of the layers remained as its base value, 90 md. As this table indicates, for three different injection pressures, case a represents the highest oil recovery value among the other cases. Thus, it is advantageous to make use of any favorable influence of gravity forces in the oil recovery even in miscible displacement. A comparison of calculated recovery factors for injection pressures of 5,000 and 5,600

psi illustrates that as miscibility develops efficiently with increasing pressure, the effect of injection well completion or gravity forces will be paramount (**Fig. 3.25**).

Similar simulation runs were conducted for the case which the permeable layer of the heterogeneous reservoir is located on the bottom of the pay zone. Simulation results indicate equal estimated properties with those provided in Table 3.15.

**Table 3.15—Performance of the homogeneous reservoir at 1.2 pore volume of injection**

**a) Injection pressure: 4,400 psi (immiscible displacement)**

case	$K_v$ , md	Recovery Factor, %	GOR, Mscf/STB	Injection-well completion layer	Production-well completion layer
a	0.009	45.56	72.67	1	2
b	0.009	32.53	31.73	2	2
c	0.009	45.55	72.67	2	1
d	0.009	32.53	31.73	1	1
a	9	50.95	57.24	1	2
b	9	50.74	57.51	2	2
c	9	50.95	57.24	2	1
d	9	50.74	57.51	1	1

**b) Injection pressure: 5,600 psi (miscible displacement)**

case	$K_v$ , md	Recovery Factor, %	GOR, Mscf/STB	Injection-well completion layer	Production-well completion layer
a	0.009	69.93	10.97	1	2
b	0.009	49.16	33.54	2	2
c	0.009	69.93	10.97	2	1
d	0.009	49.16	33.54	1	1
a	9	79.6	11.5	1	2
b	9	79.8	11.7	2	2
c	9	79.6	11.5	2	1
d	9	79.8	11.7	1	1

Reservoir performance was the same for each completion case with higher vertical permeability ratios, whether the permeable layer is located on the top or on the bottom of the reservoir. This behavior could be attributed to the equal transmissibility of the fluid flowing through the  $z$  direction in each case. Transmissibility factor for the flow of fluid from gridblock  $i$  to gridblock  $i+1$ , in the  $z$  direction is as follows:

$$T = 0.01266\Delta y \left[ \frac{(k\Delta x)_i \times (k\Delta x)_{i+1}}{(k\Delta x)_{i+1} \Delta x_i + (k\Delta x)_i \Delta x_{i+1}} \right] \dots\dots\dots (16)$$

**Table 3.16—Heterogeneous-reservoir performance at 1.2 pore volume (22,700 MMScf) of miscible or immiscible injection gas**

**a) Injection pressure:4,400 psi (Immiscible displacement)**

case	Recovery Factor, %	GOR, MScf/STB	Injection-well completion layer	Production-well completion layer	$k_1$	$k_2$
a	47.45	64.56	1	2	9	0.009
b	38.66	20.23	2	2	9	0.009
c	47.38	64.72	2	1	9	0.009
d	38.16	20.6	1	1	9	0.009

**b) Injection pressure:5,000 psi (miscible displacement)**

case	Recovery Factor, %	Gas/oil ratio, MScf/STB	Injection-well completion layer	Production-well completion layer	$k_1$	$k_2$
a	70.22	12.6	1	2	9	0.009
b	50.02	21.48	2	2	9	0.009
c	70.02	12.74	2	1	9	0.009
d	49.66	22.06	1	1	9	0.009

**c) Injection pressure:5,600 psi (miscible displacement)**

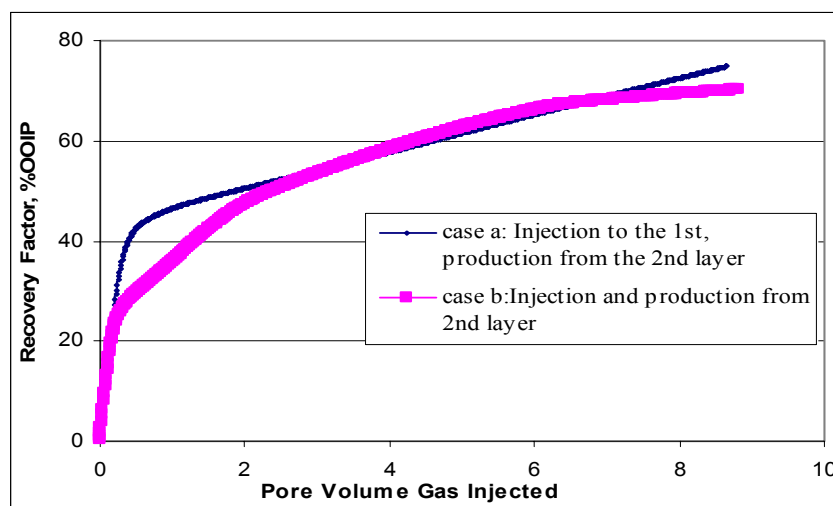
case	Recovery Factor, %	Gas/oil ratio, MScf/STB	Injection-well completion layer	Production-well completion layer	$k_1$	$k_2$
a	73.21	10.76	1	2	9	0.009
b	51.67	27.39	2	2	9	0.009
c	73.02	10.89	2	1	9	0.009
d	51.4	29.46	1	1	9	0.009

Subsequent sections are devoted to the discussion and study of the reservoir performance and fluid properties necessary to have a better understanding of fluid displacement in the heterogeneous reservoir

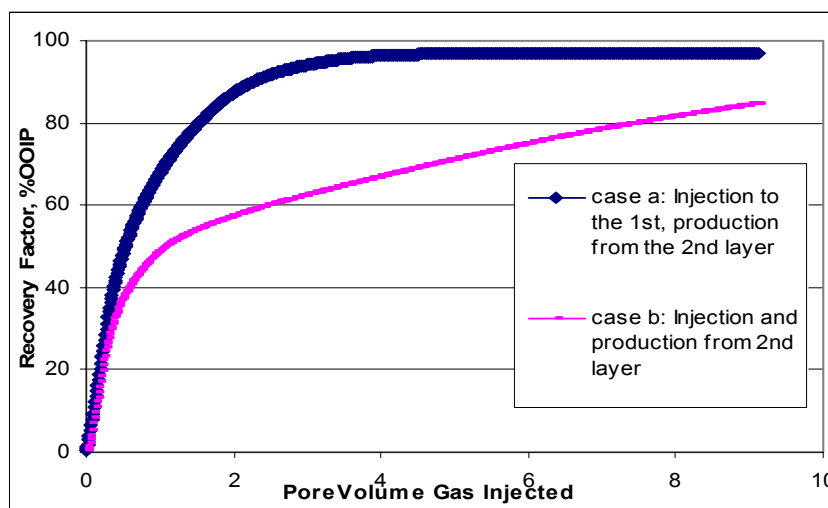
### 3.2.5.2 Saturation Profiles

Since the simulation results for pair cases a&c and b&d represent similar trends in most cases because of equal fluid transmissibility between layers, only the results for cases a and b at injection pressures of 4,400 and 5,600 psi are reported. These injection pressures are representatives of immiscible and miscible

displacement mechanisms in the reservoir. Injection pressure 5,600, which is 600 psi above the **MMP** value of the injection gas/reservoir fluid system, ascertains development of miscibility in the reservoir.



a) Effect of well-completion on immiscible oil recovery (Injection pressure: 4,400 psi)



b) Effect of well-completion pattern on miscible oil recovery (Injection pressure: 5,600 psi)

**Fig. 3.25—Significant increase in miscible oil recovery in case a completion pattern compared to immiscible displacement**

**Fig. 3.26** represents the variation in oil and gas saturations of cells (5,5,1) & (5,5,2) for different completion patterns. Various slopes in each plot indicate different rate of oil sweepout in each gridblock. Since the vertical permeability of the layers differs, the oil sweepout is also different for each layer. Breakthrough gas into a cell decrease the oil saturation of that cell to the critical oil saturation, then the injection gas initiates sweeping of the portion of the neighboring cells located on the other layer (at which the injection well is not perforated). Since then, the injection gas saturation in the cell located on the perforated layer (injection well) will reach its highest value (0.78). Unlike the immiscible saturation curves (Figs. 3.26.a and 3.26.b), continuous decreasing of oil saturation is observed for miscible fluid displacement (Figs. 3.26.c and 3.25.d).

**Figs. 3.27** through **3.29** provide considerable information to visualize the displacement of the reservoir fluid by the miscible or immiscible gas front. These profiles are the  $x$ - $z$  cross-section views of the stratified reservoir. The reservoir consist of two layers with vertical permeabilities of 9 (the first two rows of the grids) and 0.009 md. The oil saturation profiles pertain to the diagonal grids located on the shortest distance between the injector and producer wells. Case a refers to the

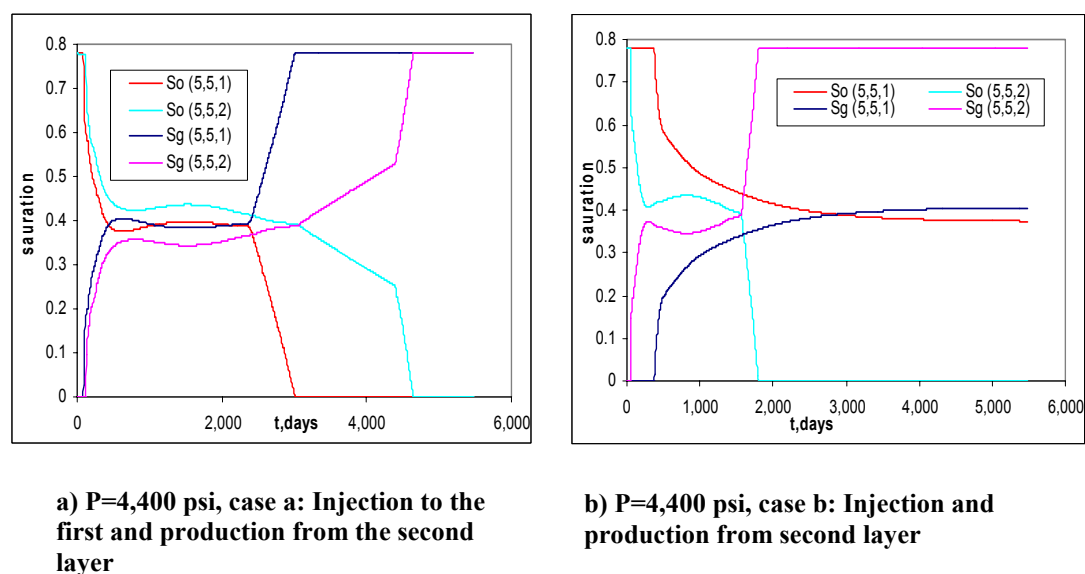


**Fig. 3.26—Oil and gas saturation profiles of grids (5,5,1) & (5,5,2)**

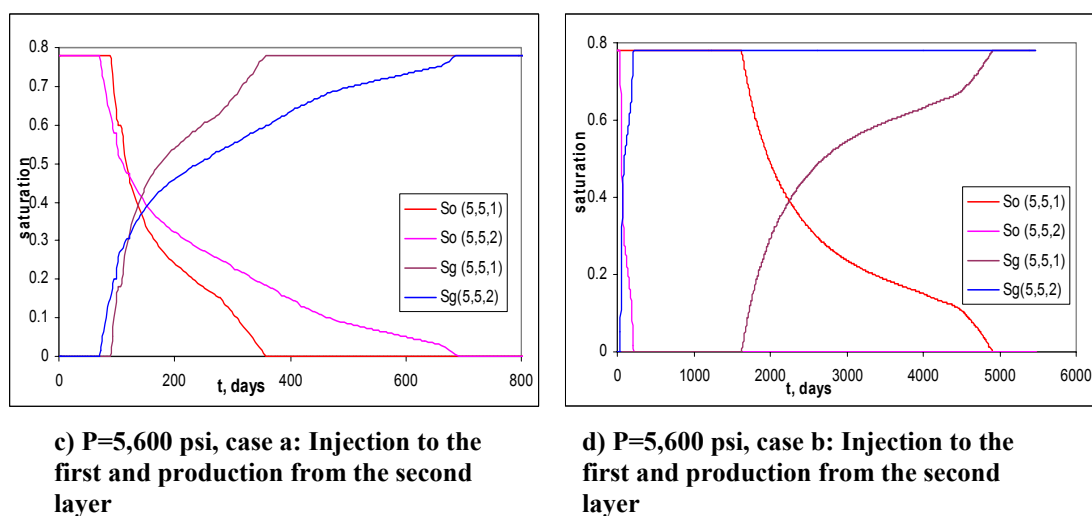
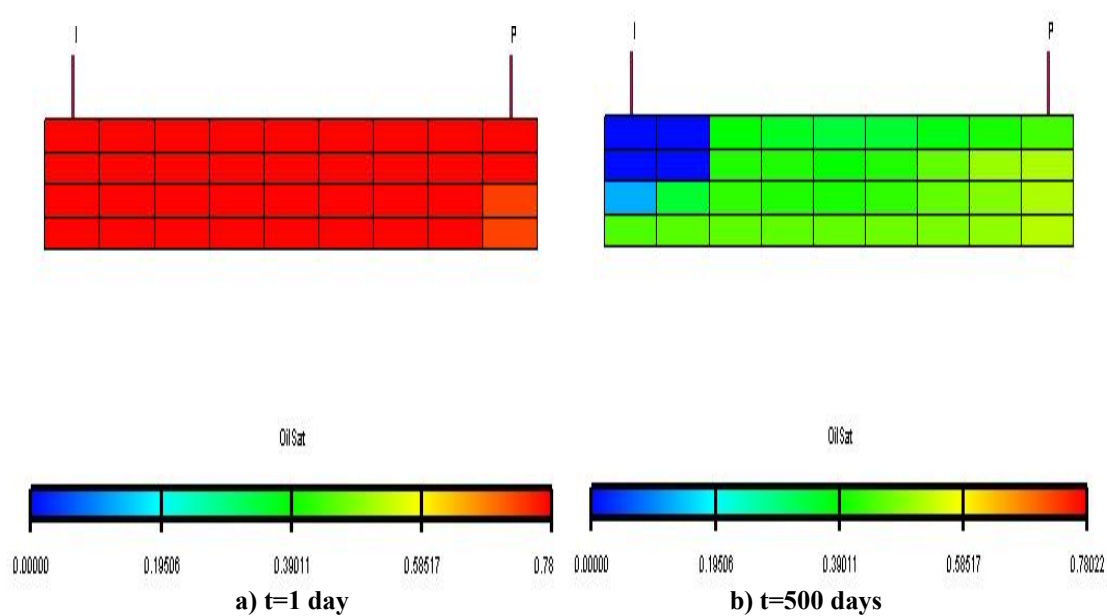


Fig. 3.26—Continued

completion case where the injection well is perforated on the first layer, whereas in case b both injection and production wells are completed in the second layer (rows three and four) with vertical permeability of 0.009 md. Lower oil saturation in these completion intervals is observed compare to neighboring grids at each time step (Figs. 3.28 and 3.29)



**Fig. 3.27—Oil saturation profiles at 4,400 psi (case a: injection to the first and production from the second layers)**



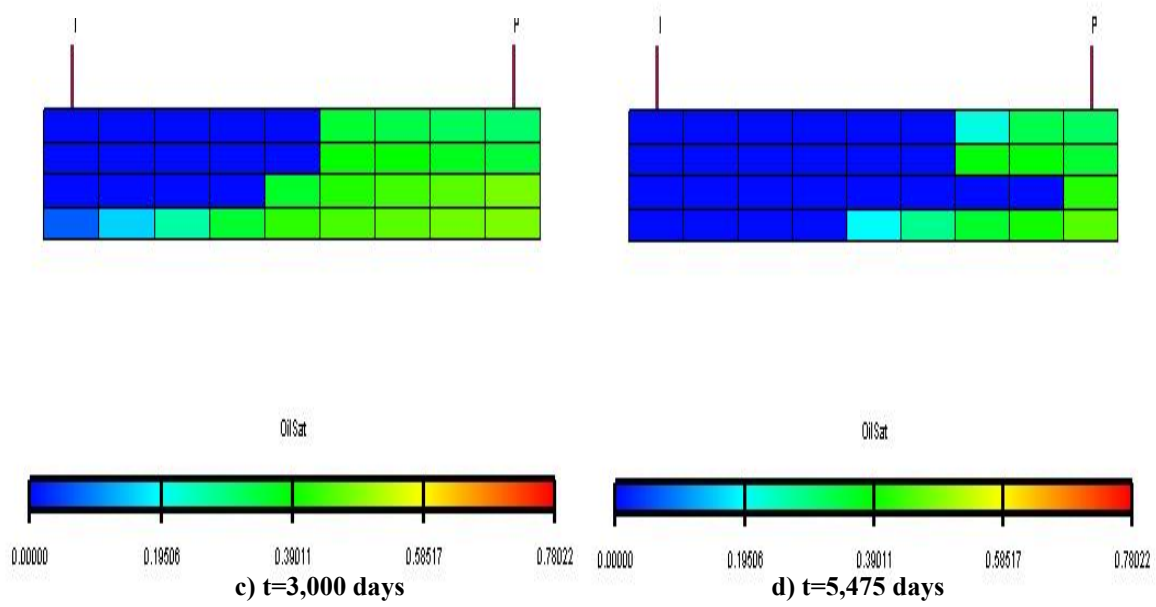


Fig. 3.27—Continued

Low vertical communication between two layers due to the high vertical permeability contrast of these layers (1000), cause the gas front to move ahead through the injection-well perforated layer. Instability in gas front is observed for both injection pressures. High portion of the stratified reservoir is swept in shorter times at the injection pressure of 5,600 psi compare to 4,400 psi.

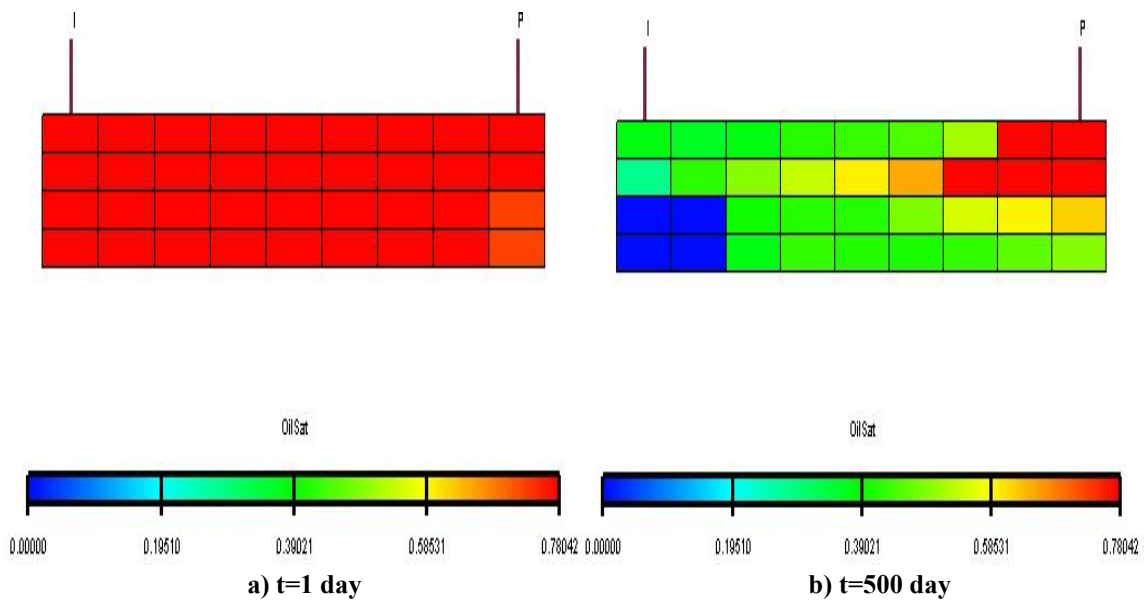


Fig. 3.28—Oil saturation profiles at 4,400 psi (case b: injection and production from the second layers)

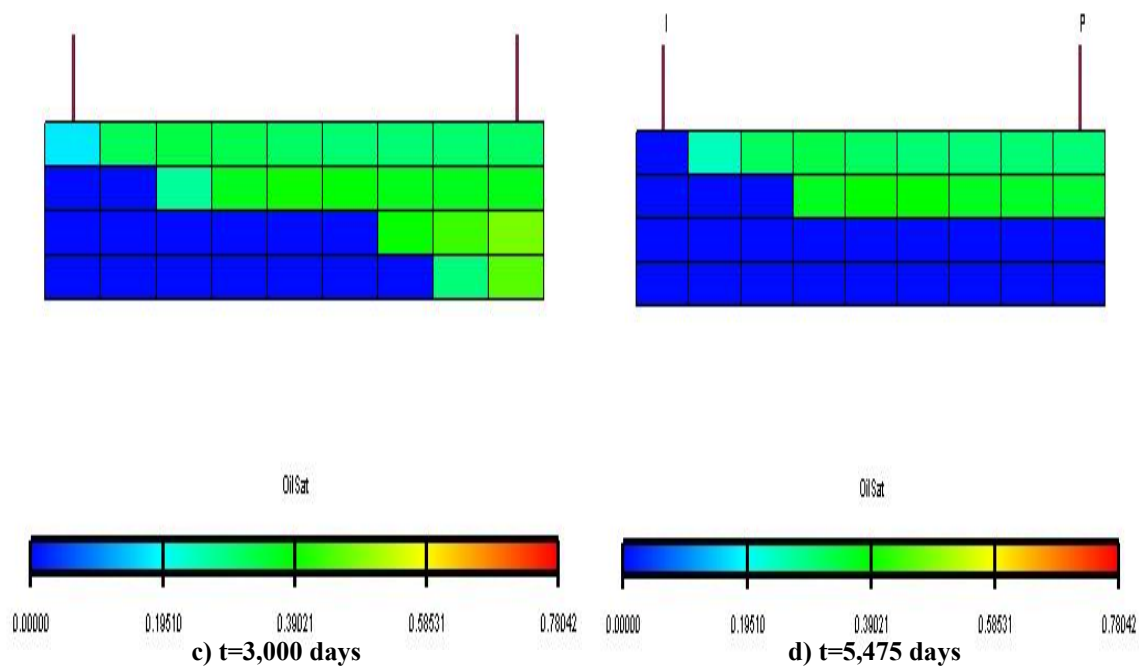


Fig. 3.28—Continued

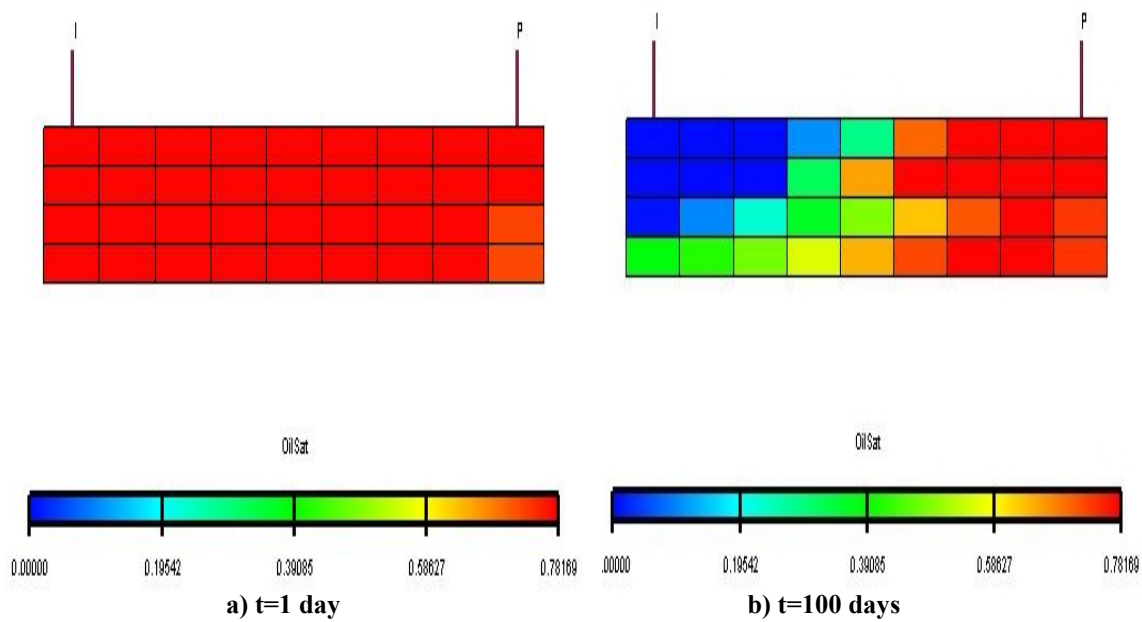
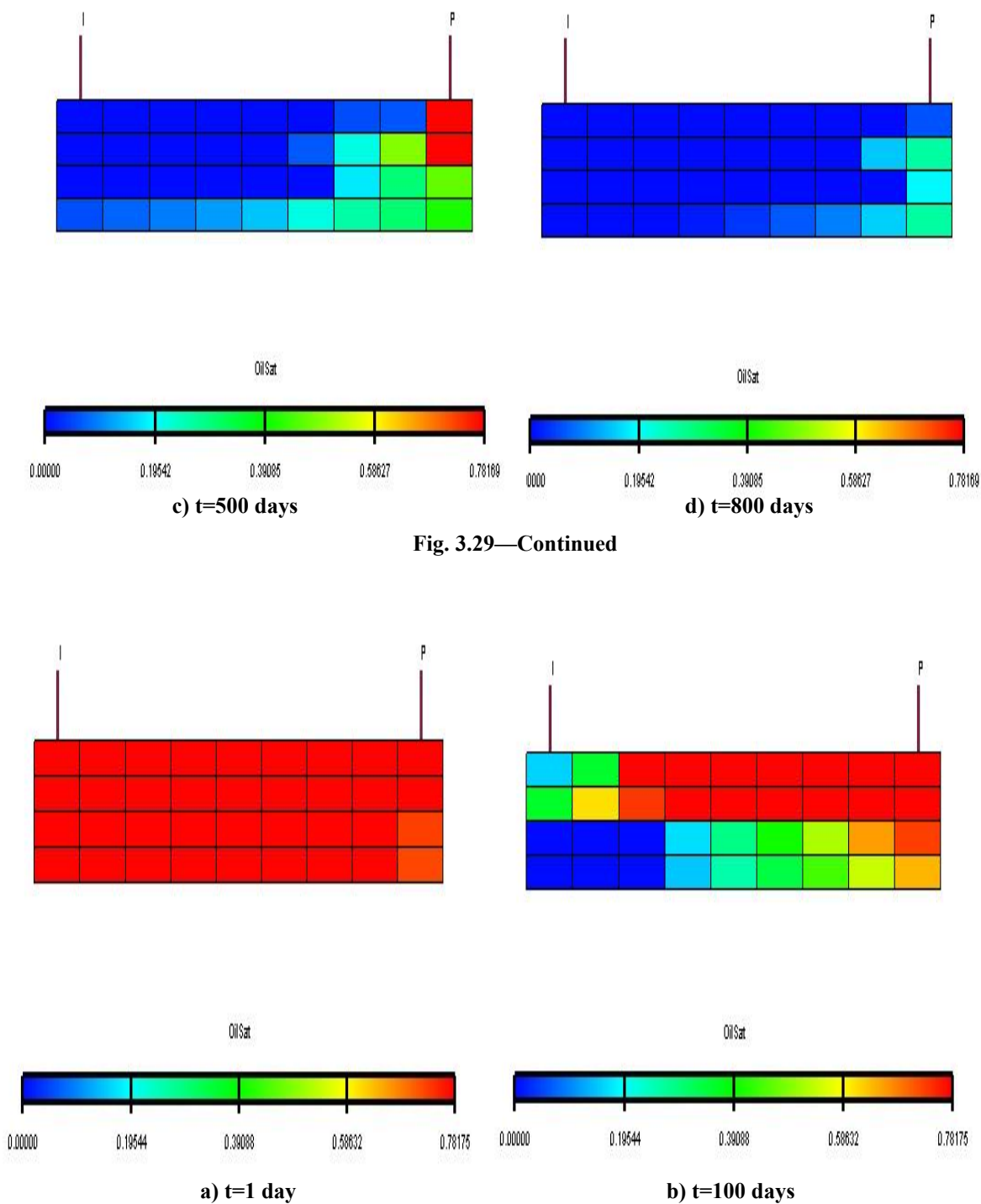


Fig. 3.29—Oil saturation profiles at 5,600 psi (case a: injection to the first and production from the second layers)



**Fig. 3.30—Oil saturation profiles at 5,600 psi (case b: injection and production from the second layers). Invaded gas into the second layer (rows three and four) sweeps this layer at earlier times**

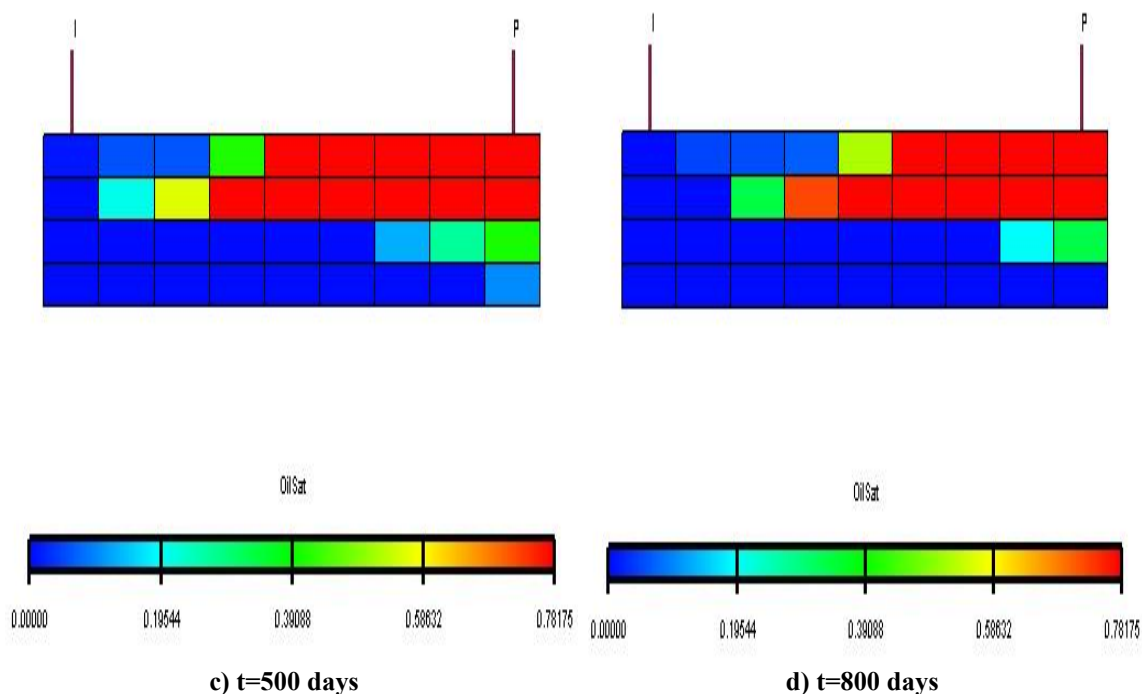


Fig. 3.30—Continued

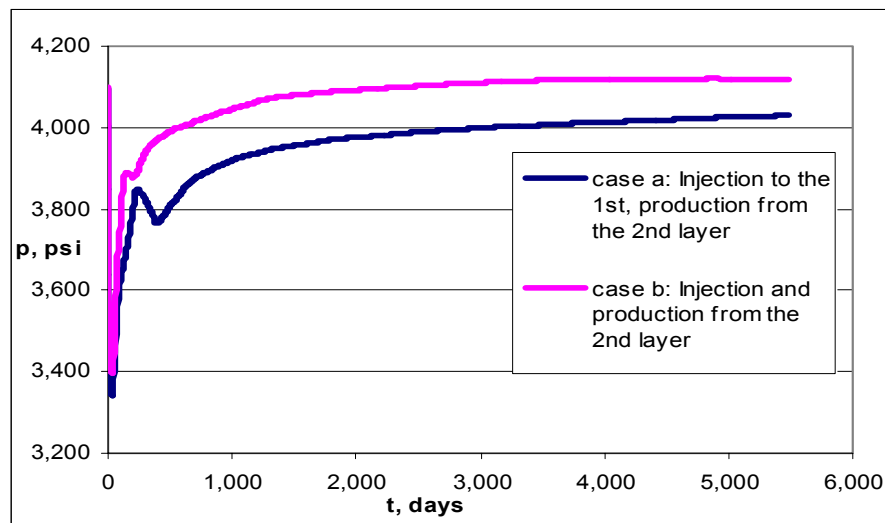
### 3.2.5.3 Pressure Variation

**Fig. 3.31** illustrates the effect of well completion on the average reservoir pressure. As was mentioned earlier, pair completion cases a&c and b&d (completion patterns provided in the Fig. 3.24) represent very similar behavior characteristics including reservoir pressure as well. As figure 3.31 indicates in case b, where the injection well is perforated on the second low permeable layer, the average reservoir pressure will be higher. It seems reasonable since the permeability difference of two layers is so high (vertical permeability ratio of 1000), the injected gas to the second layer can efficiently retrieve the pressure depletion caused by production well completed in this layer.

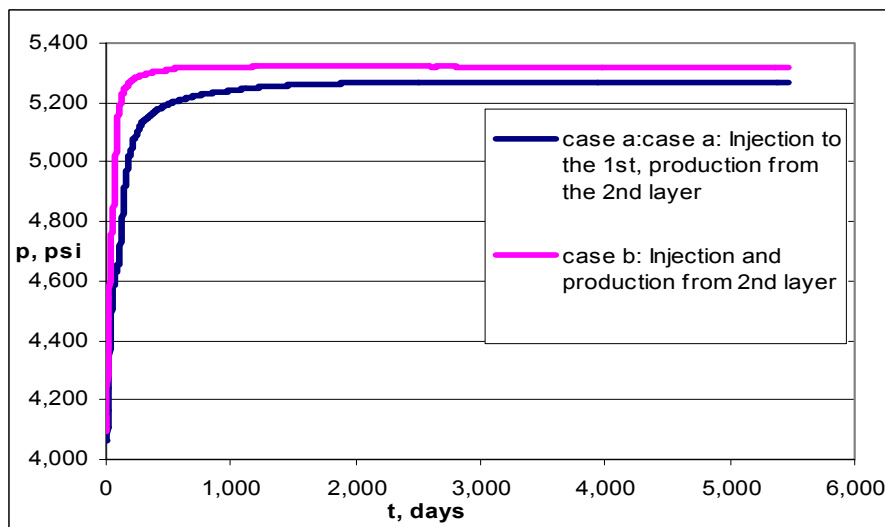
The pressure difference between a and b completion patterns is about 100 psi for immiscible displacement (Fig. 3.31.a). This pressure difference is much lower (50 psi) for miscible displacement.

**Figs. 3.32 through 3.35** show the pressure distribution in a  $x$ - $z$  cross section view of the stratified reservoir at different time steps. A key feature of the pressure

profile of the layers is depleted regions close to the production well. Reservoir pressure declines dramatically in these regions as soon as production begins. The cross-sectional model monitors the rate of movement of gas front, and high pressure regions being in contact with injected gas.



a) Injection pressure: 4,400 psi



b) Injection pressure: 5,600 psi

Fig. 3.31—Effect of well completion on average reservoir pressure

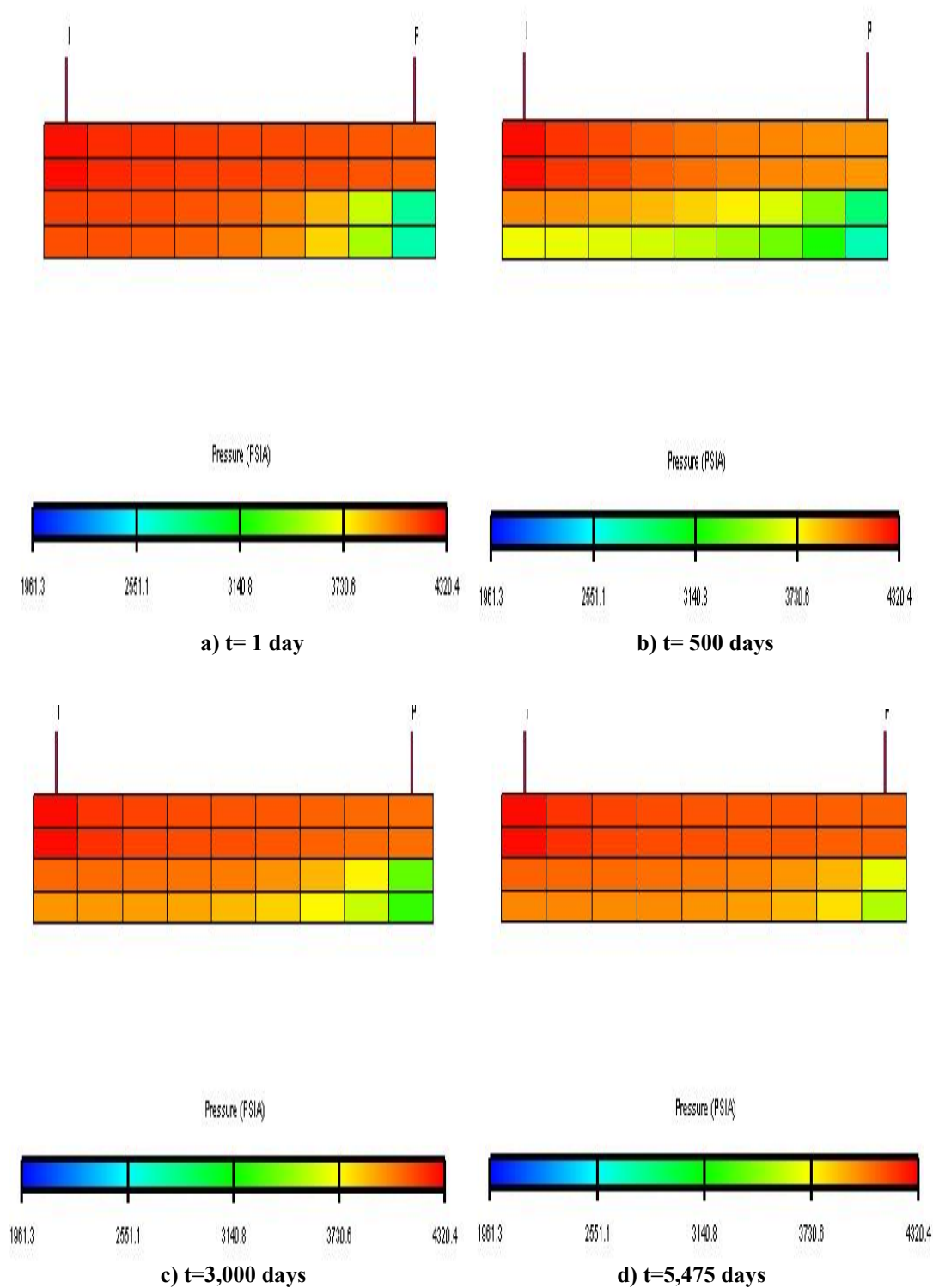


**Fig. 3.32—pressure distribution at 4,400 psi (case a: injection to the first and production from the second layers)**

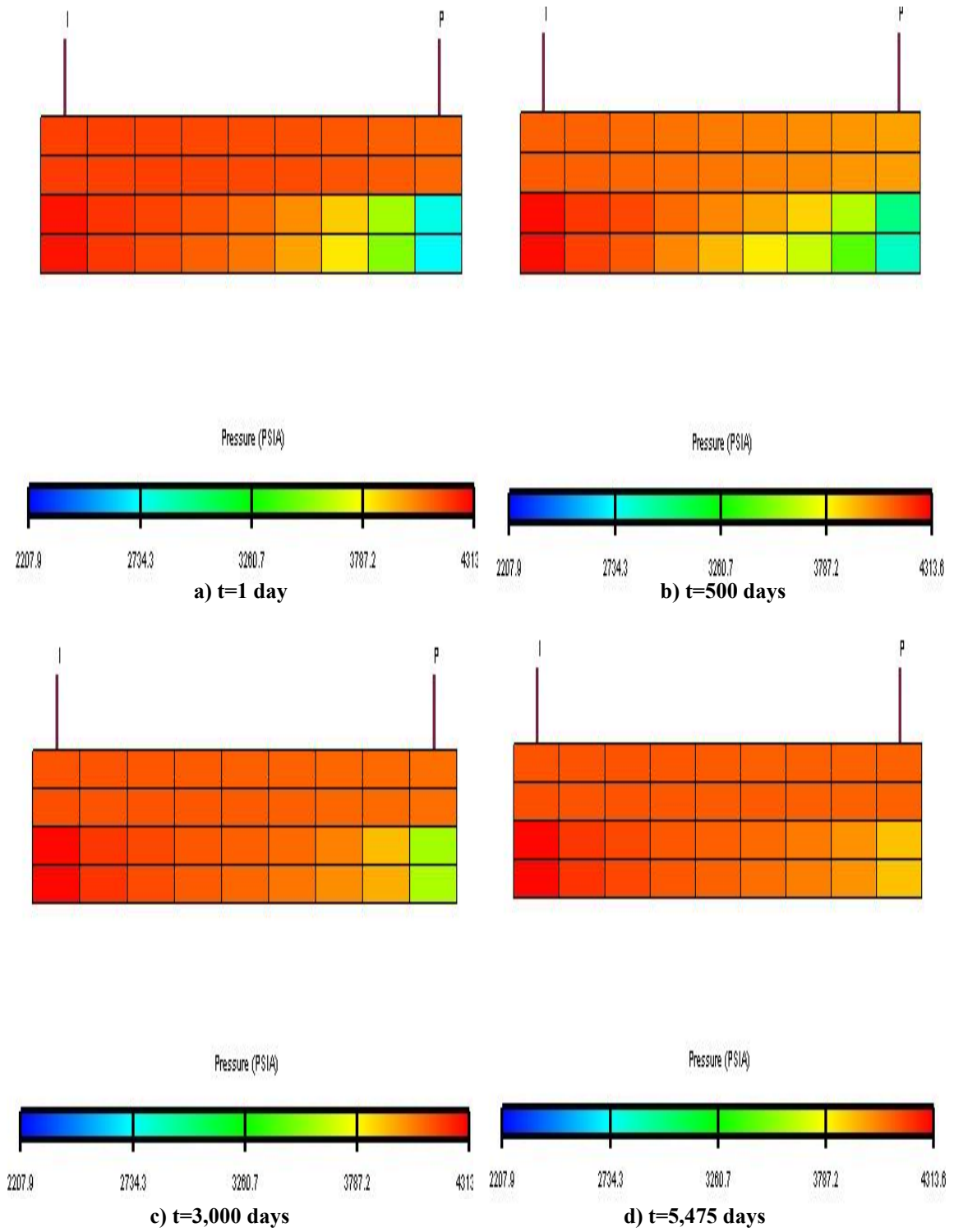


**Fig. 3.33—pressure distribution at 4,400 psi (case b: injection and production from the second layers)**

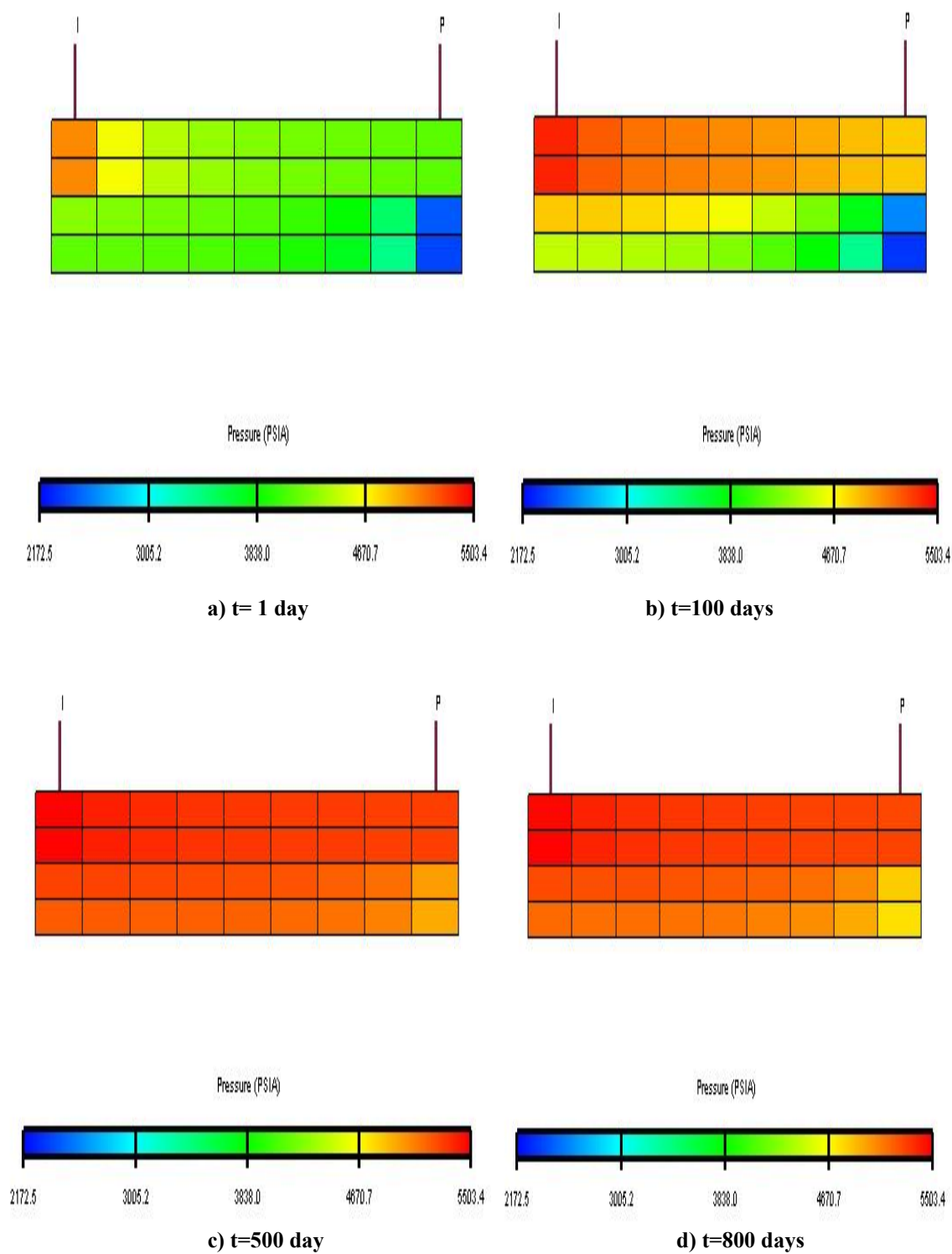


**Fig. 3.34—pressure distribution at 5,600 psi (case a: injection to the first and production from the second layers)**



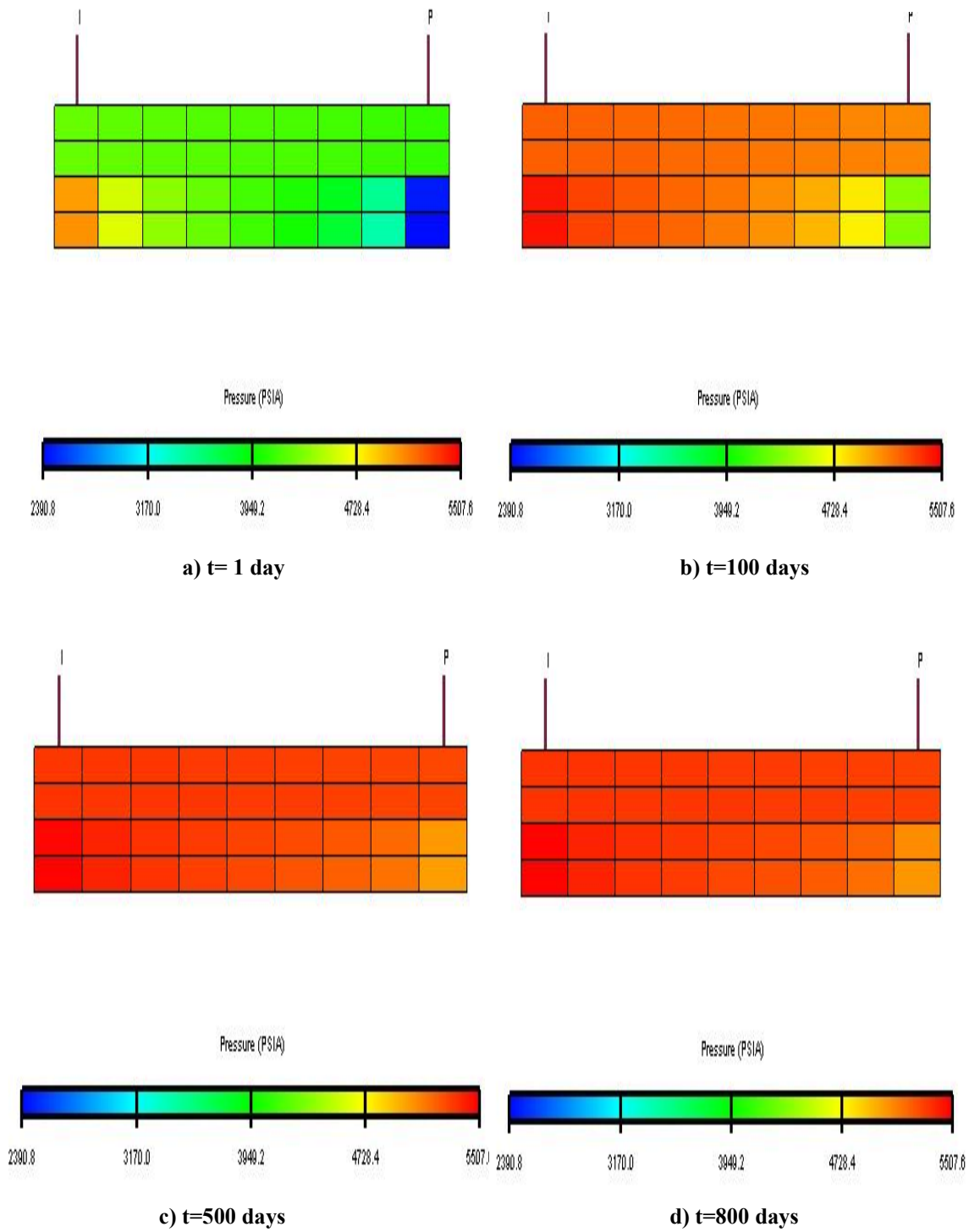
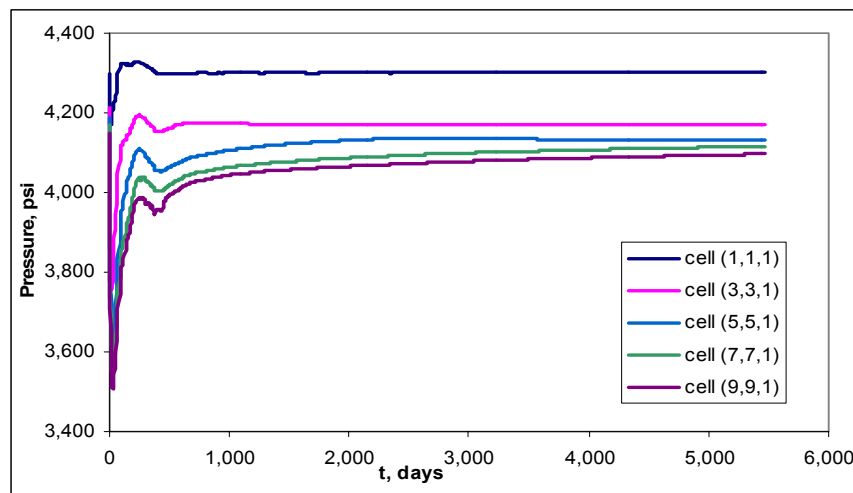
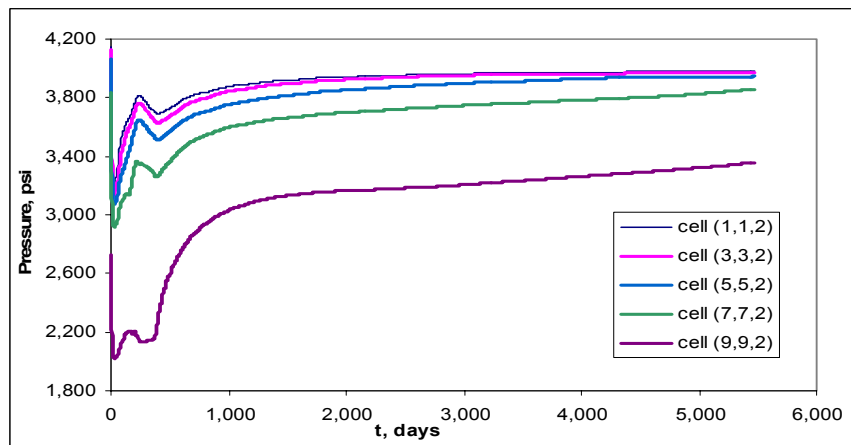


**Fig. 3.35—pressure distribution at 5,600 psi (case b: injection and production from the second layers)**

**Fig. 3.36** indicates the variation in pressure for the diagonal grids connecting injection and production wells. The average pressure difference of two layers is around 300 psi for both displacement mechanisms and the maximum achievable pressure, in regions close to the injection well, is approximately 200 psi below the injection pressure.

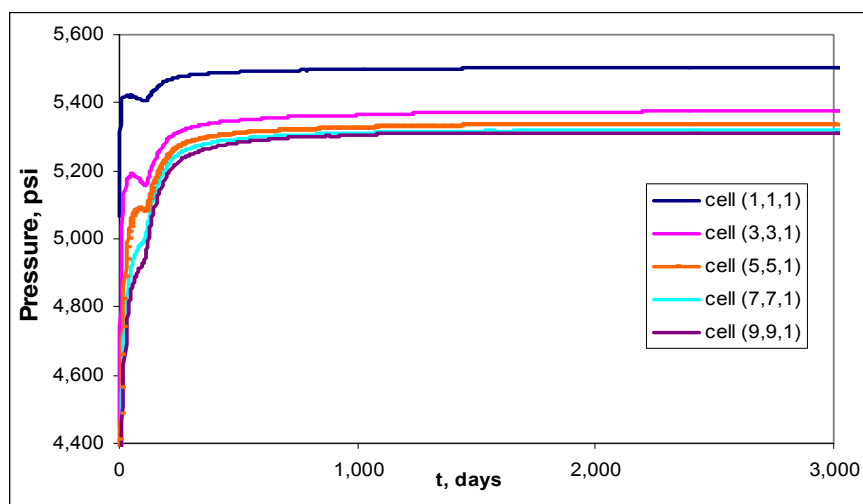


**a) Pressure distribution of the first layer at 4,400 psi (case a, Injection to the 1st and production from the 2nd layer)**

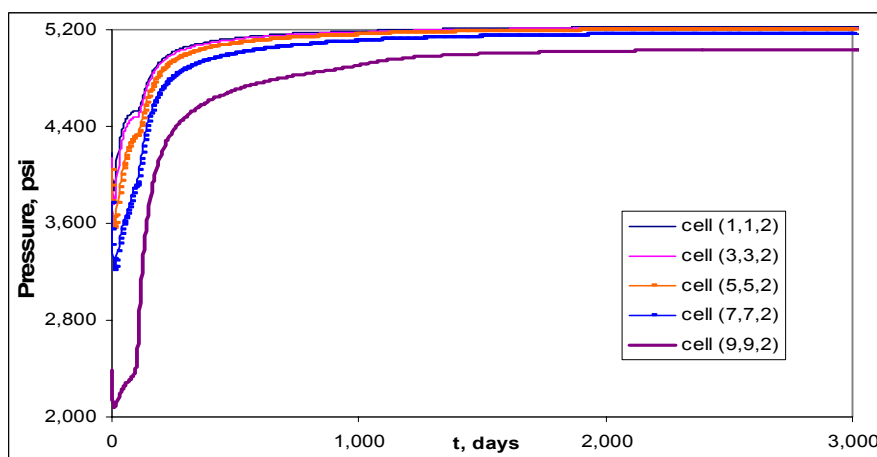


**b) Pressure distribution of the second layer at 4,400 psi (case a, Injection to the 1st and production from the 2nd layer)**

**Fig. 3.36—Variation in reservoir pressure during gas injection.**



c) Pressure distribution of the first layer at 5,600 psi (case a, Injection to the 1st and production from the 2nd layer)



d) Pressure distribution of the second layer at 5,600 psi (case a, Injection to the 1st and production from the 2nd layer)

Fig. 3.36—Continued

Unlike miscible displacement (5,600 psi), after the initial instability period a decreasing trend is observed in immiscible gas injection of the reservoir. This pressure depletion which occurs at the same time of injection into the both layers

(Figs. 3.36.a and 3.36.b) could be attributed to the loss of injection-gas rate or increase in liquid saturation (liquid drop out).

The production-well constraints are minimum bottomhole pressure of 1,000 psi and maximum gas production rate of 30,000 Mscf/day. The initial production-well bottomhole pressure (cell (9,9,2) in Fig. 3.36) is 1,000 psi. After a short time of production, bottomhole pressure increases and the production well constraint switches to the constant gas production rate of 30,000 Mscf/day. Since the maximum gas production rate remains constant with time, the more gas accumulated in the porous media, the higher the pressure will be.

The observed increasing pressure trend is proportional to the rate of fluid accumulation in the reservoir represented by **Fig. 3.37**. Different accumulation rates accounts for different pressure trends. Low value of accumulation towards the end of the project (Fig. 3.37) indicates that the vast amount of the injected gas into the second layer will be produced in completion pattern b and the reservoir pressure remains constant

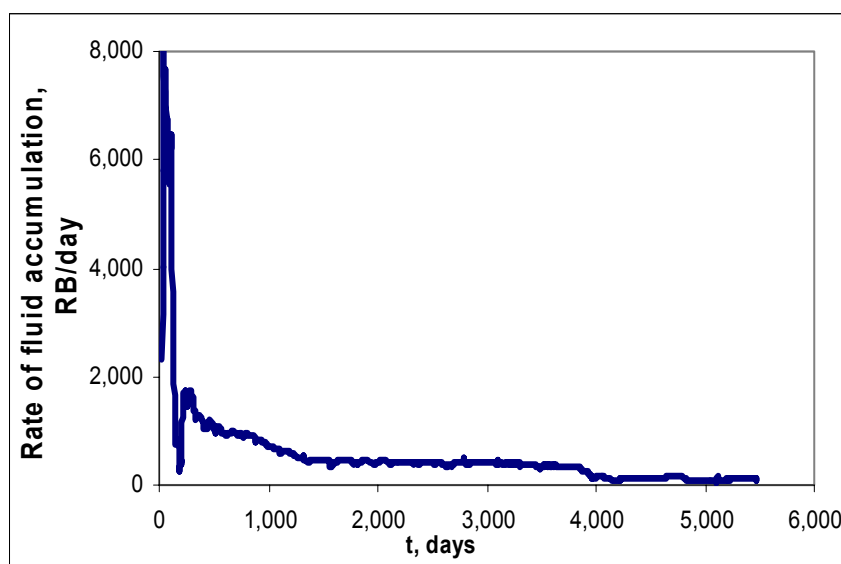


**Fig. 3.37—Fluid accumulation (Reservoir volume difference in total injected and produced fluids) during injection of gas at 4,400 psi at completion case b**

### 3.2.5.4 Fluid Viscosities

The proportionality factor relating the velocity of the fluid to the pressure gradient is called mobility. Fluid mobility is defined as the ratio of effective permeability of the rock to that fluid and fluid viscosity. The value of the mobility is dependent upon the fluid saturation.

Mobility ratio is defined as the ratio of the displacing fluid to oil mobility. In gas flooding it becomes

$$M = \frac{k_g}{\mu_g} \frac{\mu_o}{k_o} \dots\dots\dots (17)$$

in which  $k_g$  and  $k_o$  are the maximum or end-point relative permeabilities to gas and oil. **Fig. 3.38** represents a typical relative permeability curve for a gas/oil system. Therefore, the mobility ratio expresses the maximum velocity of gas flow to that of oil. Presence of unstable gas front is the problem with having free gas in the reservoir whether it evolved during depletion or is injected. The extremely low gas viscosity leads to high mobility ratios, usually resulting in early breakthrough and excessive gas production.

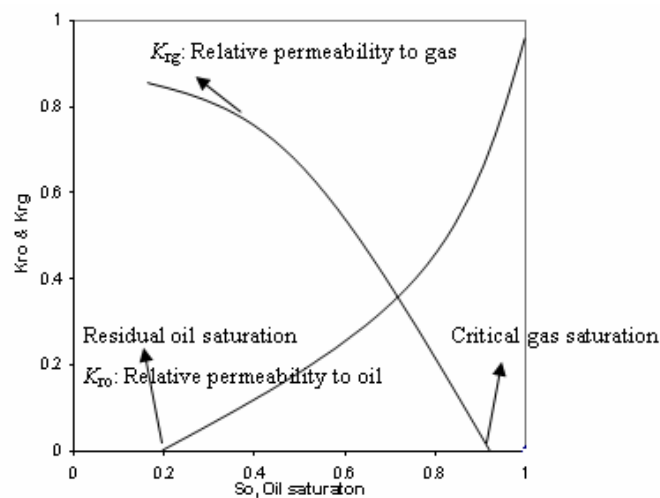
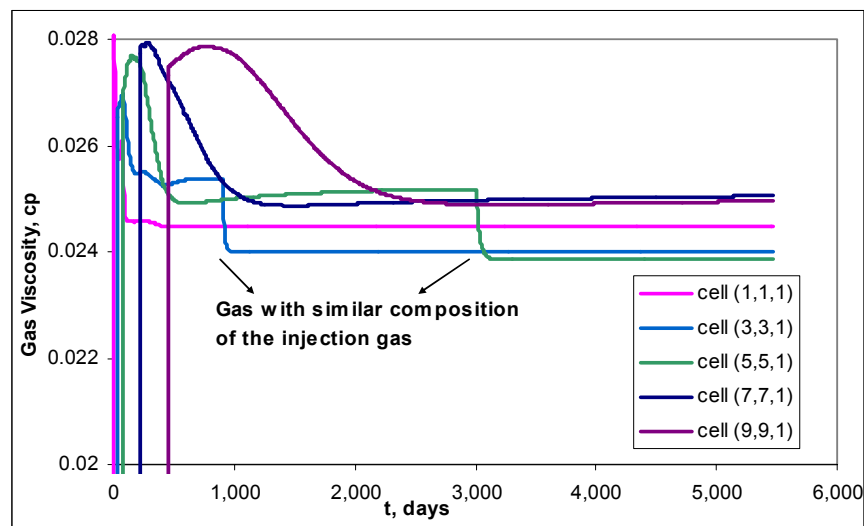


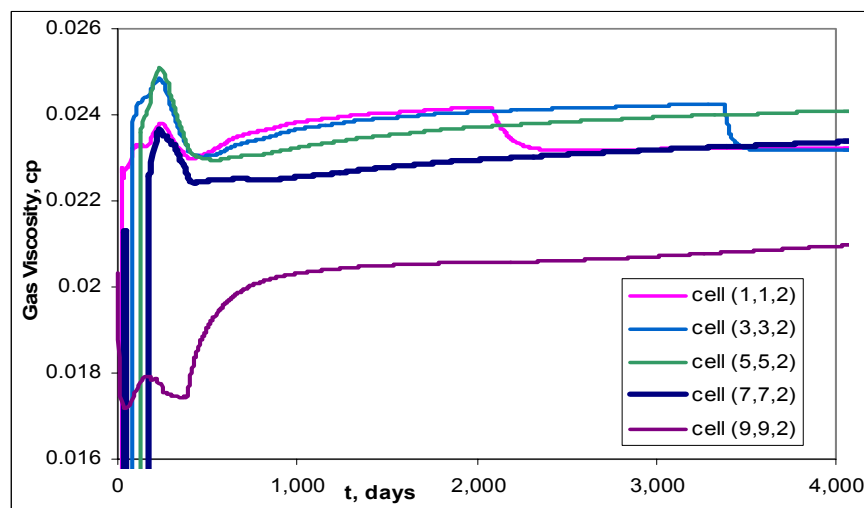
**Fig. 3.38—Typical relative permeability curve**

Mobility ratio is one of the determinant factors which influence the conformance efficiency of the reservoir.

Therefore, study of the fluid viscosity not only as an indicative of the extent of the miscibility development but also as a determinant factor in recovery performance of the reservoir will be substantial.



a) Viscosity of the gas in the first layer



b) Viscosity of the gas in the second layer

Fig. 3.39 —Variation in gas viscosity of the first and second layers at 4,400

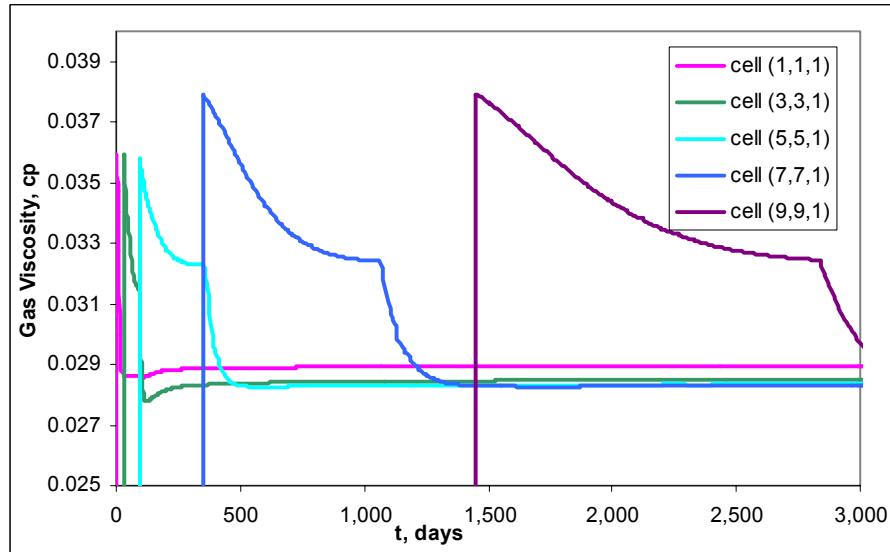
**Fig. 3.39** represents the variation of the injection gas viscosity during the immiscible displacement of the reservoir fluid. The vertical lines indicate time of gas breakthrough into each cell. The breakthrough gas into each cell is the gas which vaporizes high content of the intermediate or heavy components of the oil been in contact through its movement into the reservoir. The richer the gas in intermediate components, the greater is its viscosity. The reservoir pressure also affects the viscosity to a high degree. The gas viscosity increases with pressure.

As Fig. 3.39 indicates, the breakthrough gas into each cell has the highest viscosity, since it is rich in intermediate components of the oil. Then, viscosity keeps decreasing continuously with time till the moment at which the injection gas vaporizes most of the contacted oil. A sharp decrease in viscosity occurs when the composition of the breakthrough gas into the cell will be close to that of dry injection gas (Fig. 3.39.a). Effect of pressure is paramount in the second layer (Fig. 3.39.b). Same trend was observed in pressure distribution of the second layer in Fig. 3.36.b especially at the early times of injection. Lower pressures in grids closer to the production well, cause lower gas viscosity of that grid. Produced gas viscosity (grid (9,9,2) ) is the least viscous gas. As the pressure increases during injection, gas viscosity keeps increasing till the breakthrough gas composition approaches to composition of the dry injection gas. The sharp decrease in viscosity trends of grids (1,1,2) and (3,3,2) of Fig. 3.39.b is attributed to the variation in gas composition.

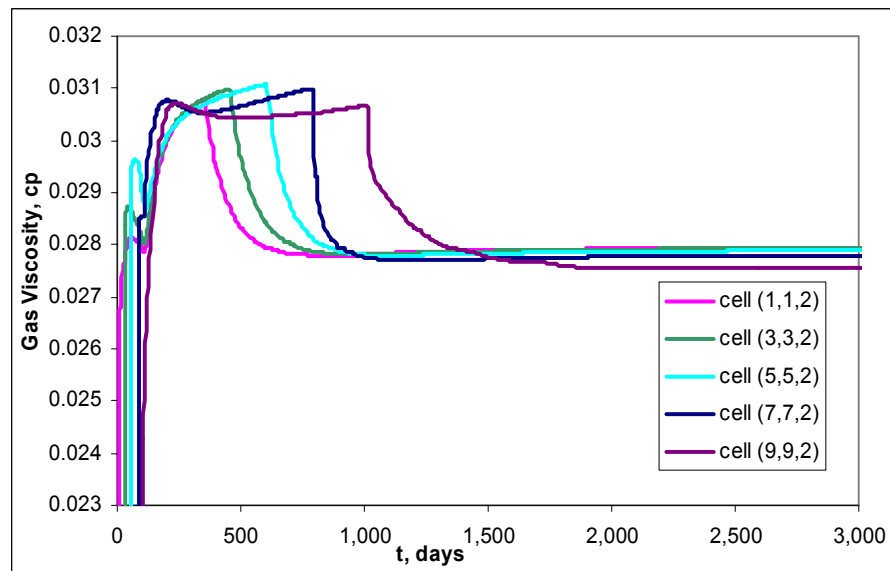
The viscosity profile for miscible displacement provided in **Fig. 3.40** could be interpreted as discussed previously. Comparison of the viscosity values for miscible and immiscible displacements results in the following conclusions:

- Injection gas viscosity increases as miscibility develops. Comparison of Figs. 3.39 and 3.40 demonstrates the significant effect of miscibility in gas viscosity.
- In both miscible and immiscible displacement mechanism, the gas viscosity of the first layer is larger than the second one (case a). The first layer is the layer at which the injection well is perforated and consequently is

at a higher pressure. Better development of miscibility or lower immiscibility factor,  $F$ , which is represented in **Fig. 3.41**, occurs in this layer. The abrupt change in immiscibility factor value in Fig. 3.41 is indicative of a front.



a) case a (Injection to the first and production from second layer), first layer



b) case b (Injection to the first and production from second layer), second layer

**Fig. 3.40** —Variation in gas viscosity during gas injection at 5,600 psi



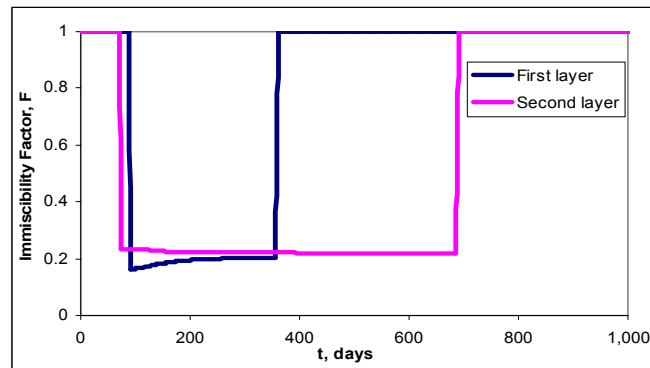


**Fig. 3.41 —Higher degree of miscibility in the first layer where the injection well is completed**

**Figs. 3.42 through 3.45** show the cross-section view of the two layers for the gas viscosity at different time steps. Tracking the front gas viscosity at different time steps for various completion patterns and injection pressures supports the above mentioned conclusions.

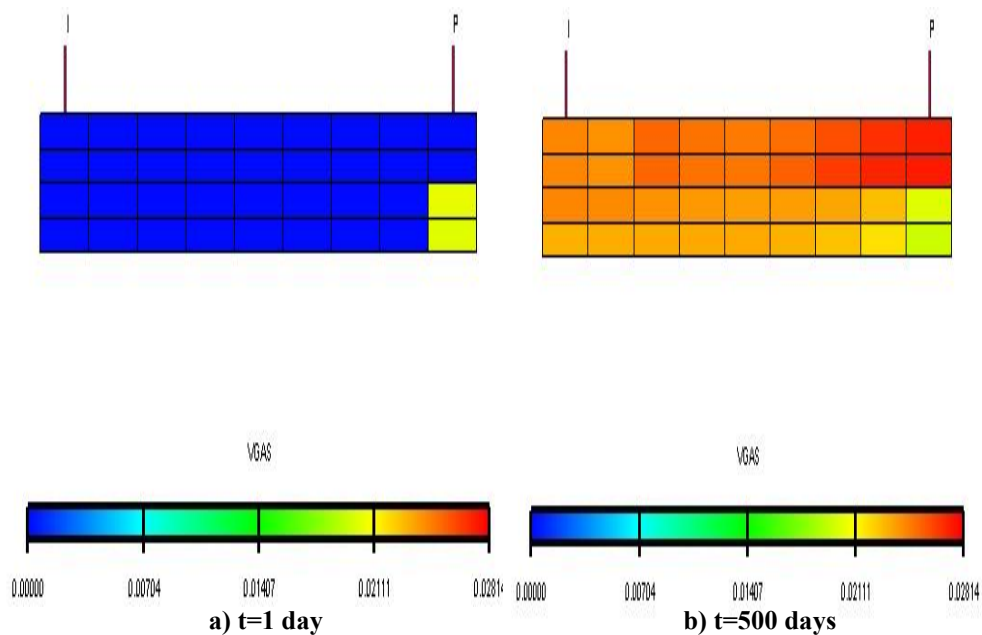


**Fig. 3.42—Variation in gas viscosity at 4,400 psi (case a: injection to the first and production from the second layers)**

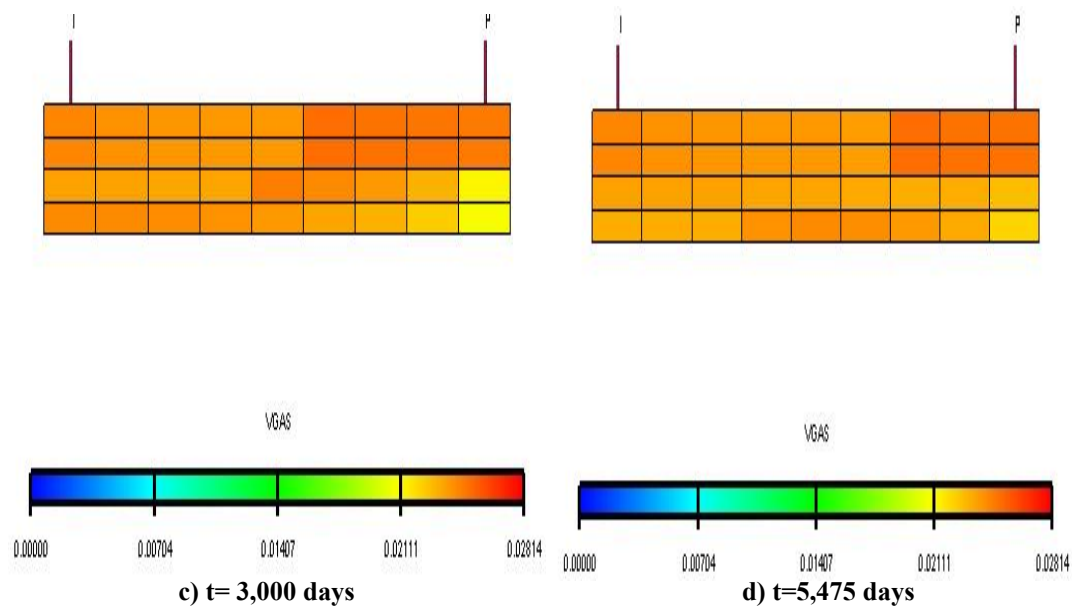


Fig. 3.42—Continued

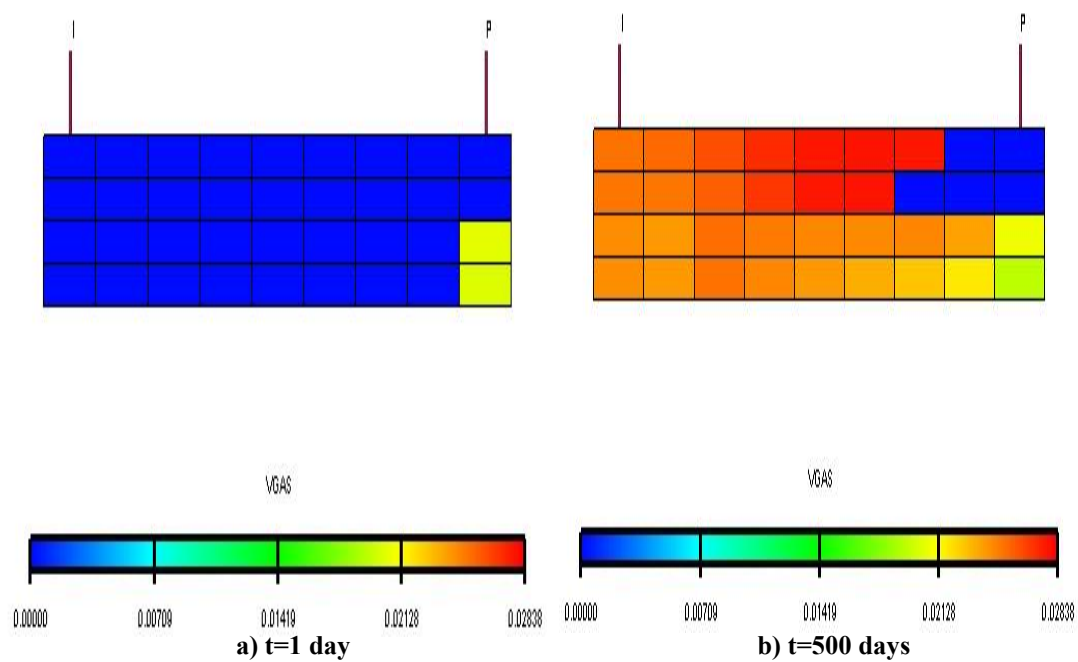


Fig. 3.43—Variation in gas viscosity at 4,400 psi (case b: injection and production from the second layers)

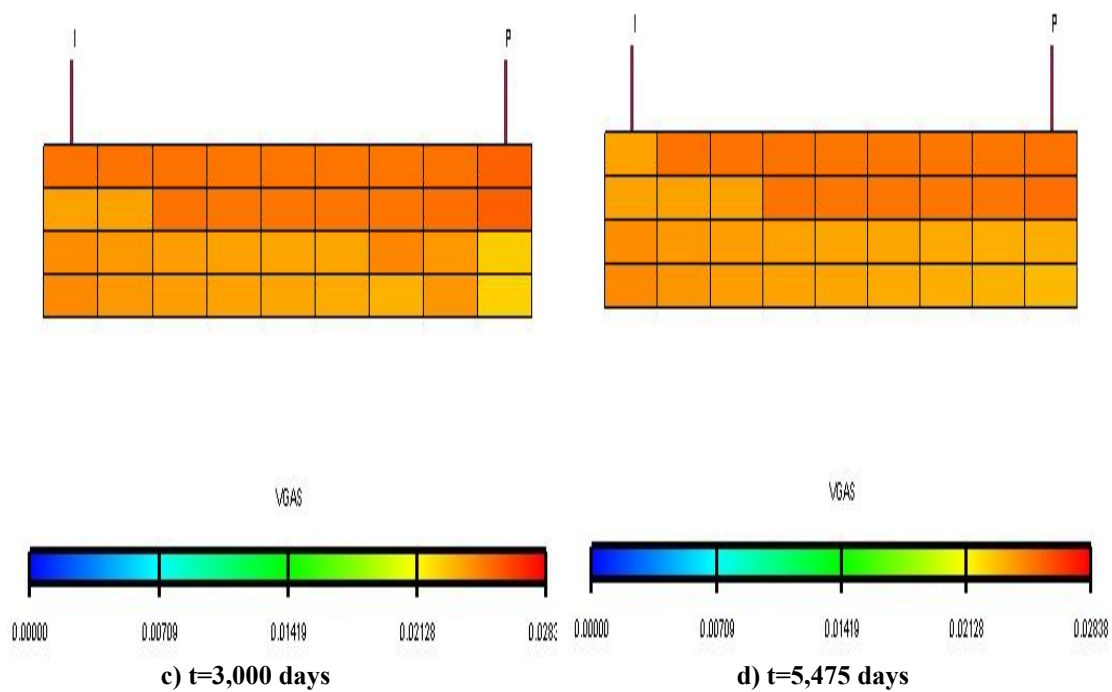


Fig. 3.43—Continued

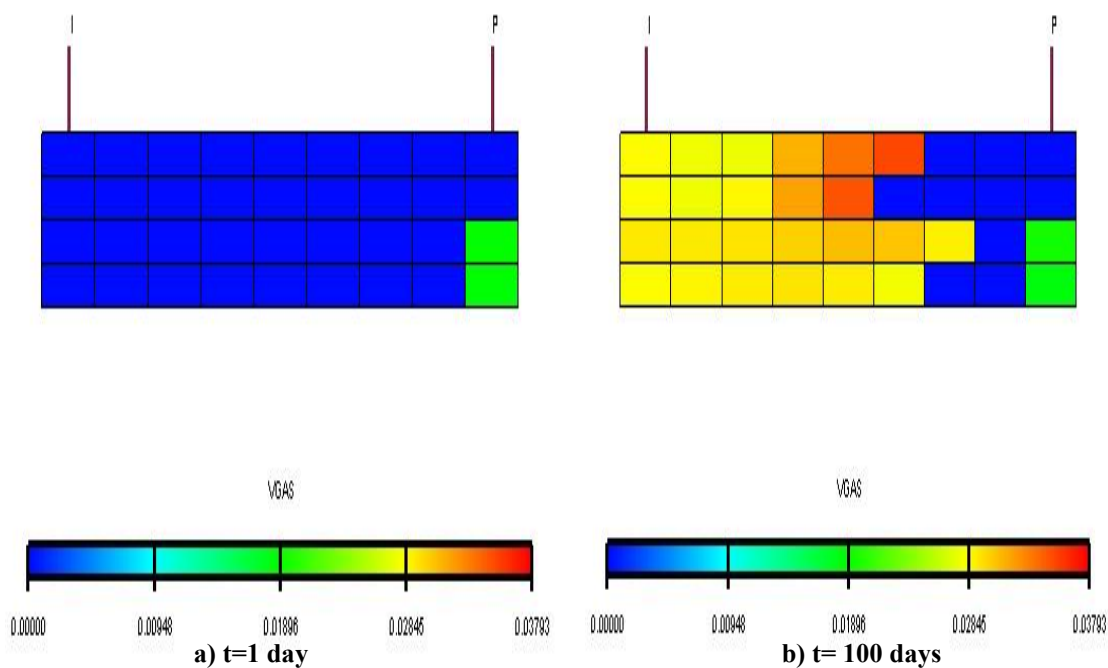


Fig. 3.44—Variation in gas viscosity at 5,600 psi (case a: injection to the first and production from the second layers)

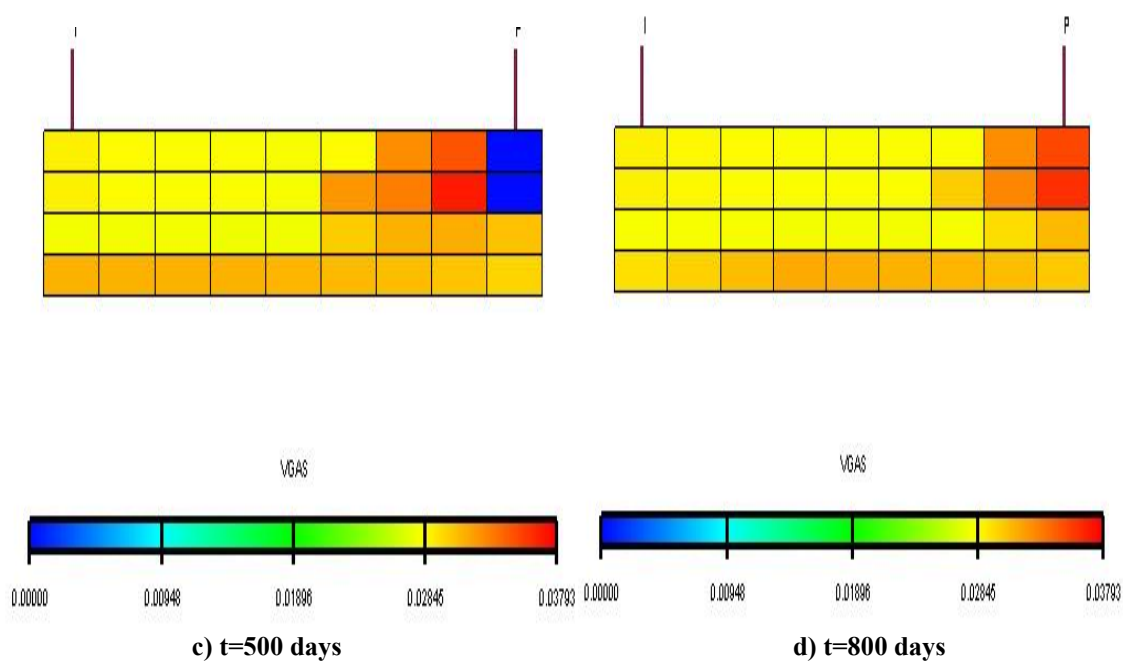


Fig. 3.44—Continued

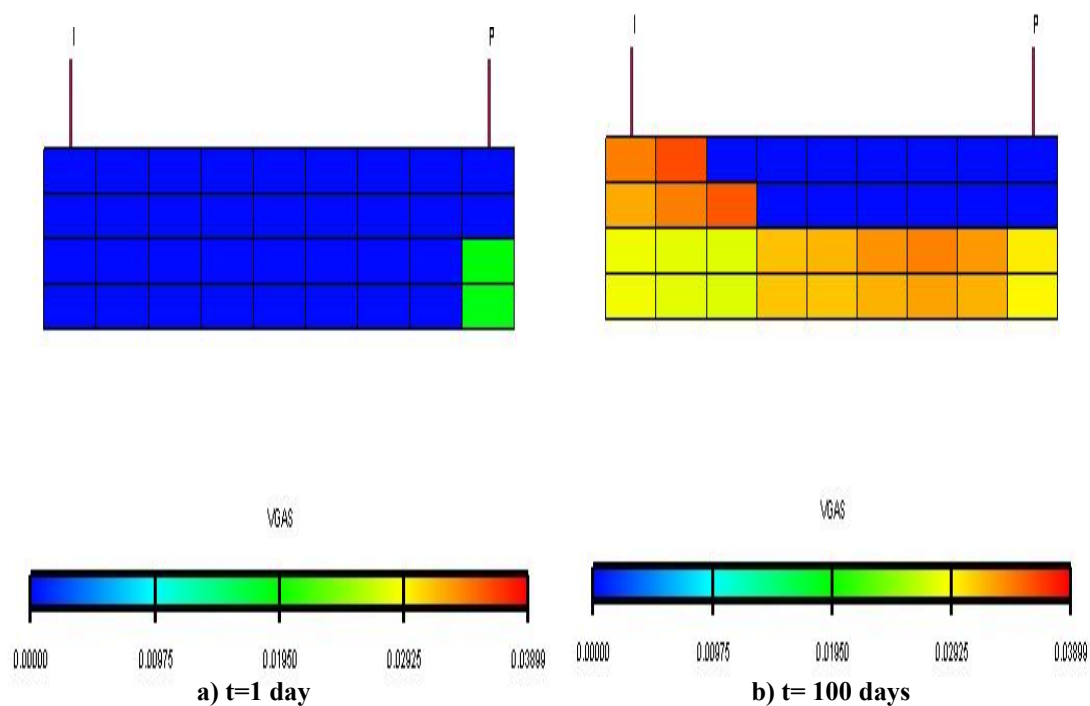


Fig. 3.45—Variation in gas viscosity at 5,600 psi (case b: injection and production from the second layers)

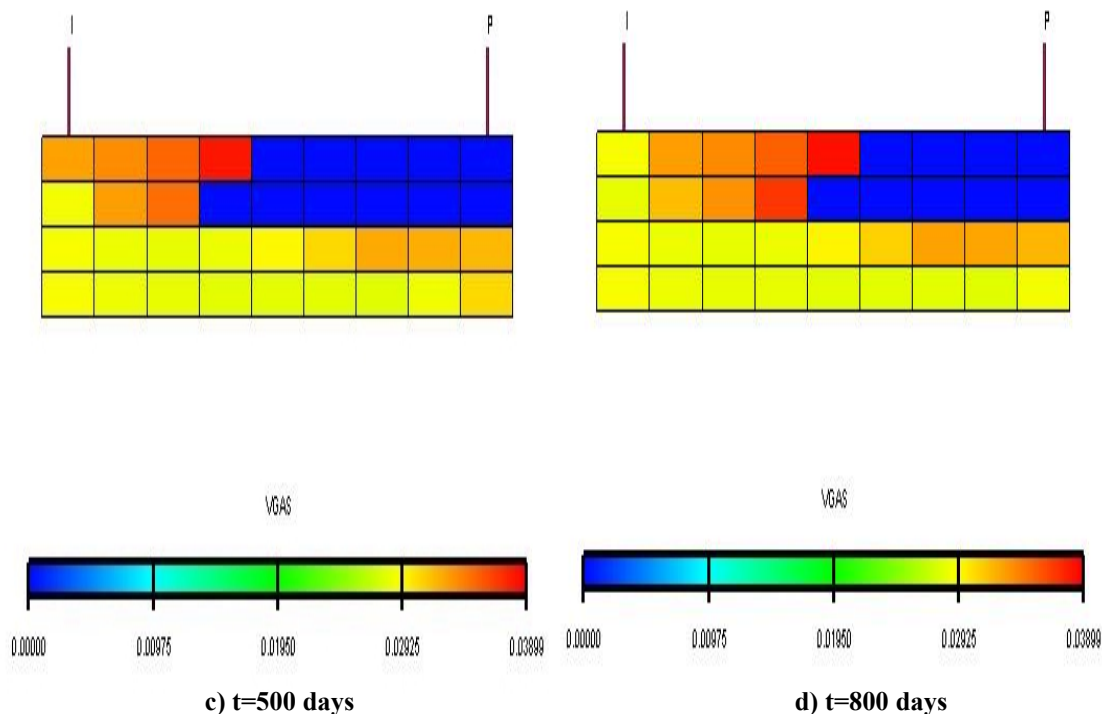
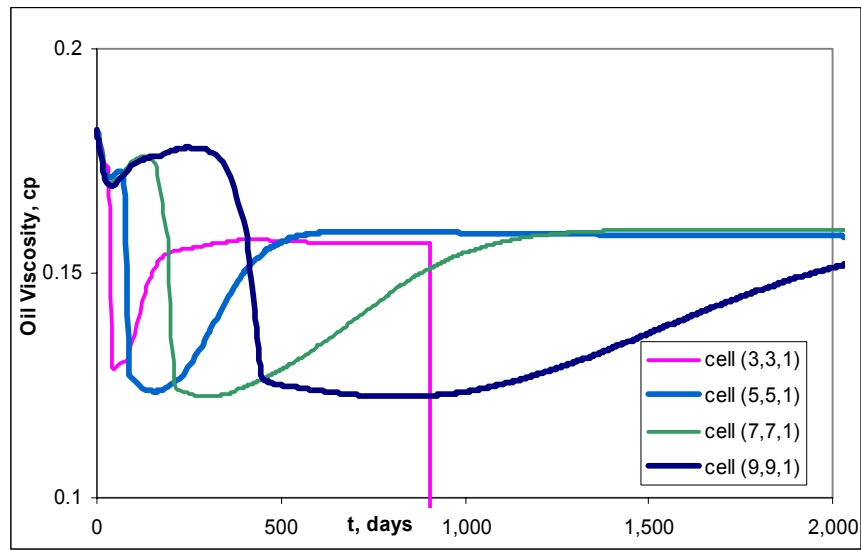


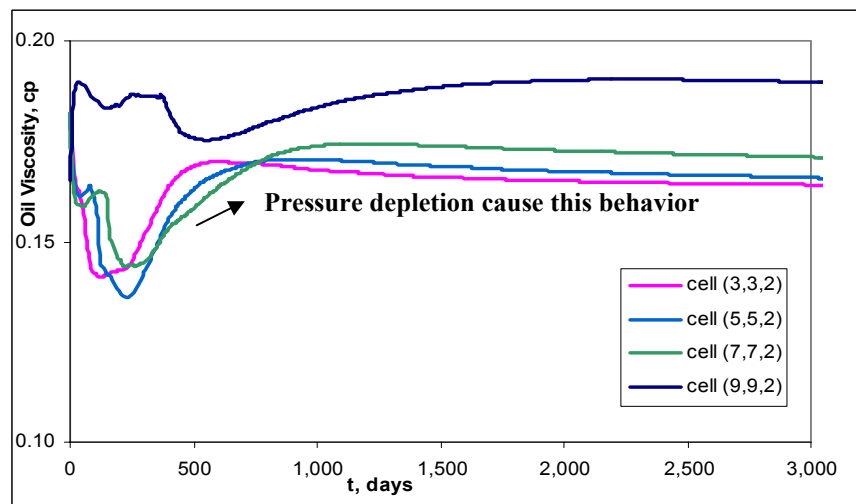
Fig. 3.45—Continued

The main parameters that affect oil viscosity are pressure, temperature, dissolved gas and fluid composition. Oil viscosity increases with a decrease in API gravity and temperature. The effect of dissolved gas is to lighten the oil and thus decrease its viscosity. The effect of increasing the pressure for undersaturated oil is to compress the liquid and to increase the viscosity. **Figs. 3.46 through 3.49** show the oil viscosity profile for different miscible and immiscible displacement mechanism in the reservoir. After a period of relatively constant oil viscosity, a sharp decrease is observed in the oil viscosity of the first layer. It is believed that light vaporized oil carried by the breakthrough gas into the cell lowers the oil viscosity substantially. Since then, oil viscosity increases gradually till it become stable at later times.

The observed trend in oil viscosity of the second layer is mostly dependent on the variation of the reservoir pressure. The reduction in oil viscosity is the result of swelling or expansion of the undersaturated reservoir fluid by the addition of dissolved gas at higher pressure.



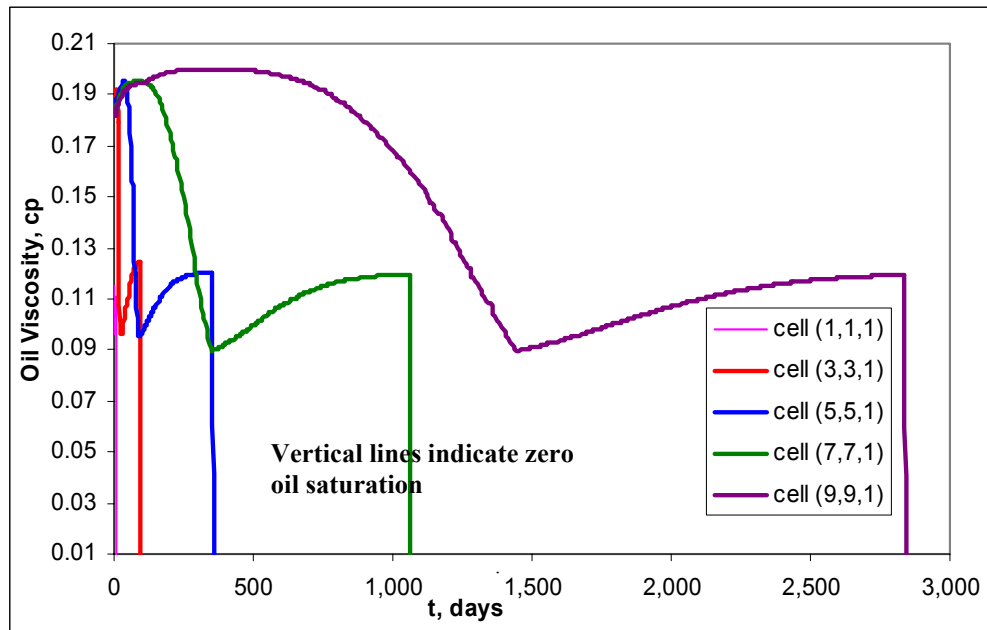
a) Variation in oil viscosity of the first layer ( $k_v = 9$  mD)



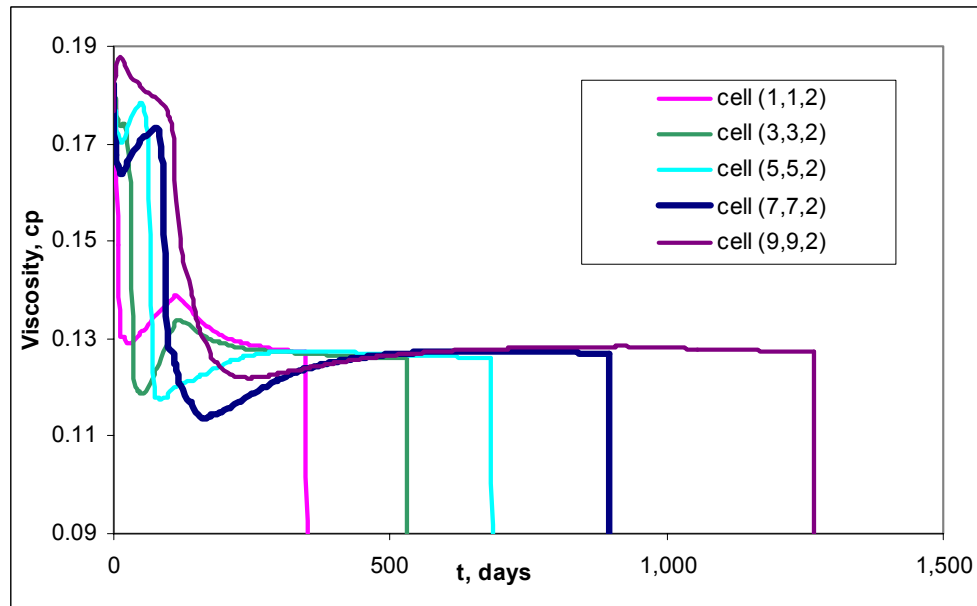
b) Variation in oil viscosity of the second layer ( $k_v = 0.009$  mD)

Fig. 3.46—Oil viscosity profile at 4,400 psi (case a)

Comparison of the viscosity values of the miscible and immiscible displacements shows lower oil viscosities in miscible displacement. Since better development of miscibility occurs in the first layer lower oil viscosity in this layer compare to the second one is predictable (Fig. 3.47).

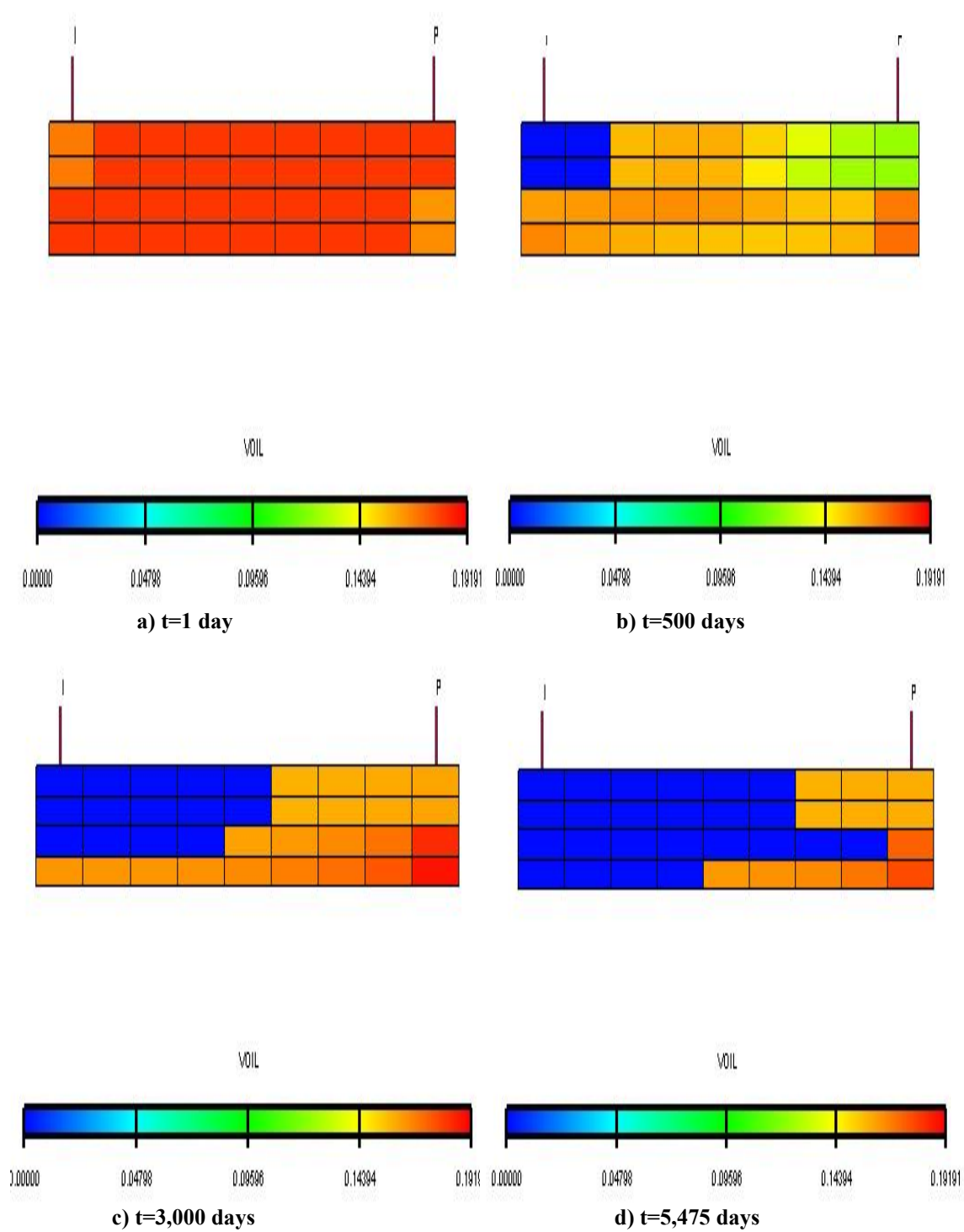


a) Oil viscosity of the first layer ( $k_v = 9$  mD)



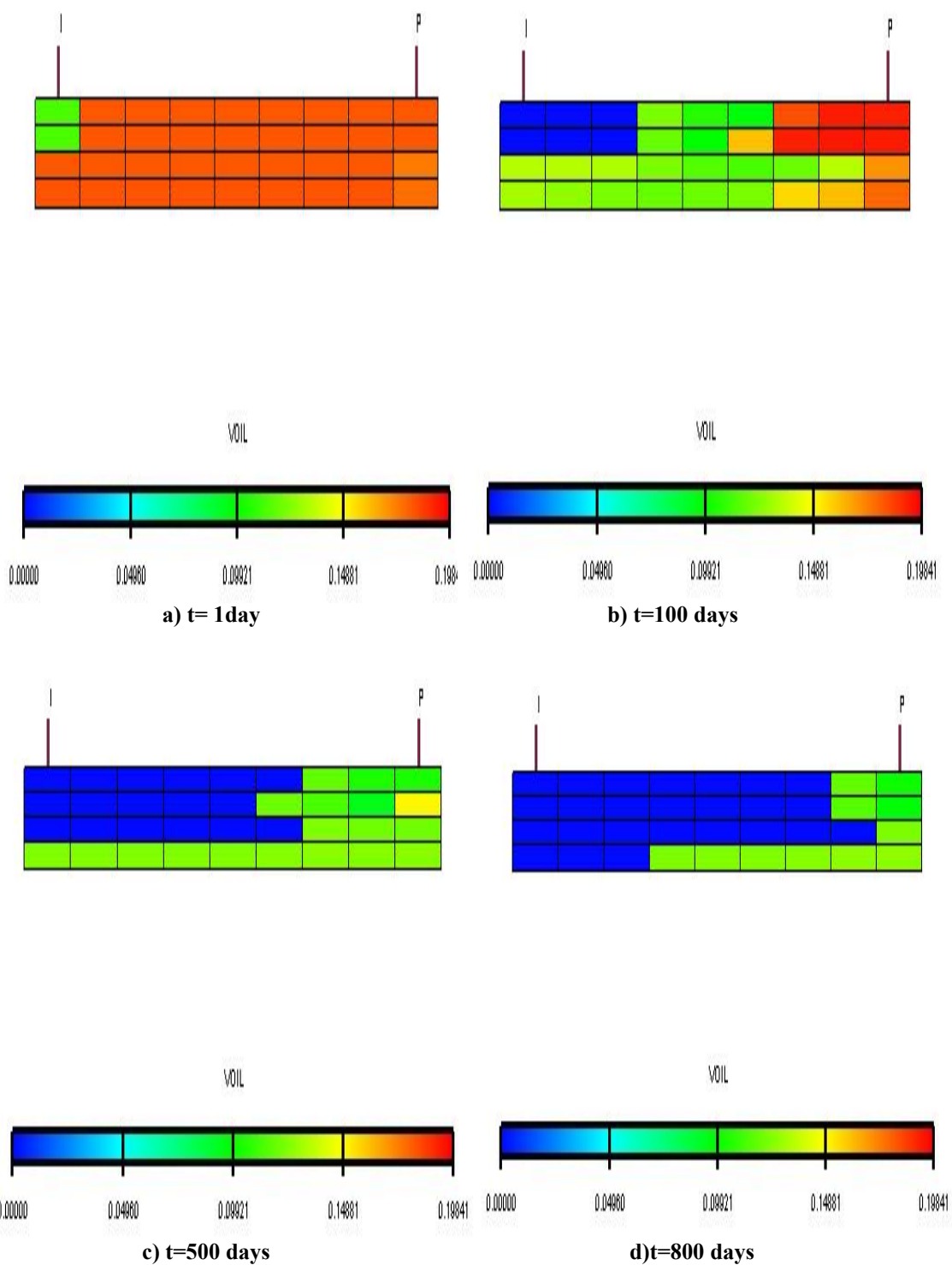
b) Viscosity of the second layer ( $k_v = 0.009$  mD)

Fig. 3.47—Variation in oil viscosity during miscible gas injection (case a, 5,600 psi)



**Fig. 3.48—Oil viscosity profile during immiscible gas injection (case a, 4,400 psi)**





**Fig. 3.49—Oil viscosity profile during miscible gas injection (case a, 5,600 psi)**

### 3.2.6 Stratification Effect

Conformance efficiency is one of the determinant factors that control maximum oil recovery from a reservoir. Conformance efficiency is defined as the fraction of the total pore volume within the pattern area that is contacted by the displacing fluid. The dominating factors that control conformance area are the gross sand heterogeneity and size distribution of the rock interstices, which usually are defined in terms of permeability variation or stratification.

In this section, lateral permeabilities are varied about their base case values (90 md) and the stratified reservoir modes were constructed to ascertain the effect of stratification on the miscible and immiscible oil recovery processes.

#### 3.2.6.1 Simulation Results

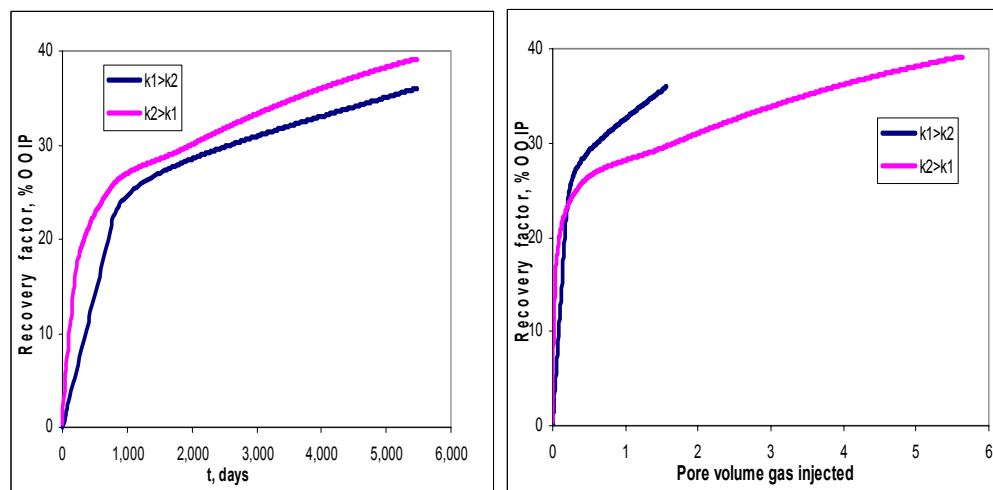
Layer permeability is the reservoir parameter varied about its base case value (90 md). The new constructed model is a two-layer stratified reservoir with permeability ratio of 30. The layers take lateral permeability values of 90 and 3 md, and vertical permeabilities of 9 and 0.3 md, respectively. The ratio of horizontal to vertical permeabilities of each layer is 0.1. In all of the simulation models the injection and production wells are completed in the first and second layers of the reservoir, respectively.

**Table 3.17** summarizes the simulation results regarding recovery performance of the stratified reservoir under miscible and immiscible gas injection. The calculated oil recoveries are provided at 1.2 pore volume of gas injected into the more permeable ( $k_1 > k_2$ ) or less permeable ( $k_2 > k_1$ ) layer. The injection and production wells are completed in the first and second layers of the reservoir, respectively. Recovery performance of the stratified reservoir during 15 years of miscible or immiscible gas injection of the reservoir is presented in **Figs. 3.50** through **3.52**. The predicted recoveries are presented as function of time and volume of injected gas at the same time. Comparison of the simulation results leads to the following conclusions:

- Significant increase in oil recovery is observed in miscible displacement mechanism. Incremental oil recovery between injection pressures of 5,000 and 5,600 psi indicates minimum miscibility pressure (5,000 psi) as the optimum injection pressure from economic point of view.
- Comparison of the estimated recovery values for two different cases,  $k_1 > k_2$  and  $k_2 > k_1$ , indicate the key factor that determines the effect of layering on oil recovery at a particular injection pressure, is the vertical location of the high-permeability streak in the stratified reservoir. If the high permeability layer is located in the lower half of the reservoir ( $k_2 > k_1$ ), the oil recovery improves since the combination of the stratification and gravity effects retard the segregation of the gas into the top portion of the reservoir cross-section. This effect is more evident in miscible displacement mechanism where the gas is injected at pressures equal to or above MMP value. It should be noted that in making this comparison, the determinant time factor in evaluating the incremental oil recovery or project economics should be taken into account. Reported recovery values for the second case, where the permeable layer is located on the lower half of the reservoir ( $k_2 > k_1$ ), are in earlier times of project life compare with those of the first case.
- Lower production-well GORs and high potential of gas injectivity (smaller times required to inject 1.2 pore volume of gas) when  $k_2 > k_1$  make this case advantageous in comparison for the case where  $k_1 > k_2$ .

**Table 3.17—Comparison of oil recovery and GOR at 1.2 pore volume of injected gas**

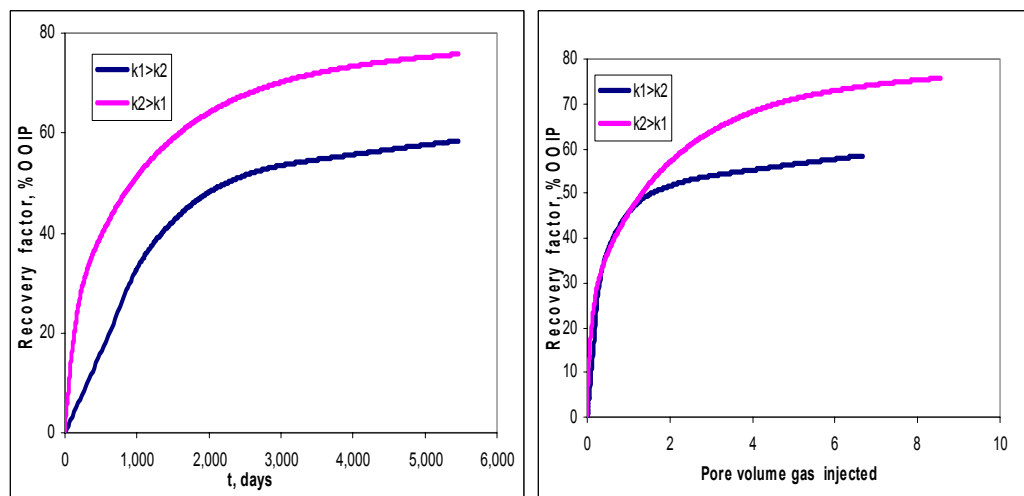
Injection Pressure,  psi	Predicted oil recovery and GOR at 1.2 pore volume of injected gas					
	$K_1 > K_2$			$K_2 > K_1$		
	t, days	Rec., %OOIP	GOR, Mscf/STB	t, days	Rec., %OOIP	GOR, Mscf/ STB
4,400	4,378	33.8	46.44	1,546	28.6	115.84
5,000	1,955	47.7	31.5	854	48.4	20.97
5,600	1,633	48.7	42.73	784	48.8	17.63



a) Recovery performance versus time

b) Recovery factor versus pore volume of injected gas

Fig 3.50—Estimated oil recovery at injection pressure of 4,400 psi



a) Recovery performance versus time

b) Recovery factor versus pore volume of injected gas

Fig 3.51—Estimated oil recovery at Minimum miscibility pressure of 5000 psi

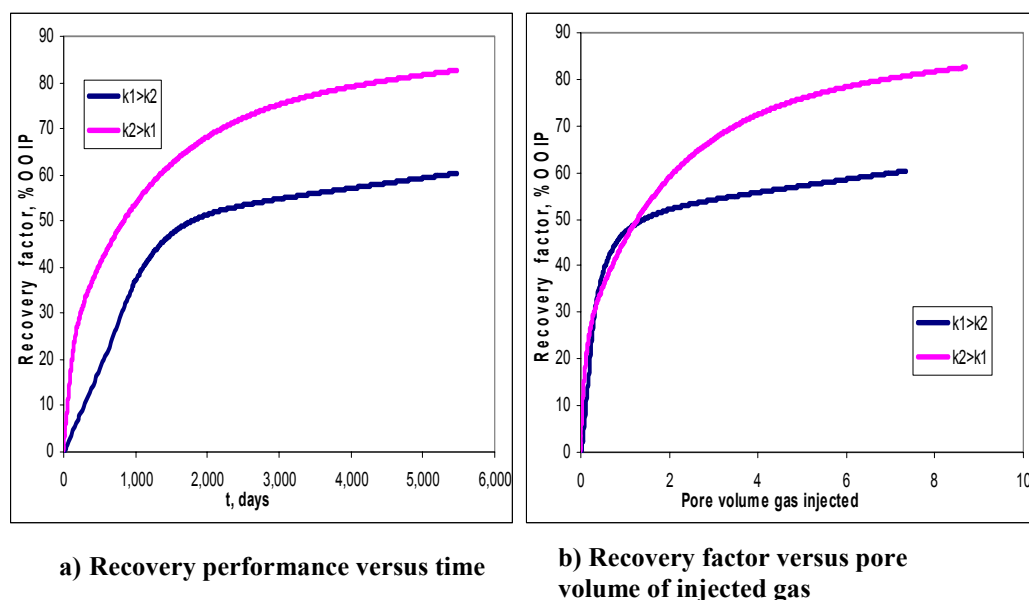
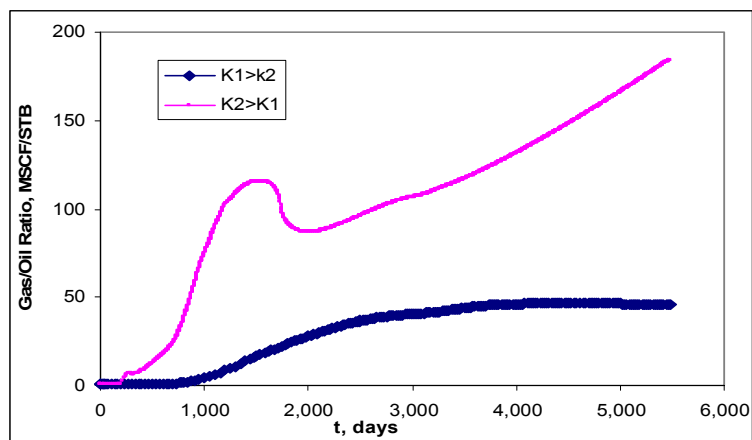


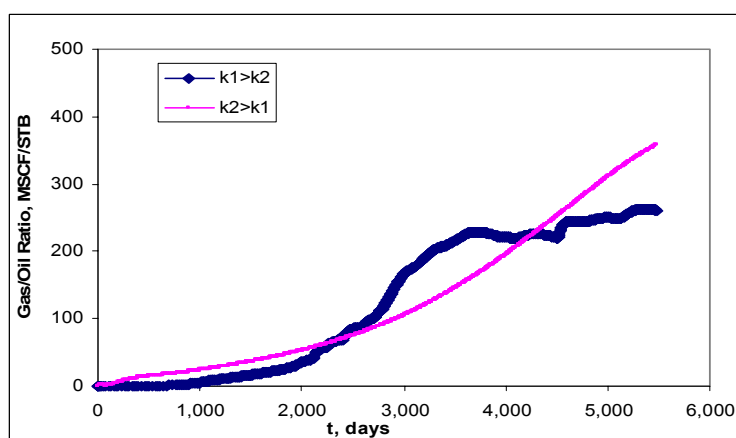
**Fig 3.52—Estimated oil recovery at injection pressure of 5600 psi**

**Fig. 3.53** indicates the production-well GOR for different injection pressure and stratified models. Predicted GOR values at 1.2 pore volume of injection are presented in Table 3.17. It's better to make our comparison on the basis of cumulative produced gas (proportional to the area between x-axis and plots of Fig. 3.53) instead of particular GOR value at 1.2 pore volume of injection. Cumulative injection gas at 1.2 pore volume of injection is equal to 22,700 MMscf. Total produced gas at injection pressures of 4,400 and 5,000 psi are 19,974 and 18,493 MMscf for the case when the first layer is more permeable ( $k_1 > k_2$ ). The correspondent values when the more permeable layer is located on the lower half of the reservoir ( $k_2 > k_1$ ) are 23,918 and 23,406 MMscf respectively.

In these two cases lower production gas in miscible flooding compare to immiscible one is beneficial. Cumulative gas production in miscible and immiscible flooding of the stratified reservoir is greater than total injection gas for the case where injection well is perforated in the less permeable layer ( $k_2 > k_1$ ). The incremental produced gas is attributed mostly to the presence of the solution gas in the produced undersaturated oil from the second layer.



a) injection pressure: 4,400 psi



b) injection pressure: 5,000 psi

Fig 3.53—Comparison of GOR at immiscible and miscible gas flooding

**Fig. 3.54** shows the gas production rates of the layers for a typical injection pressure of 5,000 psi. Unlike Fig. 3.54.a, higher gas production rate from the second layer is observed ( $k_2 > k_1$ ) at early times of injection. This is mostly the solution gas associated with the production oil from this layer (**Fig. 3.55.b**). The point of intersection of the gas production curves is the time when the gas production rate of the layers is the same and the production-well constrain switches to the constant gas production rate of 30,000 Mscf/day toward the end of the project.

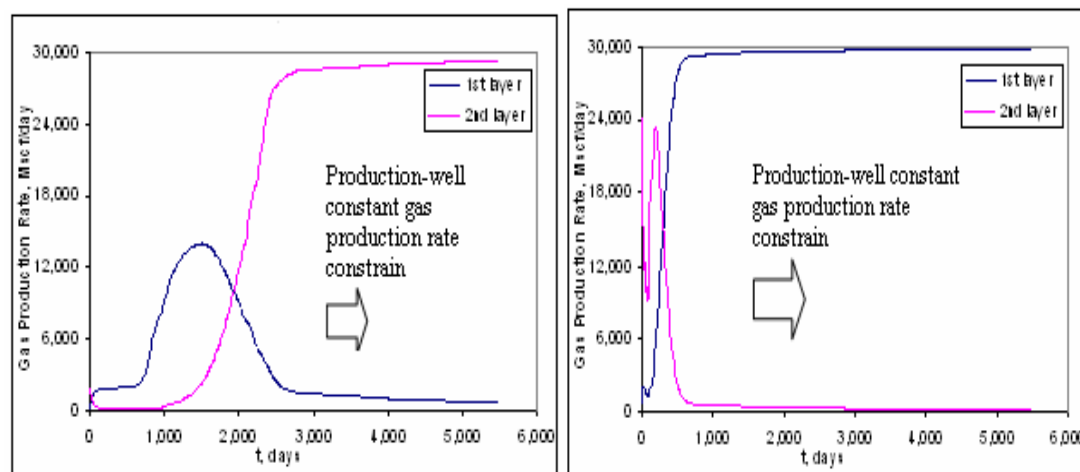
a)  $k_1 > k_2$ b)  $k_2 > k_1$ 

Fig 3.54—Gas production rate of the individual layers at 5,000 psi

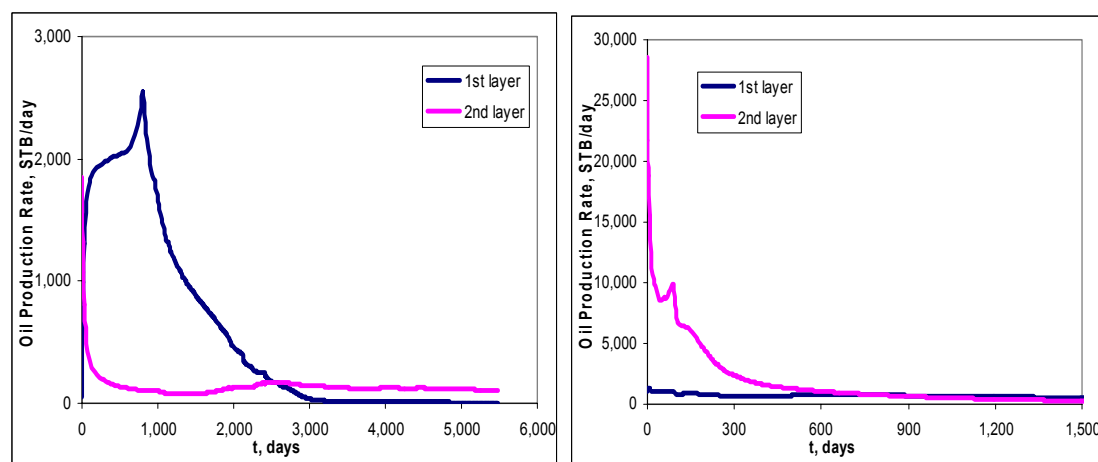
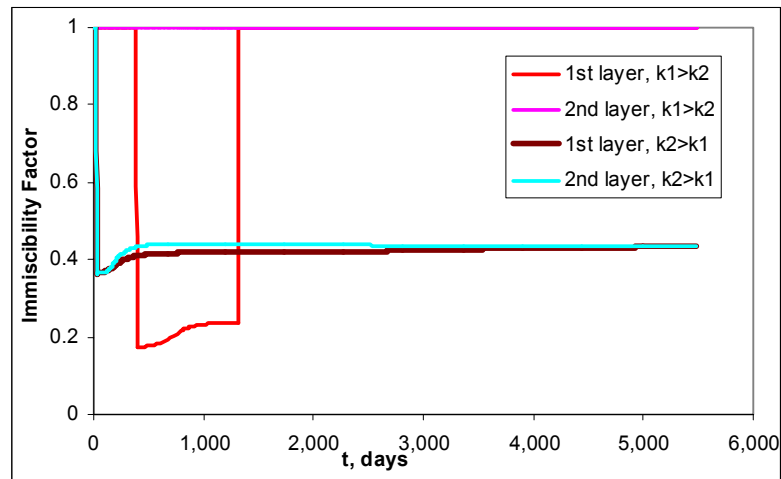
a)  $k_1 > k_2$ b)  $k_2 > k_1$ 

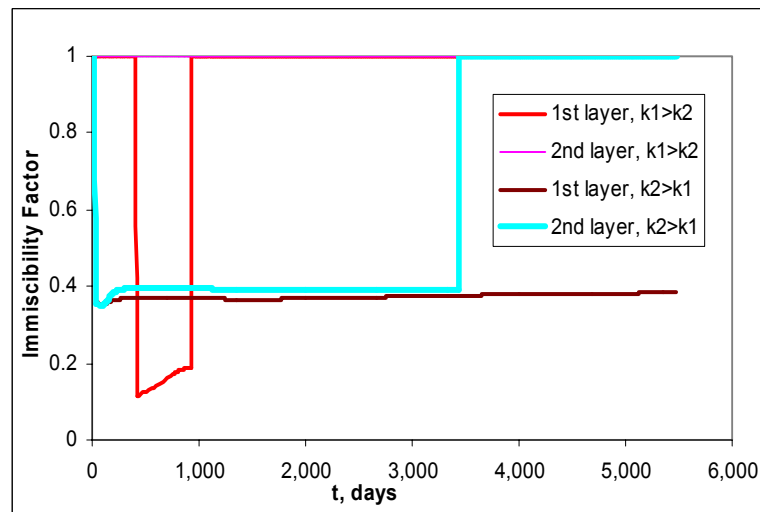
Fig 3.55—Oil production rate of the individual layers at 5,000 psi

Fig. 3.56 gives substantial information regarding development of miscibility in the stratified reservoir. This miscibility data is only for typical grid (5,5) of the reservoir. It should be noticed that even at pressures far above the minimum

miscibility pressure, thorough miscibility displacement doesn't occur. Immiscibility factor for single phase take value one, whereas it reduces with increasing pressure. Miscibility develops efficiently in the first layer where the injection well is completed.



a) Injection pressure: 5,000 psi



b) Injection pressure: 5,600 psi

Fig 3.56—Dependence of miscibility to pressure



**Figs. 3.57 through 3.60** indicate the x-z cross-section view of the region of the reservoir located between injector and producer wells. Extent of the oil sweepout and location of the gas front in each layer and at different time steps are of great interest.

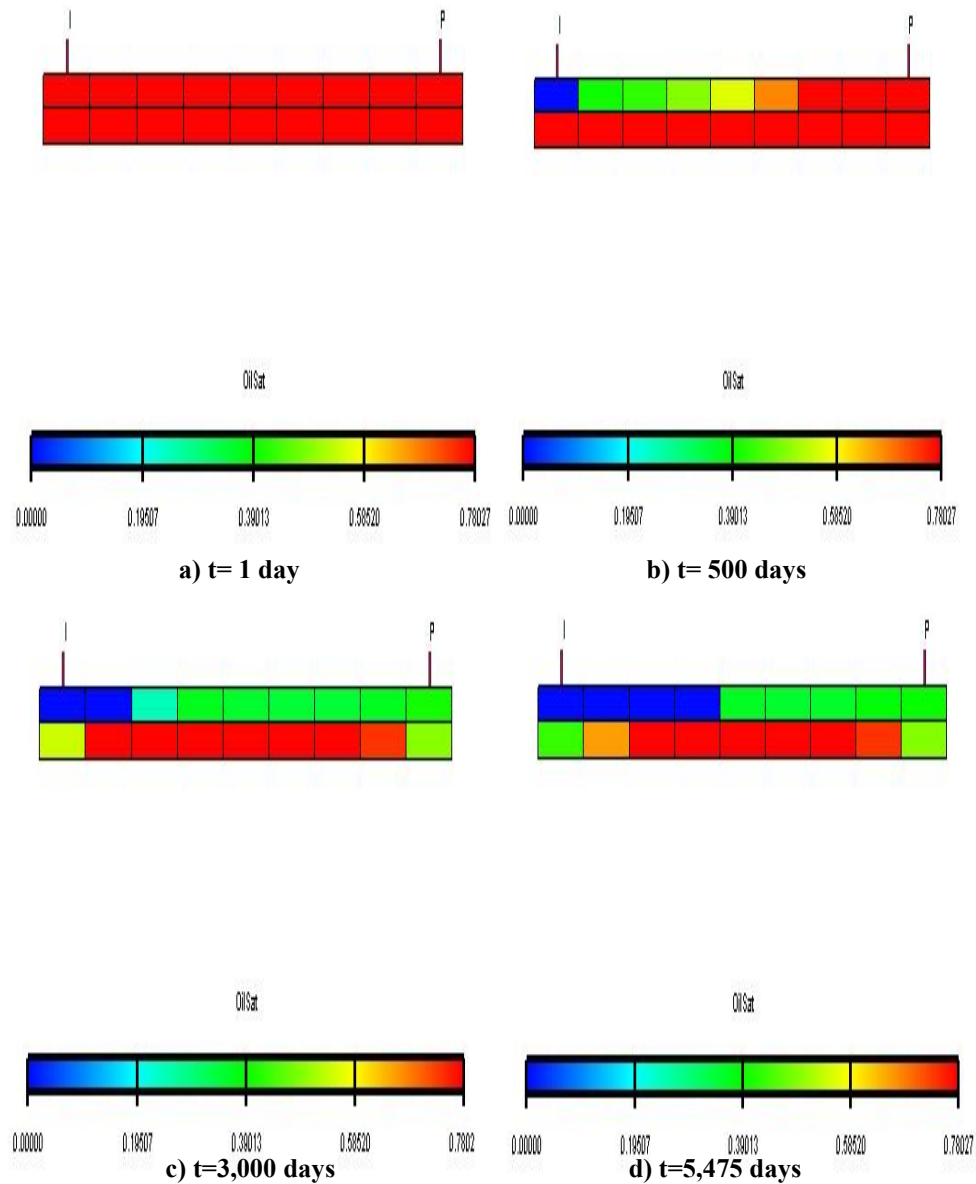


**Fig. 3.57—Oil saturation profile at injection pressure of 4,400 psi (x-z cross-section view,  $K_1 > K_2$ )**

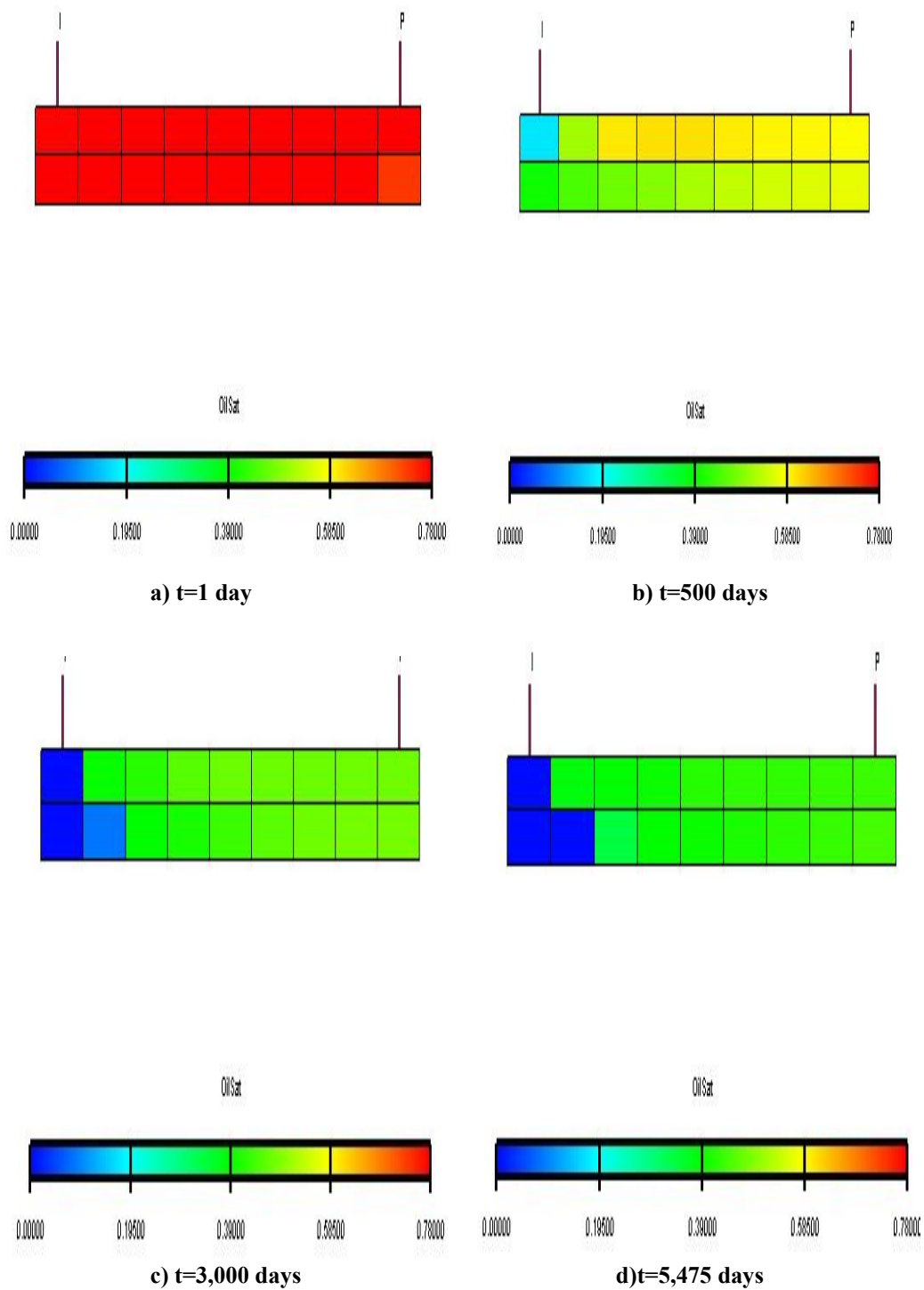


**Fig. 3.58—Oil saturation profile at injection pressure of 4,400 psi (x-z cross-section view,  $K_2 > K_1$ )**

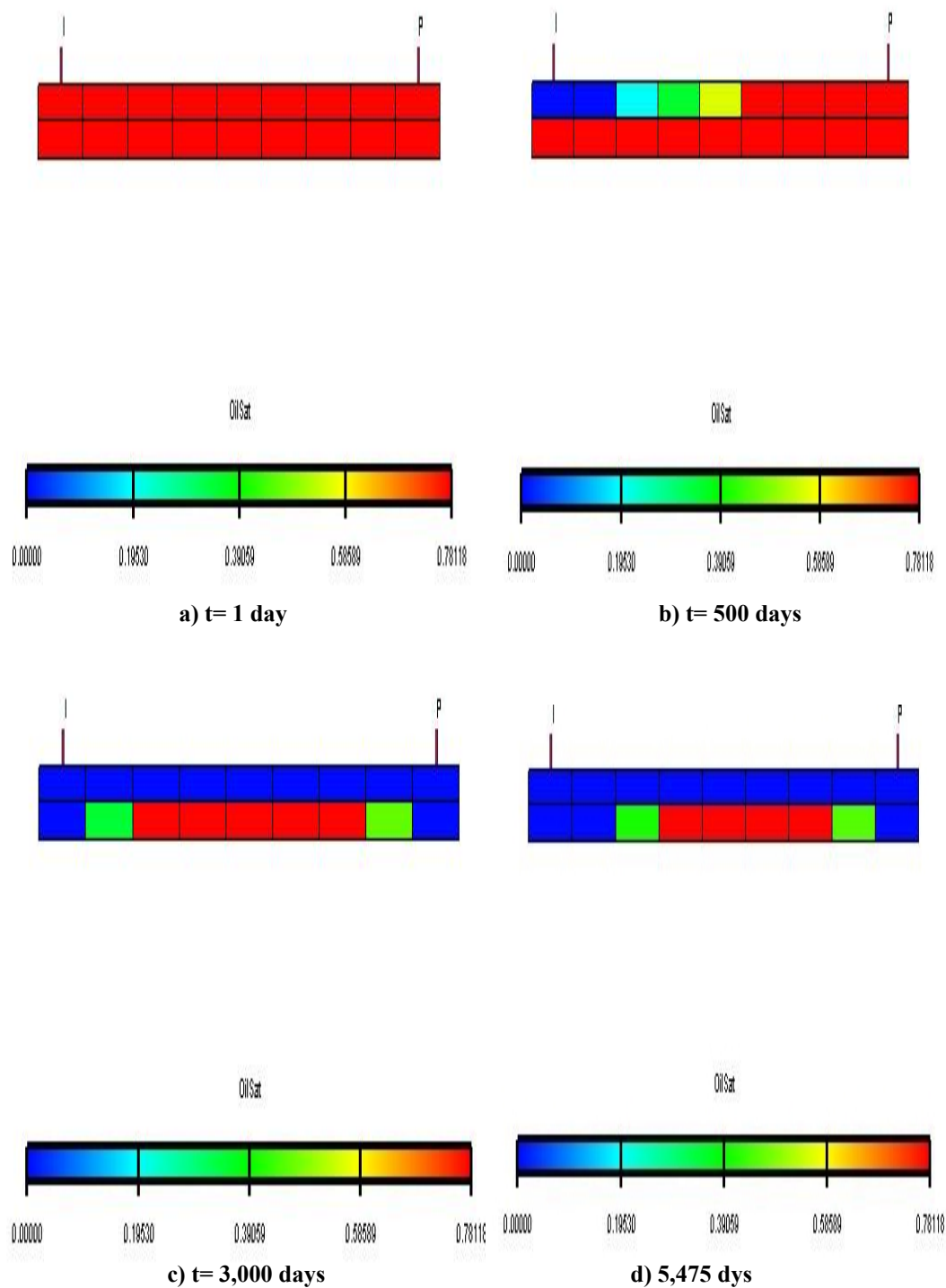


**Fig. 3.59—Oil saturation profile at injection pressure of 5,000 psi (x-z cross-section view,  $K_1 > K_2$ )**

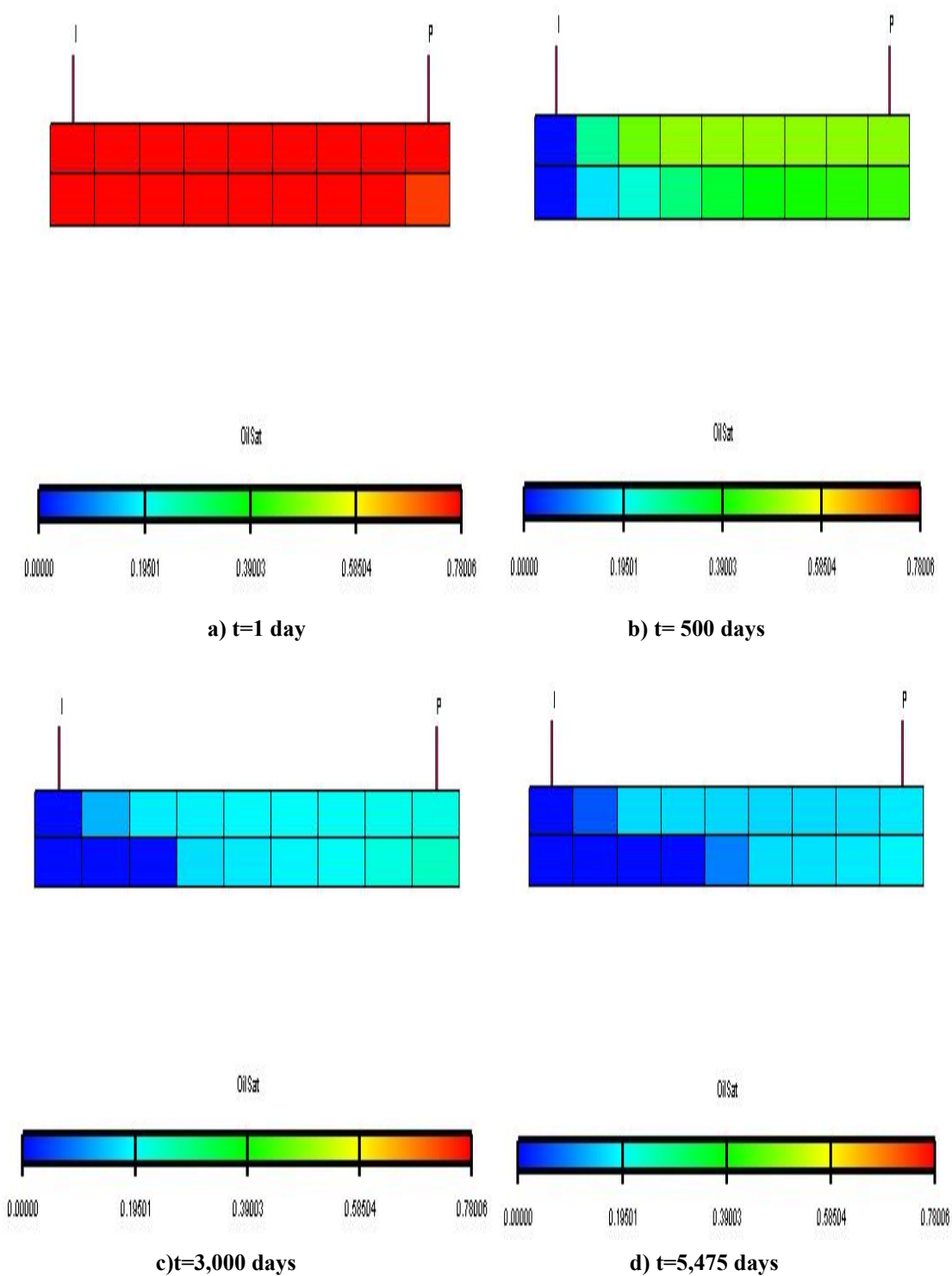


**Fig. 3.60—Oil saturation profile at injection pressure of 5,000 psi ( x-z cross-section view,  $K_2 > K_1$ )**

### 3.2.7 In What Conditions Miscible Flooding Is a Competitive EOR Method?

Oil recovery by miscible flooding has not been applicable as widely as waterflooding. Unlike the case for miscible flooding, waterflooding can be employed successfully from both technical and economic point of view in most oil recovery projects. In this part of the study, appropriate questions, when evaluating a gas injection design are discussed with more details.

The benefit of gas injection is mostly because of the fact that it exhibits better surface tension effect than water. High cost includes operating and equipment costs, solvent availability, and pressure/composition requirements for miscibility are the major limiting factors in miscible flooding. Nevertheless, the interfacial tension benefit can often outweigh the extra expense.

The benefit of gas injection can be easily concluded from the relation of capillary pressure as a function of interfacial tension and pore throat radius.

Capillary pressure is proportional to the interfacial tension and inversely proportional to the pore throat radius. This indicates that as long as the water-oil interfacial tension is greater than the gas-oil interfacial tension, gas injection, no matter how immiscible, would be of benefit since the smaller pore throats will be accessed during gas injection. However, adverse mobility ratio (originates from large oil/gas viscosity ratio) associated in most gas injection projects makes this recovery method risky.

Therefore, understanding the interaction between interfacial tension and adverse mobility ratio is subject of great importance for a gas injection project to be a competitive process in a given reservoir. It should be noticed that typical relative permeability experiments are conducted in constant interfacial tension and viscosity ratios. Since these parameters are constant during performing these experiments, one can see the effect of interfacial tension and viscosity ratio. For displacements where these are not held constant, it's difficult to know if the differences in recovery are due to the interfacial tension, solubility, viscosity ratio changes as well as mixing zones and end effects.

The dominate factor on the microscale constant interfacial tension relative permeability experiment, is determined on the basis of the difference in incremental oil recovery between the high and low interfacial tension conditions. If experiments show that the interfacial tension is dominant with very little influence from the viscosity ratio, which is the case in most slim tube studies, then finding the optimum solvent should be the next goal. If viscosity ratio is the dominant factor, then high cost of miscible flooding in the field project should be avoided.

Next section is the simulation approach that is followed to investigate the effect of mobility ratio and interfacial tension on the recovery of the reservoir.

### **3.2.7.1 Reservoir Description**

A 18\*18\*3 cross-section model is used in this simulation to make a quarter of a five-spot pattern (**Table 3.17**).

The three layers of the reservoir are homogeneous with constant porosity, permeability and thickness values. The relative permeability data are provided in the Tables 3.10 and 3.11. However, it should be noted that miscible gas recoveries are not sensitive to the shape of the relative permeability curves. As miscibility develops, the saturation curve approaches to the straight line with different end-points relative permeabilities.

Setting the average water viscosity to 0.31 cp, which is close to the reservoir oil viscosity, gives rise to an exceptionally low and favorable mobility ratio for water-oil displacement.

The varied fluid composition and injection gases are provided in **Table 3.19**. The first dry injection gas a is intended to represent a dominated mobility ratio displacement, whereas the rich injection gas b represents an interfacial tension dominated factor occurring in the reservoir.

The initial reservoir pressure is 4,200 psi and the saturation pressure of the reservoir fluid with API gravity of 33 is 2,255 psi.

Estimated reservoir pore volume and originally oil in place are 52.275836 and 40,775,152 MMRB.

Injection and production wells are located on the corners of the grid model to make a five-spot pattern. Gas injection well is perforated in the first and second layers of the reservoir, whereas, water injection and production wells are completed in the second and third layers. Constant injection pressure and reservoir volume water injection rate are the injection well constraints. The water injection rate is determined in such a way that same order of injected water and injected gas pore volumes at the end of the project would be injected.

Minimum flowing bottomhole pressure of 1,000 psi is the production-well constrain especially at the early times of production where pressure declines dramatically. Maximum gas production rate of 30,000 Mscf/day is considered as the other production-well constrain in gas injection project.

Table 3.18—Reservoir properties				
Reservoir grid data				
NX=NY=18, NZ=3				
DX=DY=293.3 ft, DZ=27 ft				
Porosity				0.13
Datum (subsurface), ft				8421
Oil/water contact, ft				8600
Capillary pressure at contact, psi				0
Initial pressure, psi				4200
Water properties				
Compressibility, $\text{psi}^{-1}$				$3 \times 10^{-6}$
Density, $\text{lbm/ft}^3$				63
Rock compressibility, $\text{psi}^{-1}$				$4 \times 10^{-6}$
<u>Laver</u>	<u>Horizontal</u> <u>permeability</u>	<u>Vertical</u> <u>permeability</u>	<u>Thickness,</u> <u>ft</u>	<u>Depth</u> <u>to top</u> <u>(ft)</u>
1	90	0.9	27	8340
2	90	0.9	27	8367
3	90	0.9	27	8394

### 3.2.7.2 Simulation Results

The injection gas composition varies in such a case to have interfacial tension and mobility ratio dominated displacement mechanisms of the particular reservoir fluid.

Mobility ratio of the light injection-gas a (viscosity of 0.02 cp) and the reservoir fluid is around 15.6, whereas the calculated mobility ratio of the oil and the intermediate injection-gas b equals 7.8.

Recovery comparison is based on the differences between the estimated recovery for the gas and water injection projects. Unit mobility ratio is employed in simulating waterflooding project.

Table 3.19—Reservoir fluid and injection gas compositions

<u>Component</u>	<u>Reservoir Fluid</u>	<u>Injection gas a</u>	<u>Injection gas b</u>
N <sub>2</sub>	0.139	0.461	0.67
CO <sub>2</sub>	0.049	0.266	5.03
C <sub>1</sub>	34.279	78.923	60.95
C <sub>2</sub>	4.364	18.34	23.76
C <sub>3</sub>	3.486	2.01	9.59
iC <sub>4</sub>	2.633	0	0
iC <sub>5</sub>	4.875	0	0
C <sub>6</sub>	3.771	0	0
C <sub>7+</sub>	46.464	0	0

**Heptanes plus properties:**

**Molecular weight: 202**

**Specific gravity: 0.86**

**Oil viscosity: 0.313 cp**

**Injection-gas a viscosity :0.02 cp**

**Injection-gas b viscosity :0.04 cp**

**Figs. 3.61 and 3.62** provide the oil recovery comparison results in mobility and interfacial surface tension dominated displacement mechanisms. The calculated recoveries at 1.2 pore volume of gas or water injection are 41.98 and 49.95 % OOIP



for mobility dominated mechanism, and 75.46 and 50.32 % OOIP for interfacial tension dominated mechanism, respectively.

As results indicate, for a mobility dominated displacement mechanism the viscous instabilities are more important than the interfacial tension effect and the injection gas composition is less important from an interfacial surface tension point of view. In these cases waterflooding with favorable mobility ratio yields higher oil recovery values (Fig. 3.61)

Absence of unfavorable mobility ratio in miscible flooding results in significant oil recovery due to the low interfacial tension between the injection gas and reservoir fluid (Fig. 3.62).

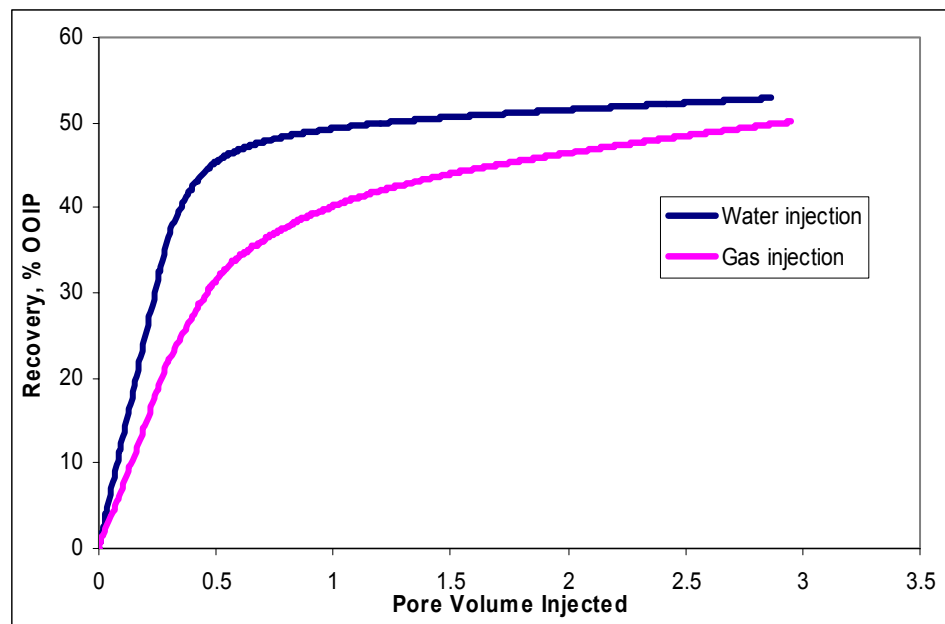


**Fig. 3.61—High mobility ratio in gas injection project decreases the oil recovery from the reservoir**

**Fig. 3.63** indicates higher GOR values in the mobility dominated displacement mechanism. Unfavorable mobility ratio causes gas fingering, instability of the front, early gas breakthrough and subsequently lower sweep efficiency.

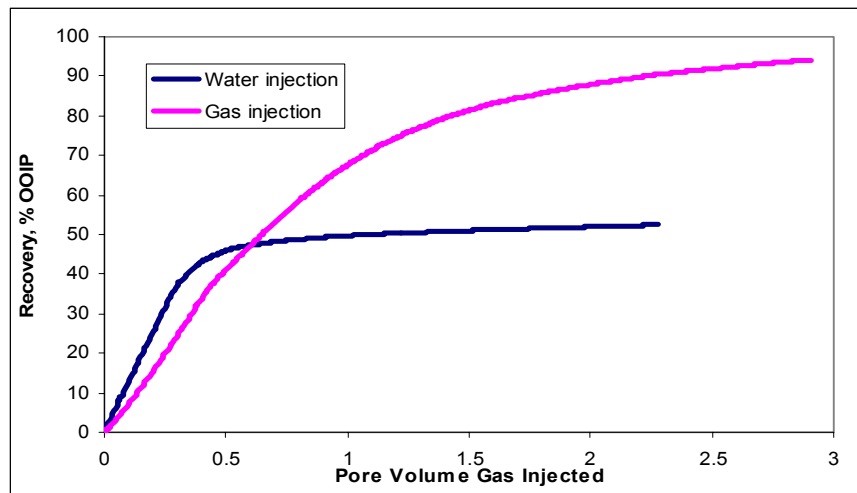


**Fig. 3.62—Absence of unfavorable mobility ratio in miscible flooding improves the oil recovery to a high degree**

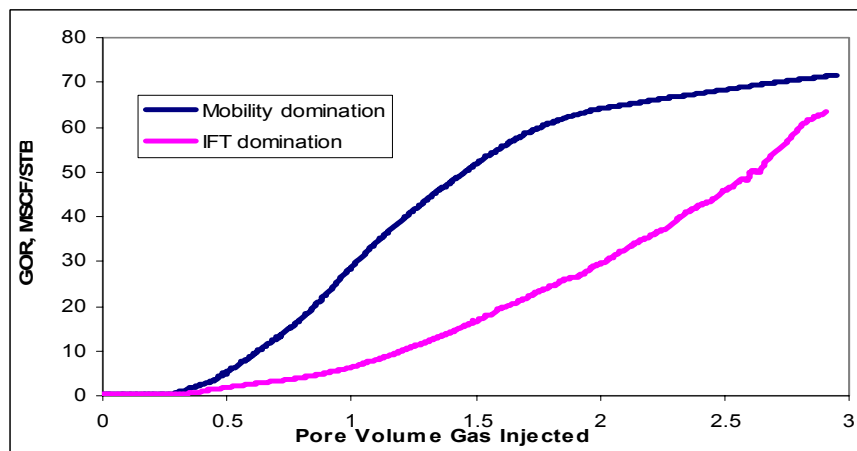
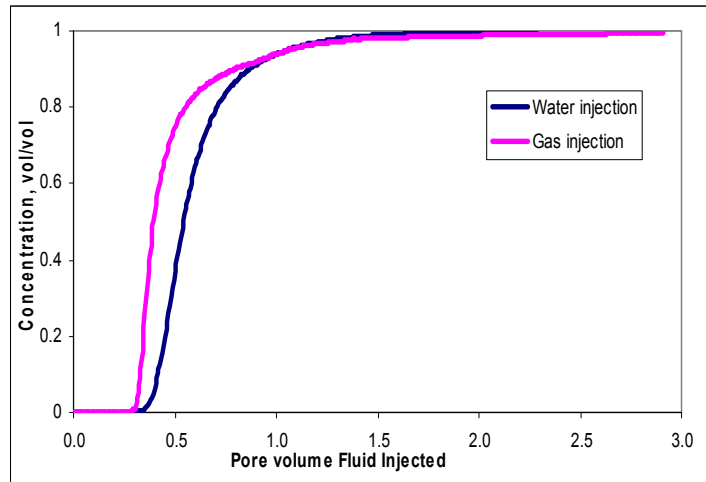


**Fig. 3.63— Comparison of GOR for two displacement mechanisms**

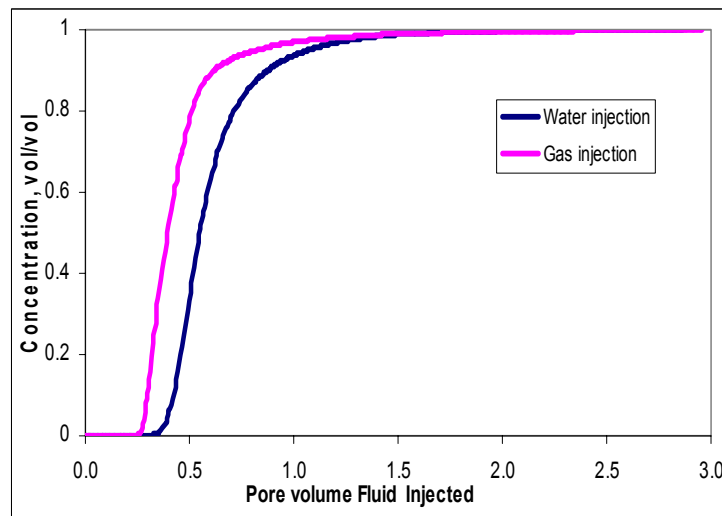
. Tracer has been added to the injection well stream with unit initial concentration to track the movement of the gas or water front through the reservoir. Production-well tracer concentration is good indicative of the unfavorable watercut or GOR values. **Fig. 3.64** shows the variation in tracer concentration in the production stream during injection.

Estimated gas breakthrough in mobility dominated and IFT dominated mechanism occurs after continuous injecting of 0.22 and 0.24 pore volume of

injected gas, whereas water breakthrough in the production well is observed after 0.3 pore volume of water injection. Therefore, the earliest breakthrough is observed in the mobility dominated mechanism.



**a) Production-well tracer concentration in waterflooding and mobility dominated gas injection**



**b) Production-well tracer concentration in waterflooding and IFT dominated gas injection**

**Fig. 3.64—Comparison of tracer concentration in gas and water injection projects**

### 3. CONCLUSIONS

The first part of this study presented an evaluation of the existing MMP correlations published in the literature for lean hydrocarbon gases. The reliability of individual correlations was evaluated by determining, on average, how close the appropriate MMPs and EOS-based analytical calculations are. As a general observation, the evaluated MMP correlations studied in this investigation were not sufficient for preliminary MMP-calculation purposes. Many of these correlations have proven not to honor the effect of fluid composition properly. The methods of Firoozabadi *et al.*<sup>35</sup> and Eakin *et al.*<sup>36</sup> were found to be the most reliable of the correlations tested. In most cases EOS-based analytical methods seemed to be more conservative in predicting MMP values. Hence, experimental MMP measurements would also be required for the design of gas-injection projects and calibration of fluid model.

Following an acceptable estimate of MMP, numerous compositional simulation models were used to investigate the effect of key parameters in miscible or immiscible recovery performance of the reservoir.

Distinct recovery trends were observed using different miscible and immiscible relative permeabilities. For the same injection pressure and pore volumes of injection gas as those of immiscible relative permeability curve, the incremental oil recovery using miscible  $k_r$ , was substantial.

Incremental oil recovery was determined by injection pressure. Pressure was the key parameter in determining whether or not the injection gas will be miscible with the in-situ oil. A multiple-contact miscible process was proven viable to increase the oil recovery to a high degree. Oil recoveries were usually greater when the gas-injection process was operated under miscible conditions. Miscibility can be achieved by injecting gas at pressures equal to or greater than MMP. At pressures higher than the MMP, the incremental recovery obtained was not substantial.

Part of the success of miscible-injection projects can be attributed to the variation in fluid viscosities toward lower mobility ratios during injection. Comparison of the viscosity values for miscible and immiscible displacements indicated that injection-gas viscosity increases as miscibility develops. Injection gas lowers the oil viscosity substantially. This reduction is the result of oil swelling or expansion of the undersaturated fluid by the addition of dissolved gas at higher pressures, which lightens the oil and consequently decreases the oil viscosity.

Comparison of estimated oil recoveries illustrated that stratification may result in a significant increase or slight decrease in the oil recovery. The major factor on the stratification effects was the vertical location of the higher-permeability layer. A high-permeability layer located in the lower half of the reservoir may improve the oil recovery potential. The maximization of oil recovery for this case may be the result of a combination of vertical displacement caused by gravity override and horizontal displacement of the oil by the high-permeability layer.

The effect of  $k_v/k_h$  ratio on the recovery performance of the particular reservoirs is of significant importance. Lower vertical permeabilities resulted in lower oil recoveries due to lower vertical communication between layers.

Predicted recoveries for different injection-well completion patterns indicated that injection to the top of the formation would be more favorable and beneficial to reservoirs having higher permeabilities to allow the gas to displace the oil downward.

Miscibility, defined as development of a zero interfacial tension between fluids, does not need to occur in order to obtain the maximum oil recovery. If a system is viscosity-dominated, the injection-gas composition may not be important from an interfacial tension perspective. In this situation, an alternative waterflooding recovery method may show more productivity improvement even with less investment. Therefore, understanding the effect of adverse mobility ratio and interfacial tension on the recovery of the reservoir is of great importance for a gas injection project to be implemented successfully.

## NOMENCLATURE

API=American petroleum institute

$A_i$  and  $B_i$  = constants characteristic for each component

CGD=condensing gas drive

$\sigma_i$  = component surface tension, dyne/cm

$\sigma_0$  = reference surface tension, dyne/cm

EOR=efficient oil recovery

$f$  = mole fraction of the injection gas

$f_{Vi}$ , volume fraction of oil components

FCMP=first contact miscibility pressure

GOR= gas/oil ratio, Mscf/STB

IFT=interfacial tension

IMPES=implicit-pressure explicit-saturation

$\rho_L^m$  = liquid phase molar density, g - mole/cc

$\rho_v^m$  = vapor phase molar density, g - mole/cc

$K_{c7+}$ = paraffinicity characterization factor

$K_{ro}^{immis}$  = immiscible oil relative permeability

$K_{ro}^{mis}$  = miscible oil relative permeability

LPG=Liquified petroleum gas

$M_{c7+}$ =molecular weight of heptane plus fraction, lb/lbmol

MMP= minimum miscibility pressure, psi

MMRB= million reservoir barrel

MMSTB= million standard tank barrel

MMscf=million standard cubic feet

Mscf=thousand standard cubic feet

$M_{c5+}$ =molecular weight of pentane plus in the live oil

$n$ =number of components in the solvent

OOIP= originally oil in place, STB

$P_{pc}$ =pseudo critical pressure of the reservoir fluid, psi

$P_{pr}$ = pseudo reduced pressure of the reservoir fluid

PR-EOS= Peng-Robinson equation of state

RBA= rising bubble apparatus

STO= standard tank oil

STB= standard tank barrel

$S_{cr}$  = critical saturation

$S_{cr}^{immis}$  = immiscible critical saturation

$S_{cr}^{mis}$  = miscible critical saturation

$T$ = temperature,  $^{\circ}F$

$T_{bi}$  = boiling-point temperature of component  $i$ ,  $^{\circ}F$

$T_{ci}$  = critical temperature of the  $i$ th component,  $^{\circ}R$

$T_{pr}$ =pseudo reduced temperature of the reservoir fluid

$T_{pc}$ =pseudo critical temperature of the reservoir fluid,  $^{\circ}R$

$T_R$ = reservoir temperature,  $^{\circ}F$

VGD=vaporizing-gas drive

$x$ = molecular weight of  $C_2$  through  $C_6$  components in injection gas, lbm/mol

$x_{int}$  =mole percent of intermediate components( $C_2$  through  $C_5$ )

$x_{vol}$  = mole fraction of volatile components in the oil ( $C_1$  and  $N_2$ )

$y$ = corrected molecular weight of  $C_{7+}$  in the stock-tank oil, lbm/mole

$y_{c2+}$  = mole fraction of the ethane plus fraction in the reservoir fluid

$y_i$ = mole fraction of component  $i$  in the solvent

$\gamma_o$  =oil specific gravity

$\gamma_{o,c7+}$  =specific gravity of the heptane plus fraction of the oil

$z$ = mole percent methane in injection gas

$z_i$  = mole percent of component  $i$

$z_i^{gas}$  = mole percent of component  $i$  in the injection gas

$z_i^{oil}$  = mole percent of component  $i$  in the reservoir oil

## SUBSCRIPTS

b=boiling

c=critical

g=gas

$i$ =component  $i$

immis= immiscible flooding

int=intermediates, mole fraction

L= liquid phase

mis= miscible flooding

o=oil

pc=pseudocritical

pr=pseudoreduced

v= vapor phase

vol=volatile components, mole fraction



## REFERENCES

1. Stalkup, F.I., Jr.: "Miscible Displacement," *SPE Monograph Series*, 1984
2. Kehn, D.M., Pyndus, G.T., and Gaskell, M.H.: "Laboratory Evaluation of Prospective Enriched Gas Drive Projects," *Trans.*, AIME (1958) **213**,382-85.
3. Helfferich, F.G.: "Theory of Multicomponent, Multiphase Displacement in Porous Media," *SPEJ* (Feb. 1981) 51-62.
4. Zick, A.A.: "A Combined Condensing/Vaporizing Mechanism in the Displacement of Oil by Enriched Gases", paper SPE 15493 presented at the 1986 SPE Annual Technical Conference and Exhibition, New Orleans, LA., 5-8 Oct
5. Stalkup, F. I.: "Displacement Behavior of the Condensing/Vaporizing Gas Drive Process", paper SPE 16715 presented at the 1987 SPE Annual Technical Conference and Exhibition, Dallas, TX, 27- 29 Sept
6. Holm, L.W. and Josendal, V.A.: "Effect of Oil Composition on Miscible –Type Displacement by Carbon Dioxide," *SPEJ* (Feb. 1982)87-98
7. Metcalfe, R.S. and Yarborough, L.: "Effect of Phase Equilibria on the CO<sub>2</sub> Displacement Mechanism," *SPEJ* (Aug. 1979)242-52
8. Yellig, W.F. and Metcalfe, R.S.: "Determination and Prediction of CO<sub>2</sub> Minimum Miscibility Pressure," *JPT* (Jan. 1980) 160-68
9. Holm, L.W. and Josendal, V.A.: "Mechanism of Oil Displacement by CO<sub>2</sub>," *JPT* (Dec. 1974) 1427-36
10. Khazem, M.M., Danesh, A., Tehrani, D.H., Todd, A.C. and Burgass, R.: "Dynamic Validation of Phase Behavior Models for Reservoir Studies of Gas Injection Schemes," paper SPE 28627 presented at the 69th SPE Annual Technical Conference and Exhibition , New Orleans, LA, 25-28 Sept
11. Collins, R.E.: *Flow of Fluids Through Porous Media*, Reinhold Publishing Co., New York (1961) 201.

12. Gardner, J.W. and Ympa, J.G.J: "An Investigation of Phase Behavior-Macroscopic Bypassing Interaction in CO<sub>2</sub> Flooding," paper SPE 18065 presented at the 1982 SPE/DOE Symposium on Enhanced Recovery, Tulsa, OK, April 4-7.
13. Thomas, F.B. and Okazawa, T.: "Does Miscibility Matter in Gas Injection?" Petroleum Society of CIM and CANMET, 95-51
14. Christiansen, R.L. and Kim, H.: "Apparatus and Method for Determining the Minimum Miscibility Pressure of a Gas in a Liquid," Canadian Patent 1 253 358
15. Eakin, B.E., Mitch, F.J.: "Measurement and Correlation of Miscibility Pressure of Reservoir Oils" paper SPE 18065 presented at the Annual Technical Conference and Exhibition, Houston, TX, 2-5 Oct.
16. Benham, A.L., Dowden, W.E., and Kunzman, W.J.: "Miscible Fluid Displacement- Prediction of Fluid Miscibility," *JPT* (Oct. 1960) 229-37; *Trans. AIME*, **219**.
17. Davis, P.C., Bertuzzi, A.F., Gore, T.L., Kurata, F.: "Phase and Volumetric Behaviour of Natural Gases at Low Temperatures and High Pressures", *Trans. AIME* (1954) **201**, 245.
18. Metcalfe, R.S., Fussell, D.D., Shelton, J.L.: "A Multicell Equilibrium Separation Model for the Study of Multiple Contact Miscibility in Rich-gas Drives" paper SPE 3995 presented at the 1972 SPE Annual Technical Conference and Exhibition, San Antonio, TX, 8-11 Oct.
19. Cook, A.B., Walter, C.J., and Spencer, G.C.: "Realistic K-values of C<sub>7+</sub> Hydrocarbons for Calculating Oil Vaporization During Gas Cycling at High Pressure," *JPT* (July 1969)901;*Trans. AIME*, **246**.
20. Kue, S.S.: "Prediction of Miscibility for the Enriched Gas Drive Process", paper SPE 14152 presented at the 1985 SPE Annual Technical Conference and Exhibition, Las Vegas, NV, 22-25 Sept.
21. Turek, E.A., Luks, K.D., Baker L.E.: "Calculation of Minimum Miscibility Pressure", SPE Res. Eng. (Nov. 1987) 501.

22. Flock, D.L., Nouar A.: " Prediction of the Minimum Miscibility Pressure of a Vaporizing Gas Drive" paper SPE 15075 presented at the 1986 SPE Annual Technical Conference and Exhibition, Oakland, CA, 2-4 April.
23. Shelton, J.L., Yalborough, L.: "Multiple Phase Behavior in Porous Media During CO<sub>2</sub> or Rich Gas Flooding," *JPT* (Sept. 1977), 1171.
24. Jensen, F., Michelson, M. L.: " Calculation of First Contact and Multi Contact Minimum Miscibility Pressures," *In Situ* (1990) **14**, 1.
25. Monroe, W.W., Silva, M.k., Larsen L. L., Orr. F.M.: " Composition Paths in Four- Component Systems: Effect of Dissolved Methane on 1-D CO<sub>2</sub> Flood Performance," *SPE Res. Eng.*,(1987) **2**, 479.
26. Johns, R. T., Dindoruk, B. and Orr, F. M., Jr.: " Analytical Theory of Combined Condensing/Vaporizing Gas Drives", *SPE Adv. Tech. Ser.* (1993) 2, No. 3, 7.
27. Johns, R.T., Orr, F.M. Jr: " Miscible Gas Displacement of Multicomponent Oils," paper SPE 30798 presented at the 1995 SPE Annual Technical Conference and Exhibition, Dallas, TX, 22-25 Oct.
28. Wang, Y., Orr, F. M., Jr.: " Calculation of Minimum Miscibility Pressure", paper SPE 39683 presented at the 1998 SPE Annual Technical Conference and Exhibition, Tulsa, OK, 19-22 April.
29. Johns, R.T., Orr, F.M. Jr: " Miscible Gas Displacement of Multicomponent Oils," paper SPE 30798 presented at the 1995 SPE Annual Technical Conference and Exhibition, Dallas, TX, 22-25 Oct.
30. Metcalfe, R.S., Fussell, D.D., Shelton, J.L.: "A Multicell Equilibrium Separation Model for the Study of Multiple Contact Miscibility in Rich-gas Drives" paper SPE 3995 presented at the 1972 SPE Annual Technical Conference and Exhibition, San Antonio, TX, 8-11 Oct.
31. Glasø, Ø.: "Generalized Minimum Miscibility Pressure Correlation" paper SPE 12893 presented at the 1985 SPE Annual Technical Conference and Exhibition, Dec. 1985

32. Yurkiw, F.J., Flock, D.L.: "A Comparative Investigation of Minimum Miscibility Pressure Correlations for Enhanced Oil Recovery," *JCPT* (1994) 33, N0. 8, 35.
33. Sebastian, H.M., Wenger, R.S., Renner, T.A.: "Correlation of Minimum Miscibility Pressure for Impure CO<sub>2</sub> Streams," *JPT* (Dec 1985) 2076.
34. Alston, R. B., Kokolis, G. P., James, C. F.: "CO<sub>2</sub> Minimum Miscibility Pressure: A Correlation for Impure CO<sub>2</sub> Streams and Live Oil Systems," *SPEJ* (April, 1985) 268.
35. Firoozabadi, A., Aziz, K.: "Analysis and Correlation of Nitrogen and Lean-Gas Miscibility Pressure", paper SPE 13669 presented at the 1986 SPE Annual Technical Conference and Exhibition, 8 Nov.
36. Eakin, B.E., Mitch, F.J.: "Measurement and Correlation of Miscibility Pressure of Reservoir Oils" paper SPE 18065 presented at the Annual Technical Conference and Exhibition, Houston, TX, 2-5 Oct.
37. Pedrood, P.: "Prediction of Minimum Miscibility Pressure in Rich Gas Injection," M. Sc. Thesis, Tehran University, Tehran (1995)
38. Glasø, Ø.: "Generalized Pressure-Volume-Temperature Correlations," *JPT* (May, 1980) 785-95
39. Kay, W.B.: "Density of Hydrocarbon Gases and Vapors at High Temperatures and Pressure" *Ind. Eng. Chem.*, (1936) **28**, 1014
40. Orr, F.M., Jr. and Silva, M.K.: "Effect of Oil Composition on Minimum Miscibility Pressure-Part 2:Correlation", *SPE Res. Eng.*,(1987) 2,479.
41. Todd, M.R. and Longstaff, W.J.: "The Development, Testing , and Application of a Numerical Simulator for Predicting Miscible Flood Performance," *JPT* (July 1972) 874-82
42. Coats, K.H.: "An Equation of State Compositional Model," *SPEJ* (Oct 1980) 363

## APPENDIX A

### Data file for compositional model

```

--RUNSPEC section-----
RUNSPEC
--Request the FIELD unit set
FIELD
--Water is present
WATER
OIL
GAS
--AIM solution method
AIM
--9 components in study (plus water )
COMPS
9 /
--Peng-Robinson equation of state to be used
EOS
PR /
DIMENS
9 9 2 /
WELLDIMS
2 2 2 2 3 1 10 1 /
TABDIMS
1 1 40 40 1/
MULTSAVE
1 /
NSTACK
40 /
--Grid section-----
GRID
INIT
DX
162*293.3 /
DY
162*293.3 /
DZ
162*40 /

```

```

TOPS
81*8340 /
PORO
162*0.13 /
PERMX
162*90 /
PERMY
162*90 /
PERMZ
162*9 /
--Properties section-----
PROPS
NCOMPS
9 /
-- Peng-Robinson correction
EOS
PR /
PRCORR
-- Standard temperature and pressure in Deg F and PSIA
STCOND
60.0 14.7 /
-- Component names
CNAMES
N2
Co2
C1
C2
C3
C4
c5
c6
c7+
/
-- Critical temperatures Deg R
TCRIT
227.16 548.46 343.08000 549.774 665.64000 755.1 838.62 913.5
1325.16 /
-- Critical pressures PSIA
PCRIT
492.31 1071.3 667.78 708.34 615.76 543.45 487.17 436.62

```

```

277.28/
VCRIT
1.4417 1.5057 1.5698 2.3707 3.2037 4.1328 4.9657 5.6225
12.445 /
-- Accentric factors
ACF
.04 .2250 .013 .0986 .1524 .1956 0.2413
.299 .64515 /
-- Molecular Weights
MW
28.014 44.010 16.043 30.070 44.097 58.124
72.151 84 202 /
-- Omega_A values
OMEGAA
.45724 .45724 .45724 .45724 .45724
.45724 .45724 .45724 .45724 /
-- Omega_B values
OMEGAB
.077796 .077796 .077796 .077796 .077796
.077796 .077796 .077796 .077796 /
-- Default fluid sample composition
ZMFVD
1 0.0092 0.0032 0.4125 .0868 .0727 0.049 0.0289 0.0429 0.2948
/
-- Boiling point temperatures Deg R
TBOIL
139.32000 350.46 200.88 332.28 415.98 484.02
550.62 606.69 991.21 /
-- Reference temperatures Deg R
TREF
140.58 527.4 201.06 329.4 415.8 527.4 527.4 520.2 519.67 /
-- Reference densities LB/FT3
DREF
50.192 48.507 26.532 34.211 36.333 35.69 38.93 42.763 53.813 /
-- Parachors (Dynes/cm)
PARACHOR
41 78 77 108 150.3 187.2 228.9 271 524.93 /
-- Binary Interaction Coefficients
BIC

```

-0.0170

0.0311      0.1200

0.0515      0.1200 0.0000

0.0852      0.1200 0.0000 0.0000

0.1033      0.1200 0.0000 0.0000 0.0000

0.0922      0.1200 0.0000 0.0000 0.0000 0.0000

0.0800      0.1200 0.0000 0.0000 0.0000 0.0000 0.0000

0.0800      0.1000 0.0000 0.0000 0.0000 0.0000 0.0000      0.0000 /

-- Reservoir temperature in Deg F

RTEMP

217.5 /

--Saturation tables

SWFN

0.22    0       7

0.3    0.07    4

0.4    0.15    3

0.5    0.24    2.5

0.6    0.33    2

0.8    0.65    1

0.9    0.83    0.5

1       1       0       /

SGFN

0       0       0

0.04    0       0.2

0.1    0.022    0.5

0.2    0.1       1

0.3    0.24    1.5

0.4    0.34    2

0.5    0.42    2.5

0.6    0.5       3

0.7    0.8125   3.5



```

      0.78   1       3.9   /
SOF3
0          0          0
0.15       0          0
0.38       0.00432    0
0.4         0.0048     0.004
0.48       0.05288    0.02
0.5         0.0649     0.036
0.58       0.11298    0.1
0.6         0.125      0.146
0.68       0.345      0.33
0.7         0.4        0.42
0.74       0.7        0.6
0.78       1          1          /

```

```

DENSITY
1* 63 1* /

```

```

ROCK
4200 0.000004 /

```

```

PVTW
4200 1.0 0.000003 0.31 0.0 /

```

```

--Solution section-----

```

```

SOLUTION

```

```

OUTSOL

```

```

SOIL /

```

```

RPTSOL

```

```

SOIL /

```

```

EQUIL

```

```

8340 4200 8450 0 7000 0 1 1 0 /

```

```

=====

```

```

SUMMARY

```

```

BSOIL

```

```

--FIRST LAYER

```

```

1 9 1 /

```

```

2 9 1 /

```

```

3 9 1 /

```

```

4 9 1 /

```

```
5 9 1 /
6 9 1 /
7 9 1 /
8 9 1 /
9 9 1 /
--2ND LAYER
1 9 2 /
2 9 2 /
3 9 2 /
4 9 2 /
5 9 2 /
6 9 2 /
7 9 2 /
8 9 2 /
9 9 2 /
/
BOVIS
--FIRST LAYER
1 9 1 /
2 9 1 /
3 9 1 /
4 9 1 /
5 9 1 /
6 9 1 /
7 9 1 /
8 9 1 /
9 9 1 /
--2ND LAYER
1 9 2 /
2 9 2 /
3 9 2 /
4 9 2 /
5 9 2 /
6 9 2 /
7 9 2 /
8 9 2 /
9 9 2 /
/
BODEN
--FIRST LAYER
```

```
1 9 1 /
2 9 1 /
3 9 1 /
4 9 1 /
5 9 1 /
6 9 1 /
7 9 1 /
8 9 1 /
9 9 1 /
--2ND LAYER
1 9 2 /
2 9 2 /
3 9 2 /
4 9 2 /
5 9 2 /
6 9 2 /
7 9 2 /
8 9 2 /
9 9 2 /
/
BSGAS
--FIRST LAYER
1 9 1 /
2 9 1 /
3 9 1 /
4 9 1 /
5 9 1 /
6 9 1 /
7 9 1 /
8 9 1 /
9 9 1 /
--2ND LAYER
1 9 2 /
2 9 2 /
3 9 2 /
4 9 2 /
5 9 2 /
6 9 2 /
7 9 2 /
8 9 2 /
```

```
9 9 2 /  
/  
BGVIS  
--FIRST LAYER  
1 9 1 /  
2 9 1 /  
3 9 1 /  
4 9 1 /  
5 9 1 /  
6 9 1 /  
7 9 1 /  
8 9 1 /  
9 9 1 /  
--2ND LAYER  
1 9 2 /  
2 9 2 /  
3 9 2 /  
4 9 2 /  
5 9 2 /  
6 9 2 /  
7 9 2 /  
8 9 2 /  
9 9 2 /  
/  
BDENG  
--FIRST LAYER  
1 9 1 /  
2 9 1 /  
3 9 1 /  
4 9 1 /  
5 9 1 /  
6 9 1 /  
7 9 1 /  
8 9 1 /  
9 9 1 /  
--2ND LAYER  
1 9 2 /  
2 9 2 /  
3 9 2 /  
4 9 2 /
```

```

5 9 2 /
6 9 2 /
7 9 2 /
8 9 2 /
9 9 2 /
/
FRPV
FOPR
WWCT
P/
FGPT
FPR
FGIR
FGIT
FGIPG
FGIP
FOIPR
FMWIN
FMWIA
WGOR
P/
FOPT
RUNSUM
--Schedule section-----
SCHEDULE
RPTSCHED
SOIL RECOV /
WELSPECS
--WELL specifications
WELSPECS
I  Field  1  1 8340 GAS /
p  Field  9  9 8380 OIL /
/
--WELL completions
COMPDAT
I  1  1  1 1 OPEN 1 /
P  9  9  2 2 OPEN 1 /
/
--Wells are controlled by min BHP of 1000 psi and MAX Gas Rate of 30,000
WCONPROD

```

```

P  OPEN GRUP 2* 30000 2* 1000 /
/
--Injection gas composition
WELLSTRE
'INJG'  0    0.00877    0.87526    0.06360    0.03906    .01331    0 0 0  /
/
WINJGAS
I  STREAM  'INJG' /
/
WCONINJE
I  GAS  OPEN  BHP  2*  4400  /
/
--Request fluid in place reports, group, and well data.
RPTPRINT
0 0 0 0 0  0 0 0 0 0 /
--NOINNER
TSTEP
5110 /
TSTEP
365 /
END

```

**VITA**

Name:

**IMAN FARZAD**

Permanent Address:

No.61, 5Parastoo Lane, 50 Vakil Abad Street,  
Mashhad, Khorasan, Iran

Education:

B.S., Chemical Engineering  
Sharif University of Technology  
Tehran, Iran

M.S., Petroleum Engineering  
Texas A&M University  
College Station, Texas